FK151121 - Hydrothermal Hunt on the Mariana Back-arc

R/V Falkor Nov 20 – Dec 17, 2015 Guam to Guam

Chief Scientists Joseph Resing and William Chadwick

Captain Heiko Volz

Operations with CTD casts and tows, AUV *Sentry* dives 366-370,

and seafloor mapping with EM302 multibeam sonar

Report compiled by Susan Merle and William Chadwick

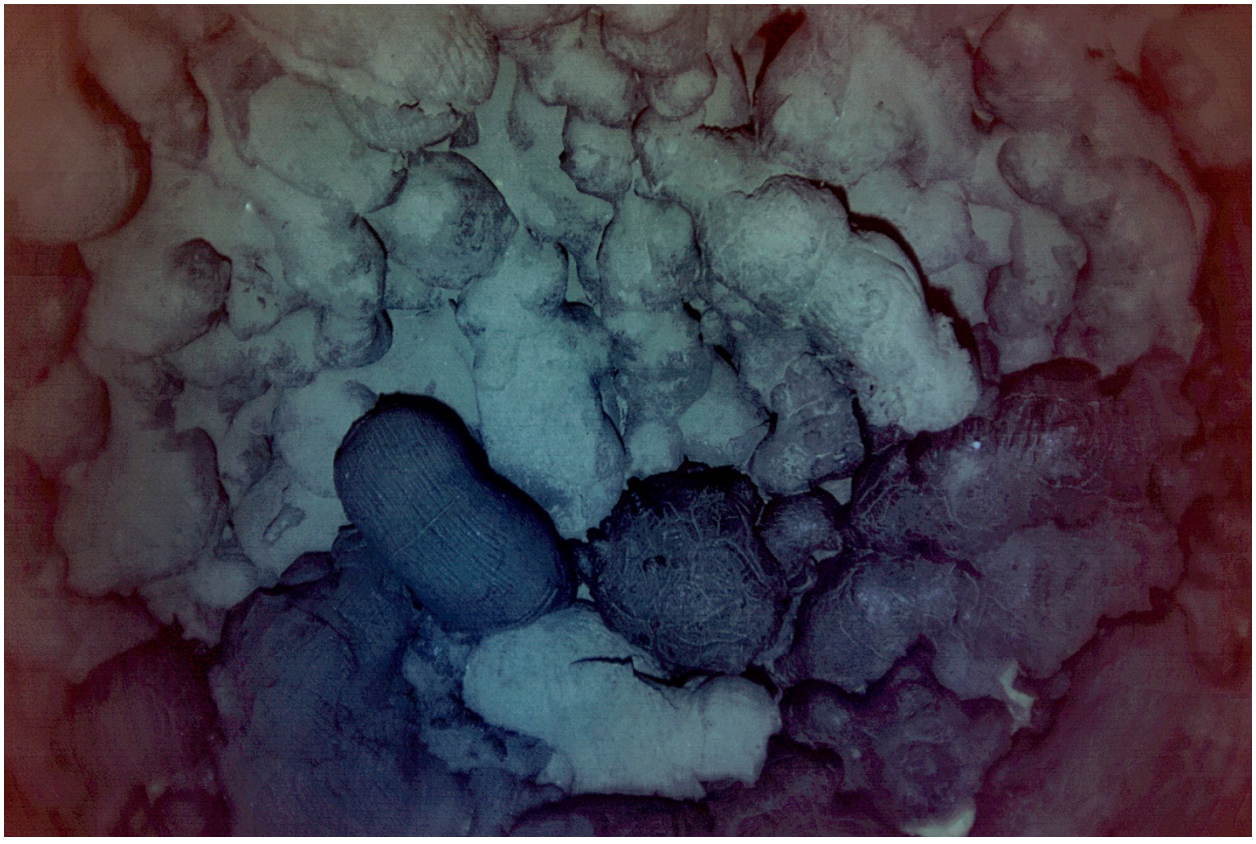

Photograph taken during Sentry dive 367 showing the edge of a newly discovered young lava flow (dark) over the surrounding older seafloor (light) on the Mariana back-arc spreading center.

blank

Table of Contents

FK151121 Expedition - Operations Summary

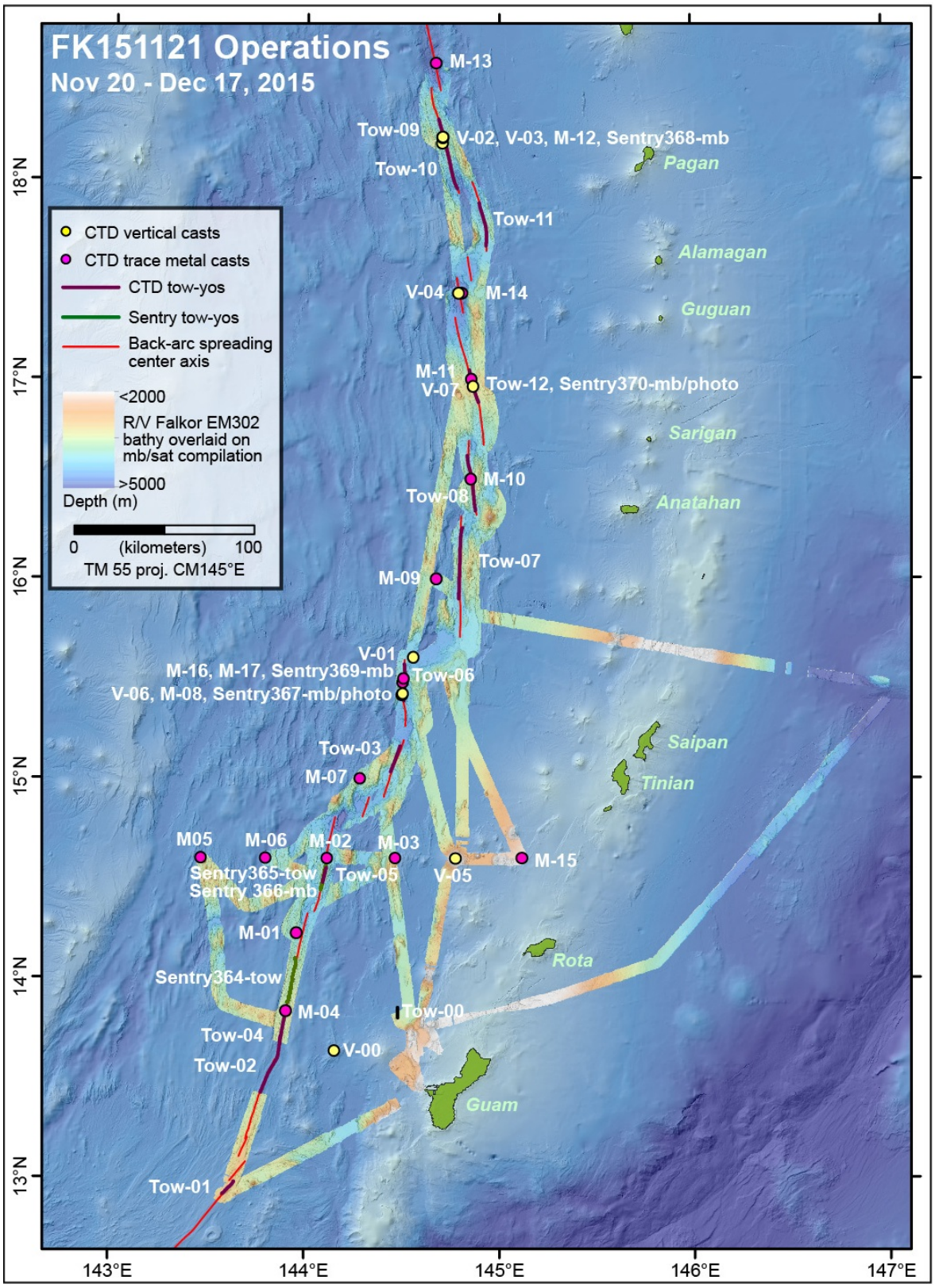

Expedition Summary

Bill Chadwick and Joe Resing

This expedition on R/V *Falkor* systematically explored 600 km of the southern Mariana back-arc for the first time, roughly from 13°N to 18.5°N. We made 12 tow-yos and 7 vertical casts with our hydrothermal CTD to search for hydrothermal plumes along the axis of the deep back-arc spreading center (3000-5000 m). We also made 17 trace metal CTD casts (<1000 m) on and off the back-arc axis to look for hydrothermal effluent coming from the shallower Mariana Arc, located further to the east. This work is aimed at understanding the potential sources and contribution of hydrothermal iron to the Pacific Ocean basin. In addition, we made 7 dives with AUV *Sentry*. The first two *Sentry* dives (364 & 365) surveyed the water column for plumes to supplement the CTD work, and the last 5 dives (365-370) focused on collecting high-resolution multibeam bathymetry of the seafloor. Two of the *Sentry* dives (367 & 370) also made photographic surveys of the seafloor.

The cruise was remarkably successful. We discovered four new hydrothermal vent fields in the Mariana back-arc, which more than doubles the number of known hydrothermal sites from three to seven. One of the newly discovered vent sites is one of the deepest ever found - at a depth of 4230 m. There are nearly 700 known vents around the world, and only three are deeper. Another remarkable (and surprising!) discovery was finding a newly erupted lava flow on the back-arc axis that was still cooling and likely only a few months old. The timing of the eruption can be constrained between multibeam sonar surveys on February 14, 2013, by R/V *Melville*, and December 1, 2015, when we resurveyed the site with the *Falkor*. We collected 24,050 km^2 of high-quality multibeam bathymetry with *Falkor's* EM302 sonar system, which is another important product from the cruise.

This expedition was the first in a two-part project to locate new vent sites (this cruise), and then to dive on those new sites with an ROV to characterize their geology, chemistry, and biology (the next cruise). The second cruise will be conducted on R/V *Falkor* in the fall of 2016, using the Schmidt Ocean Institute's new 4500-m rated ROV to visually explore and sample the new vent sites on the seafloor. The data collected on this first cruise will be invaluable to the success of the second cruise. The results from this cruise will also have a big impact in the context of our larger science goals in the Mariana region and will help test the idea that arc and back-arc hydrothermal sites have distinct ecosystems, controlled by each settings' geology and unique fluid chemistry.

We are grateful for the support we received for this project from the NOAA Ocean Exploration and Research Program, the NOAA Pacific Islands Regional Office, and the Schmidt Ocean Institute. The captain and crew of R/V *Falkor* were particularly helpful in the success of the cruise and were a pleasure to sail with. We are already looking forward to our next trip.

Cruise Participants

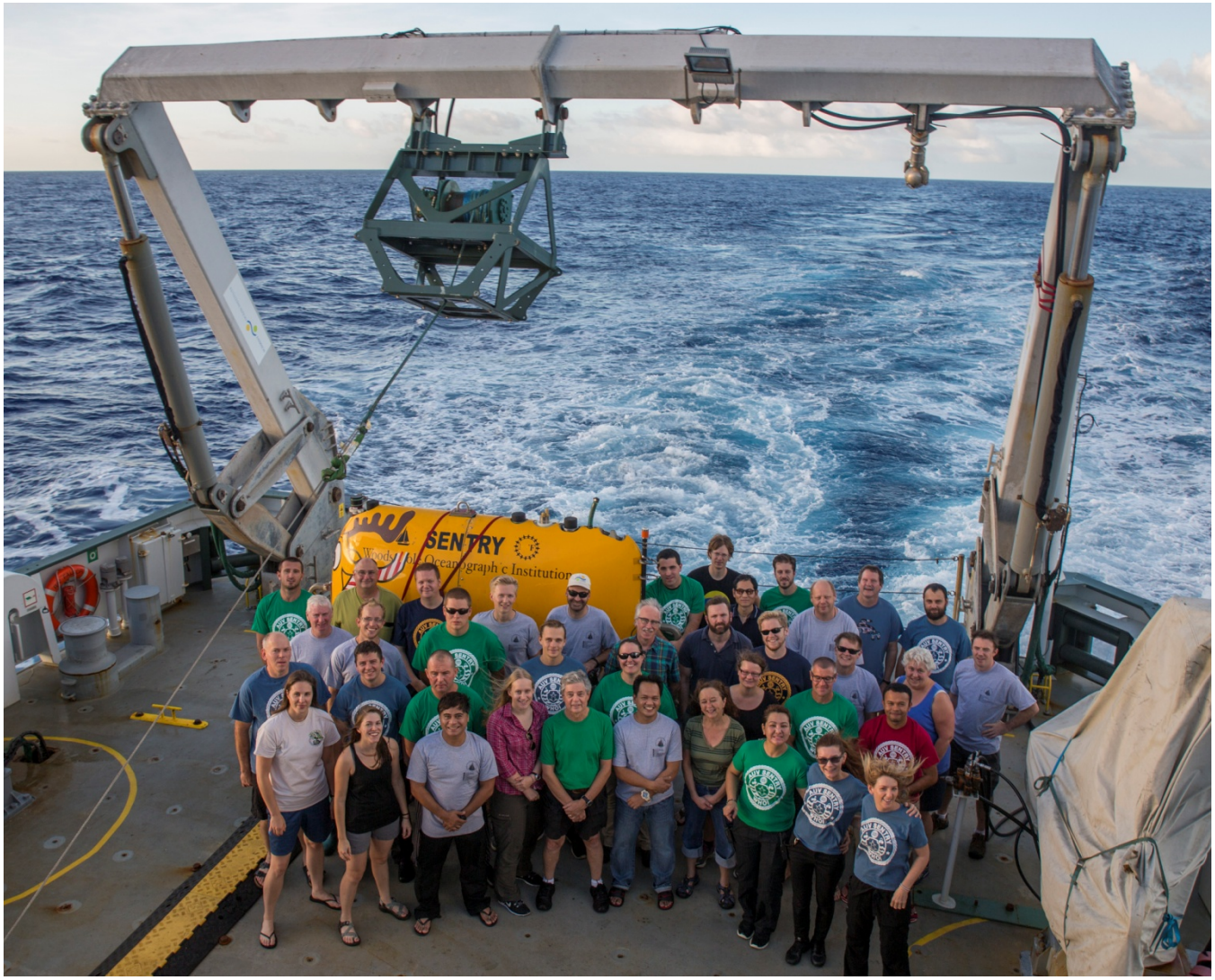

FK151121 scientific party and R/V *Falkor* crew

Front row (l to r): Pamela Barrett, Susanna Michael, Alberto Barcelo, Melissa Anderson, Edward Baker, Edwin Pabustan, Susan Merle, Mildred Dadis, Adriana Zamudio, Joyce Young.

Row 2: Joseph Resing, Arkadiusz Ochocki, Grzegorz Kuberski, Kaarel Kaspar Rais, Colleen Peters, Tamara Baumberger, Michael Utley, Archel Benitez.

Row 3: Allan Watt, Jack Hewitt, Henrik Ewert, David Butterfield, Nathan Buck, Carl Kaiser, Mike McCarthy, Sharon Walker.

Row 4: Karl Rogers, Andrew Billings, Douglas Hay, Erik Suits, Heiko Volz, Logan Driscoll, Zac Berkowitz, Hu Wang, Jason Garwood, Paul Duncan, Bill Chadwick, Todor Gerasimov, John Ahern.

(Not pictured: Thom Hoffman)

Science Party	**Affiliation**
Resing, Joseph	University of Washington, JISAO: NOAA EOI Program
Chadwick, William W.	Oregon State University, CIMRS: NOAA EOI Program
Anderson, Melissa	University of Ottawa: GEOMAR
Baker, Edward	University of Washington, JISAO: NOAA EOI Program
Barrett, Pamela	University of Washington
Baumberger, Tamara	NRC postdoctoral fellow: NOAA EOI Program
Berkowitz, Zac	*Sentry* team WHOI
Billings, Andrew	*Sentry* team WHOI
Buck, Nathaniel	University of Washington, JISAO: NOAA EOI Program
Butterfield, David A.	University of Washington, JISAO: NOAA EOI Program
Driscoll, Logan	*Sentry* team WHOI
Hoffman, Thom	UK-based filmmaker , multimedia journalist
Kaiser, Carl	*Sentry* team leader WHOI
McCarthy, Mike	*Sentry* team WHOI
Merle, Susan	Oregon State University, CIMRS: NOAA EOI Program
Michael, Susanna	University of Washington
Walker, Sharon	NOAA EOI Program
Wang, Hu	School of Ocean and Earth Science, Tongji University

Operations Log

Local time / date	**UTC time / date**	**R/V *Falkor* (FK151121) Event**	Latitude °N	Longitude °E
		Local time = UTC+10		
0830 Nov20	2230 Nov 19	Depart Guam harbor at commercial pier to avoid typhoon In-Fa.		
		Collected multibeam data during all transits, etc. no matter what the ship speed.		
		First head to NW Rota-1 to re-survey summit for surface differencing.		
		Re-survey points: Rota-S 14d 32.023' 144d 43.905'; Rota-N 13d 39.455' 144d 48.636'.		
1414	0414 Nov 20	EM302 re-survey. SOL 8. Speed ~7kts. Bumpy seas.		
1426	0426	Brought angles out from 50/50 to 65/65.		
1523	0523	End of EM302 re-survey at NW Rota-1. EOL 9. (Lines 8 and 9 are Rota)		
		Speeding up to get out of the way of the typhoon.		
0800 Nov 21	2200 Nov 20	Ship N of Saipan. Seas 2.5 - 2.8 m. Continue weather avoidance until evening, then head S as seas decrease.		
Nov 22		Heading S and mapping on our way back to Guam to pick up trace metal CTD and to conduct shore side AUV launch and recovery.		
1605 Nov 22	0605 Nov 22	**V15B-00**. CTD test cast.	13.63407	144.15655
1658	0658	CTD back on deck. End V15B-00		
1902	0902	**T15B-00**. CTD test tow.	13.81392	144.48083
2300	1300	CTD back on deck. End of test tow T15B-00	13.83988	144.47812
2307	1307	Em302 survey on way back to Guam - edge mapping. SOL 65.	13.83928	144.47777
	2203	EM302 line 73.	13.45195	144.62408
0900 Nov 23	2300 Nov 22	Arrive in port at Guam commercial pier.		
1030		*Sentry* dunk test at the pier.		
1300		Load trace metal CTD on the ship.		
1400		Depart Guam harbor with trace metal CTD on board.		
1540		***Sentry* in water for trial launch and recovery** - just offshore on Guam's W coast.		
1545		*Sentry* released.		
1625		*Sentry* back on board.		
1748	0748 Nov 23	EM302 survey. SOL 74		
0018 Nov 24	1418 Nov 23	**T15B-01**. CTD in the water for first official CTD tow on the S Back-arc spreading center 12.8 N segment also known as- Snail segment.	12.91713	143.58296
0648	2048	Turned off EM302 logging - EOL 86. The USBL beacons interfere with the multibeam data, so probably not worth logging in the future. Also the ship was crabbing so much during the CTD two-yo that the multibeam coverage was poor.		
	2055	CTD back on deck. End of T15B-01.	12.98061	143.64256

Local time / date	UTC time / date	R/V *Falkor* (FK151121) Event	Latitude °N	Longitude °E
0740	2140	***Sentry* dive 363**. *Sentry* in the water.		
		USBL not working. *Sentry* dive aborted. Problem was between the ship's USBL transducer and *Sentry*'s USBL beacon - they weren't talking.		
		Sentry back on deck. No navigation for this dive.		
1000	0000 Nov 24	Going to send *Sentry* USBL beacon down on the trace metal CTD to test it. After USBL troubleshooting will transit to next CTD tow-yo.		
1335	0335	USBL troubleshooting only partially successful. Can do tracking but no comms. Will have to troubleshoot more via email with sonardyne.		
		Trace metal CTD back on deck. Test cast.		
		Ship transiting to CTD T15B-02 site (from 12° 47.6'N to 13° 25.6'N).		
1349	0349	Started logging EM302 during transit. Line 87. Z=2873. Very Deep mode. 65/65 angles. 3801/3824 coverage. 252/432 beams. Colleen says we started in sonar test mode.	12.97750	143.62870
1357		Stopped logging bathy briefly to try to fix display		
1358		EM302 logging to line 88.		
1359		Stopping again to restart SIS.		
1400 Nov 24	0400	Logging again to line 89. Sound velocity was bogus (1500m) for a few pings near the start.		
1405	0405	EM302 mapping. 10 kts. Z=2903. Deep mode. 56/56 angles. 4290/4216 coverage. 416/432 beams. Angular coverage set to Auto.	13.01980	143.64218
1420	0420	EM302 cont. 10 kts. Z=2952. 57/59 angles. 4349/4269 coverage. 410/432 beams. Deep mode.	13.05730	143.65440
1430	0430	EM302 cont. 10 kts. Z=3033. 55/59 angles. 3956/4444 coverage. 429/432 beams. Deep mode.	13.08450	143.66340
1453	0453	EM302 cont. 10 kts. Z=2957. 56/58 angles. 4239/4512 coverage. 409/432 beams. Deep mode.	13.14770	143.68430
1515	0515	Bridge says ETA is 1.5 hrs or 1630 local.		
1530	0530	EM302 cont. 10 kts. Z=3006. 56/59 angles. 4376/4758 coverage. 429/432 beams. Deep mode.	13.24560	143.71710
1600	0600	EM302 cont. 10 kts. Z=3197. 56/57 angles. 4394/4371 coverage. 398/432 beams. Deep mode.	13.32470	143.74360
1635	0635	Stopped logging EM302 data. EOL 91		
1700 Nov 24	0700 Nov 24	**T15B-02** (Cast 2). Deploy CTD for tow-yo at southern Mariana back-arc.	13.42683	143.77742
		Position of last time CTD was at the bottom before it was recovered.	13.68459	143.87622
1252 Nov 25	0252 Nov 25	T15B-02 CTD back on deck. End of tow-yo.	13.70929	143.87912
		Ship now transits ~6.5nm north to position for trace metal CTD cast followed by AUV *Sentry* dive 364.		
1350	0350	**CTD metal cast (M15B-00) test cast.**	13.82048	143.89935
1558	0558	***Sentry* launch Dive 364 - tow-yo dive.**	13.82059	143.89921

Local time / date	**UTC time / date**	**R/V *Falkor* (FK151121) Event**	Latitude °N	Longitude °E
1426 Nov 26	0426 Nov 26	*Sentry* off bottom. Dive manually aborted.		
1604	0604	***Sentry* back on board** after 1st successful *Sentry* "yo-yo".	14.10063	143.95665
1651	0651	**M15B-01**. First official trace metal cast (Cast #3) to 1050m.	14.22527	143.95917
1755	0755	M15B-01 back on board.		
	0756	EM302 survey. SOL 94 (E to W)		
	0823	Turning. SOL 95.		
1827	0827	SOL 96. S to N transit to next CTD tow-yo site. Collecting EM302 during transit. Z=2901; 51/52 angles; 381/432 beams; 4345/4480 coverage.	14.25372	143.92140
		THANKSGIVING DINNER ON UPPER DECK.		
2037	1037	EM302 cont. (Line 98). Z=4071; 52/48 angles; 4240/3500 coverage; 393/430 beams. Good data.	14.56870	144.04600
	1131	EM302 cont. (Line 99). Z=4100; 45/49 angles; 3800/4700 coverage; 420/432 angles. Turning to the NE and continuing on.	14.69950	144.06780
2320	1320 Nov 26	EM302 cont. Z=1320; 44/38 angles; 4100/3100 coverage; 385/432 beams.	14.83950	144.31680
0056 Nov 27	1456	Arrived at waypoint for CTD. Z=4100; 52/52 angles; 4650/4735 coverage.	15.03740	144.44230
0113	1513	**T15B-03 start.** Tow-yo over central Mariana back-arc (over high in map #5).	15.03758	144.44202
1201	0201 Nov 27	**T15B-03 end.** Tow-yo over central Mariana back-arc (over high in map #5).	15.16356	144.49004
		Next: Collect multibeam during ~5 hour transit south to trace-metal cast site; followed by AUV dive. MB waypoints: CTD1 -> MB6 -> MB7 -> TMC-M2.		
1212	0212	EM302 survey between tasks. SOL 103 logging EM302 during transit. Line 103. Z=4348; Very deep mode; 49/52 angles; 4480/4690 coverage; 405/432 beams.	15.16070	144.48960
1351	0351	EM302 cont. Line 104. 9,7 knots; Z=3870; 45/51 angles; 3939/3802 coverage; 350/432 beams.	14.96070	144.33300
1640	0640	Stop logging EM302. EOL 108. Z=4298.	14.60060	144.11580
	0706	**M15B-02**. Trace-metal CTD #2 to 950 m. CTD cast #5.	14.59964	144.11702
	0802	End M15B-02.		
	0825	***Sentry*** in the water for **dive S365**. *Sentry* "Yo-yo" dive.	14.58457	144.11420
	2345	*Sentry* yo-yo midpoint on bottom - Z=3877.	14.51484	144.10147
	1010	*Sentry* back on board.	14.43861	144.08333
2025	1025	**EM302 logging** between *Sentry* dive site and next trace metal cast. Z=4114m. SOL 109.	14.39070	144.08550
2045	1045	EM302 logging during transit. Slowed down to 7.5 knots due to sea conditions. Z=3875; 50/52 angles; 4375/4300 coverage.	14.41020	144.11780
2300	1300	EM302 cont. Z=3855; 8.5 knots; 4200/3600 coverage; 417/432 beams; 52/52 angles.		
	1333	**Stop logging EM302** at site for trace metal cast west of Rota.. Z=3114.	14.59970	144.40830

Local time / date	UTC time / date	R/V *Falkor* (FK151121) Event	Latitude °N	Longitude °E
	1343	**M15B-03**. Trace-metal CTD cast #3 to 950m. CTD cast #6.	14.59968	144.46595
	1502	End M15B-03. CTD on deck.	14.60010	144.46080
0151 Nov 29	1551 Nov 28	EM302 survey between other tasks. Z=3345; 3600/2700 coverage; 52/37 angles; 415/432 beams.		
	1650	EM302 cont. Z=4350; 3620/3640 coverage; 381/432 beams.	14.60620	144.30850
0323	1723	EM302 cont. Z=2999; 4140/4500 coverage; 405/432 beams; 54/61 angles.		
	1745	EM302 cont. overlapping with other data. Z=4295;4525/3560 coverage	14.61210	144.15050
	1800	Continue heading south along the back-arc axis "edge-mapping".		
0440 Nov 29	1840 Nov 28	EM302 cont. Increasing from 9 to 10 knots. Z=3929; 3890/4052 coverage.	14.50320	144.10730
0500	1900	Data looked good at 10 knots.		
0530	1930	EM302 cont. Dropping some starboard beams. 50/40 angles so are reducing speed back down to 9 knots to see if they come back. Z=4147; 4466/3072 coverage.	14.37654	144.05330
0540	1940	Continuing multibeam transit. Now have starboard beams back. Z=4160; 50/50 angles; 9 knots. Line 116.		
0600	2000	Line 117. 9 knots; Z=4357; 50/52 angles.	14.31200	144.02000
0644	2044	Line 117. Increasing speed to 10 kts and bridge will head directly to next multibeam waypoint - instead of edge-mapping because as of now there are no previous data in this area.		
0744	2144	Line 118. 10 knots; Z=3588; 51/51 angles.	14.04290	143.94730
0834	2234	Line 119. 10 knots; Z=3428; 52/52 angles; very deep.	13.90460	143.91990
	2320	Line 120. 10 knots; 52/52 angles; very deep; Z=3446. We're going over the small patch of multibeam we collected earlier in the cruise.	13.77830	143.89470
	2355	Line 121. Ship slowing down. Now at 7 knots.		
	2358	Stop logging multibeam data. Z=3379; 51/52 angles.	13.68220	143.87540
1017	0017 Nov 29	**T15B-04 start.** Southern Mariana back-arc (Map 3; to close gap between T15B-02 and *Sentry*-364).	13.68230	143.87548
2327	1327	**T15B-04 end**.	13.84505	143.90856
0016 Nov 30	1416	**M15B-04.** Trace metal cast to 1000 m. Z=3464.	13.83366	143.90579
0136	1536 Nov 29	Trace metal CTD back on deck.		
0224	1624	EM302 survey during transit to west over small features west of the back-arc - then north to next trace metal cast. SOL 122. Z=3427.	13.83660	143.90700
0256	1656	EM302 cont. Z=3231; 410/432 beams; 3600/4020 coverage. Heading 287°.	13.79060	143.84930
0330	1730	EM302 cont. Z=2925; 9.5 knots; 4000/4050 coverage; 53/58 angles.	13.81440	143.77080
0434	1834	EM302 cont. Z=3325; 9 knots; 4000/3967 coverage; 51/52 angles; Very deep mode.	13.86700	143.60710
0443	1843	Making turn from WNW to NNW. Line 124.		
0508	1908	EM302 cont. On the new course now after the turn. Z=3609; 9 knots; 3823/4041 coverage; 52/51 angles; very deep mode; Line 124.	13.93170	143.56290

Local time / date	UTC time / date	R/V *Falkor* (FK151121) Event	Latitude °N	Longitude °E
0700 Nov 30	2100 Nov 29	EM302 cont. Z=3462; 9 knots; 4413/4162 coverage; 51/52 angles; very deep mode. Line 126.	14.20520	143.54760
0939	2339	Ship at waypoint. Slowing down and starting slow turn. Very deep mode; Z=3450; 6 knots; 4131/3967 coverage; 52/50 angles. Line 129.	14.59750	143.46840
0942	2342	Stop logging EM302 multibeam bathymetry.		
1014	0014 Nov 30	**M15B-05.** Trace metal cast to 900 m. Z=3464.	14.59999	143.46679
1118	0118	Trace metal CTD back on deck.		
1131	0131	Start logging EM302 multibeam data for transit to CTD towyo-5; using waypoints MB 8-10.		
1135	0135	EM302 cont. Z=3445 52/52 angles; 3970/4013 across; 9 knots; Line 130.	14.59450	143.47280
1347	0347	EM302 cont. Ship turning from SE to NE heading. Z=3317; 52/52 angles; 3933/3743 coverage; 9 knots; Line 132.	14.36900	143.69630
1550	0550	EM302 cont. Z=3810; 50/47 angles; 4048/3666 coverage; 8 knots; Line 134.	14.46400	143.97000
1637	0637	Stop logging EM302. Next task will be tow-yo in area of the plume found previously.		
1705	0705	**T15B-05**. Short tow to define plume seen during *Sentry* 365 tow-yo.	14.48201	144.09323
2307	1307	T15B-05 back on board.	14.55311	144.11106
0006 Dec 1	1406 Nov 30	**S366**. *Sentry* in the water for dive 366 in area where plume was discovered on S365 tow-yo and T15B-05.	14.50202	144.10045
1535 Dec 1	0534 Dec 01	*Sentry* on deck (end dive S366).	14.48260	144.09419
1601	0601	Start logging EM302 for transit to next CTD cast. Z=3932; 51/51 angles; 4700/4600 coverage; Line 136.	14.50340	144.09020
1740	0740	Stop logging EM302 at cast site.		
1756	0756	**M15B-06**. Trace metal cast.	14.59979	143.80015
1900	0900	Trace metal CTD back on deck.		
1910	0910	Start logging EM302 for transit to next CTD cast. Z=4208; Line 138	14.60430	143.80640
2130	1130	EM302 cont. Z=4475; 3303/3800 coverage; 45/44 angles; 9.8 kts.	14.78930	144.08980
2203	1203	EM302 cont. Z=3917; 3500/4500 coverage; 45/42 angles	14.84420	144.15200
2242	1242	EM302 cont. Z=3937; 51/51 angles; 355/432 beams	14.91320	144.21740
2308	1308	EM302 cont. Z=3700; 3303/3800 coverage; 45/44 angles; 385/432 beams	14.96650	144.26070
2326	1326	EM302 logging stopped at cast site.		
2347	1347	**M15B-07** Trace metal cast.		
0011 Dec 2	1411	Cast on bottom.	14.99997	144.28321
0050	1450	M15B-07 CTD on deck.		
0055	1455	EM302 start logging Line 143 heading to T15B-06. Z=3686; 1 knot.	15.00020	144.28430
0120	1520	EM302 cont. Z=3850; 4120/4180 coverage; 5.4 kts.	15.01390	144.30260
0150	1550	EM302 cont. Z=3480; 395/432 beams; 3040/3100 coverage; 9.4 kts.	15.05960	144.36330
0240	1640	EM302 cont. Z=3850; 4200/4200 coverage; 52/52 angles; 9.6 kts.	15.13740	144.46030

Local time / date	**UTC time / date**	**R/V *Falkor* (FK151121) Event**	Latitude °N	Longitude °E
0310	1710	EM302 cont. Z=4650; 3900/4500 coverage; 10.2 kts.	15.20870	144.49250
30417	1817	EM302 cont. Z=4290; 52/50 angles; 4546/4059 coverage; 3 kts; Line 147.	15.39000	144.50800
0420	1820	EM302 logging stopped at tow site.		
0459	1859	**T15B-06** at waypoint 6A (south->north tow) begin.	15.39148	144.50823
1932	0932 Dec 02	T15B-06 on deck.	15.57290	144.51041
1942	0942	EM302 start logging Line 147; Z=4134; 9 kts. Survey from N to S.	15.57833	144.50935
2004	1004	EM302 cont. Z=4155; 4100/3100 coverage; 391/432 beams; 43/39 angles. Line 148		
2022	1022	EM302 cont. Z=4111; 4300/3900 coverage; 379/432 beams; 47/47 angles. Possible plume in WCD.	15.57742	144.50935
2044	1044	EM302 cont; Z=4107; 4400/4250 coverage; 365/432 beams; 51/51 angles.	15.52727	144.50938
2115	1115	EM302 cont; Z=4040; 4560/4230 coverage; 8.5 kts.	15.47570	144.50833
2148	1148	EM302 cont; Z=4281; End N-S line over area of venting. Line 150 from N-S survey to M15B-08 (do not use).		
2155	1155	EM302 logging stopped.		
2213	1213	**M15B-08** Trace metal cast.	15.41658	144.49990
2316	1316	M15B-08 CTD on deck.		
2343	1343	***Sentry* Dive 367** in water over area of diffuse venting at south end of T15B-06.	15.42473	144.50960
0939 Dec 3	2339	EM302 start logging. Z=4249; 4345/4204 coverage; 52/50 angles; Line 151; 12 kts.	15.43718	144.51375
1042	0042 Dec 3	EM302 logging stopped at CTD V15B-01 site. Z=4607.		
1951	0051	**V15B-01** begin.		
1053	0053	V15B-01 on bottom in deep basin N of T15B-06.	15.60696	144.55838
1221	0221	V15B01 CTD on deck.		
1355	0355	EM302 start logging. Line 153 transit back to *Sentry* site. Z=4627; 2549/4086 coverage; 32/46 angles.	15.59888	144.55580
1446	0446	EM302 logging stopped as approaching *Sentry* site.		
2235	1235	*Sentry* left bottom.		
0021 Dec 4	1421	*Sentry* on deck (end dive S367).	15.40079	144.50888
0040	1440	EM302 start logging. Line 134. Z=4363; 52/51 angles; 390/432 beams; 9.2 kts. Repeat data.		
0055	1455	EM302 cont. Z=4325; 52/51 angles; 390/432 beams; 9.2 kts.	15.43128	144.51698
0152	1552	EM302 cont. Z=4390; 50/52 angles; 4800/4250 coverage; 388/432 beams; Line 155; New data.	15.56342	144.55425
0245	1645	EM302 cont. Z=4585; 43/43 angles; 4100/4000 coverage; In deep basin	15.64635	144.66843
0300	1700	EM302 cont. Line 156. Edge of EM122 Revelle 2014 data to towyo site.		
0303	1703	EM302 cont. Z=4516; 3900/4150 coverage; 42/47 angles; 401/432 beams.	15.67132	144.70037

Local time / date	UTC time / date	R/V *Falkor* (FK151121) Event	Latitude °N	Longitude °E
0330	1730	EM302 cont. Z=4550; 4320/4400 coverage; 48/47 angles; 409/432 beams.		
0451	1851	EM302 cont. Ship heading east to CTD towyo site.		
0502	1902	EM302 logging stopped.		
0531	1931	CTD in water (no tow number assigned)		
0634	2034	CTD docking head problem at 2650m; recovering.		
0736	2136	CTD on deck.		
0934	2334	EM302 start logging. Line 159.		
0937	2337	EM302 cont. Z=4180; 48/52 angles; 432/432 beams; 8565 coverage; Line 159	15.91762	144.78718
0943	2343	EM302 logging stopped. Test CTD deployment.		
1202	0202 Dec 4	EM302 start logging after CTD test. Line 160; Z=4166	15.94260	144.76178
1251	0251	EM302 logging stopped. Ship at CTD site.		
1256	0256	**M15B-09** in water.	16.00000	144.67500
1355	0355	M15B-09 on deck. Transit to CTD tow site (no multibeam).		
1512	0512	**T15B-07** in water. Z=4169	15.90833	144.79208
1900	0900	T15B-07 on deck. No anomalies/dead zone.		
1902	0902	EM302 start logging. Line 161.		
1905	0905	EM302 cont. Z=4112; 3400/3450 coverage; 49/41 angles; 400/432 beams.	16.26052	144.81465
1912	0912	EM302 cont. End Line 161 (do not use).		
1919	0919	EM302 cont. Start Line 162. Z=4073; 3700/3800 coverage; 48/45 angles; 427/432 beams. From end of tow up spreading center to beyond M15B-10 position.	16.24983	144.81000
1944	0944	Increasing speed to 10 kts.		
2025	1025	EM302 cont. Z=3772; 4100/4145 coverage; 414/432 beams; 52/48 angles.	16.39983	144.86983
2051	1051	EM302 cont. Z=3715; 3960/3870 coverage; 402/432 beams; 50/52 angles.	16.47183	144.86350
2122	1122	EM302 logging stopped. Line 164; Z=3965.	16.55333	144.84933
2205	1205	**M15B-10** start.	16.49983	144.85617
2258	1258	M15B-10 on deck.		
2308	1308	EM302 start logging. Line 165; Z=3475; 3900/3648 coverage; 51/46 angles; 5.2 kts.	16.49467	144.85617
2345	1345	EM302 cont. Z=3540; 9.5 kts; 4450/3450 coverage; 52/46 angles.	16.44500	144.81650
0025 Dec 5	1425	EM302 stop logging. Z=3880; 4340/4740 coverage; 52/50 angles.	16.36200	144.85100
0046	1446	**T15B-08** in water. Data logging problems at 800m going down and 1644m coming up.	16.34622	144.87595
2114	1116 Dec 6	T15B-08 on deck.		
2157	1157	EM302 start logging. Line 167; Z=4044; 47/51 angles; 231/432 beams.	16.63183	144.83633
2245	1245	EM302 cont. Z=4145; 432/432 beams; 50/52 angles; 9.5 kts.	16.72017	144.88783
2252	1252	EM302 cont. Z=4170; 4200/3800 coverage; 9 kts.	16.74000	144.89500

Local time / date	**UTC time / date**	**R/V *Falkor* (FK151121) Event**	Latitude °N	Longitude °E
2320	1320	EM302 cont. Z=3981; 420/432 beams; 52/52 angles; Line 168.	16.81150	144.90433
2351	1351	EM302 cont. Z=3512; 4100/4000 coverage; 430/432 beams; 8.9 kts.	16.89017	144.89283
0015 Dec 7	1415	EM302 cont. Z=3313; 432/432 beams; 52/52 angles.	16.94417	144.87817
0040	1440	EM302 cont. Slowing down and turning to CTD cast site. End line 169; Start line 170.		
0043	1443	EM302 logging stopped.		
0052	1452	**M15B-11** in water at 16.5°N.	16.99977	144.85694
0152	1552	M15B-11 on deck.		
0208	1608	EM302 start logging. Z=3420; Line 171; 3.7 kts. Heading to Alice Springs area.	17.00233	144.85667
0234	1634	EM302 cont. Z=3640; 52/52 angles; 422/432 beams.	17.04767	144.85067
0325	1725	EM302 cont. Z=4100; 4600/3300 coverage; 49/52 angles; 410/432 beams.		
0340	1740	EM302 cont. Z=4475; 45700/3550 coverage; 49/52 angles; 424/432 beams.	17.22533	144.83067
0400	1800	EM302 cont. Z=4588; 3840/4000 coverage; 42/52 angles; 344/432 beams.	17.27983	144.82450
0450	1850	EM302 cont. Z=4749; Line 173; 3033/2647 coverage; 32/34 angles.	17.25648	144.80750
0542	1942	EM302 cont. Z=4504; Line 174; 8051 coverage; 47/42 angles; 10 kts.	17.57083	144.79097
0701	2101	EM302 cont. Z=3645; Line 175; 7025 coverage; 52/52 angles; 10 kts.	17.78460	144.76618
0850	2250	EM302 cont. Z=3972; Line 177; 9044 coverage; 52/48 angles; 10 kts.	18.08417	144.73167
0920	2320	Ship slowing as approach Alice Springs tow site; 7 kts.		
0923	2323	EM302 cont. Z=3837; Line 178; 7509 coverage; 49/52 angles; 5 kts.	18.16967	144.72150
0927	2327	EM302 logging stopped.		
0949	2349	**T15B-09** CTD tow at Alice Springs.	18.17332	144.72120
2223	1223 Dec 7	T15B-09 end tow.	18.32163	144.67771
2232	1232	EM302 cont. Line 180; Z=3834; Heading to *Sentry* launch site	18.29633	144.68450
2316	1316	EM302 logging stopped. Alice Springs *Sentry* dive site.		
2328	1328	***Sentry* Dive 368** *Sentry* in water at Alice Springs area.	18.21431	144.70411
0900 Dec 8	2300	Ship leaving *Sentry* site to do CTD cast.		
0928	2328	**V15B-02** CTD in water (3rd from north of 4 Alice Spring targets in Hessler 1991)	18.18250	144.71967
1213	0213 Dec 8	V15B-02 on deck. Ship returning to *Sentry* tracking area.		
1512	0512	**M15B-12** Trace metal CTD in water.	18.21210	144.70669
1645	0645	M15B-12 on deck.		
1916	0916	**V15B-03** "Pogo" 18deg12.6'-12.8' in area of Alice Springs vents	18.20943	144.70682
2305	1305	V15B-03 on deck	18.21342	144.70653

Local time / date	**UTC time / date**	**R/V *Falkor* (FK151121) Event**	Latitude °N	Longitude °E
330430 Dec 9	1830	*Sentry* Dive 368 end; *Sentry* on surface.	18.21431	144.70413
0448	1848	*Sentry* on deck; USBL pole up.		
0456	1856	EM302 start logging. Line 181; Z=3693; 4442 across; 41/40 angles; 3.8 kts; noisy data heading to first waypoint	18.18167	144.71367
0501	1901	EM302 cont. Data looking better; 8 kts.		
0518	1918	EM302 cont. Ship turning onto waypoint; Line 182; 10 kts.		
0533	1933	EM302 cont. Z=3723; 8622 across; 52/52 angles; Line 182; 10 kts.	18.20000	144.73850
0716	2116	EM302 cont. Z=4483; 8814 across; 47/46 angles; Line 183; 10 kts.	18.46967	144.69933
0816	2216	**M15B-13** Trace metal CTD in water.	18.58343	144.67038
0914	2314	M15B-13 CTD on deck.		
0921	2321	Ship testing small boat.		
1026	0026 Dec 9	EM302 start logging after boat test; filled hole in previous survey after max depth reset.		
1029	0029	EM302 cont. Z=5080; 6109 across; 34/31 angles; Line 185	18.56317	144.64950
1213	0213	EM302 cont. Z=3880; 8351 across; 52/46 angles; Line 187	18.28050	144.62717
1220	0220	EM302 cont. Turning to *Sentry* recovery point.		
1306	0306	EM302 cont. Starting slow turn to south near starting point.		
1307	0307	EM302 cont. Z=3717; 8219 across; 51/49 angles; 10 kts; Line 188	18.17650	144.70967
1315	0315	EM302 logging stopped. Z=3792; 7984 across; 49/49 angles; Line 188	18.16167	144.72067
1350	0350	EM302 start logging again to cover new area. Z=3886; 9724 across; 52/49 angles; Line 189; 12 kts.	18.04267	144.75567
1418	0418	EM302 cont. Z=4324; 8889 across; 44/50 angles; Line 189; 12 kts and slowing.	17.95933	144.77150
1419	0419	EM302 logging stopped. Setting up for CTD.		
1434	0434	**T15B-10** CTD tow in water. Sothern half of Map 10 Central Trough Segment. Z=4237	17.95865	144.78067
0730 Dec 10	2130	T15B-10 CTD on deck.	17.95865	144.78067
0737	2137	EM302 start logging. Z=3798; 8190 across; 52/47 angles; 6 kts; Line 190	18.18767	144.72367
0836	2236	EM302 cont. Z=3556; Line 191; 7888 across; 51/50 angles; 9.4 kts (data looks good)	18.09200	144.80250
0908	2308	EM302 cont. Z=3848; Line 191; 8029 across; 45/46 angles; 9.1 kts (data looks good)	18.01710	144.83360
1132	0132 Dec 10	EM302 cont. Z=4020; 7203 across; 59/44; 9.6 kts; Line 193 (near south end of segment 9; data looks good)	17.67700	144.93383
1218	0218	EM302 cont. Z=4559; 7976 across; 47/43; 9.5 kts; Line 194 (at north end of segment 8)	17.59267	144.85367
1316	0316	EM302 cont. Z=3947; Line 195 (ship turning west for CTD V15B-04)	17.43567	144.84583]
1338	0338	EM302 logging stopped.		
1405	0405	**V15B-04** CTD in water.	17.43185	144.78992
1753	0753	V15B-04 CTD on deck.		
1832	0832	**M15B-14** Trace metal CTD in water. Z=4873	17.43190	144.79957

Local time / date	**UTC time / date**	**R/V *Falkor* (FK151121) Event**	Latitude °N	Longitude °E
1919	0919	M15B-14 CTD on deck.		
1948	0948	EM302 start logging. Line 197; 5.5 kts. (Will map at 12kts but slow to 10kts in new data areas).	17.44500	144.80933
2009	1009	EM302 cont. Z=4837; 2970/2650 coverage; Line 198; Turn	17.44305	144.77083
		EM302 cont. Z=4700; 2900/4100 coverage; 32/52 angles; 411/432 beams; 10 kts; Line 199 (Heading south)	17.42217	144.75800
2112	1112	EM302 cont. Z=4655; 3600/3600 coverage; 40/41 angles; 423/432 beams	17.27872	144.76192
2157	1157	EM302 cont. Z=3866; 402/432 beams; 51/52 angles; 12 kts.	17.29450	144.76350
2333	1333	EM302 cont. Z=3473; 405/432 beams; 49/49 angles	16.82467	144.82717
0005 Dec 11	1405	EM302 cont. Z=4047; 4360/3650 coverage; 368/432 beams; Line 203 (near data overlap area)		
0038	1438	EM302 cont. Z=4075; 422/432 beams; 50/46 angles; 10.8 kts	16.62333	144.83167
0210	1610	EM302 cont. Z=3700/ 3630/4190 coverage; 42/50 angles	16.39000	144.93000
0256	1656	EM302 cont. Z=3585; 4000/4000 coverage; 371/432 beams; Approaching data gap	16.26667	144.90500
0330	1730	EM302 cont. Z=4372 Turning on to data gap area.		
0340	1740	EM302 cont. Z=3911; 432/432 beams; 51/52 angles	16.22450	144.79450
0457	1857	EM302 cont. Z=3659; 7625 across; 52/50 angles; 10 kts.	16.03600	144.80267
0600	2000	EM302 cont. Z=4277; 8301 across; 50/49 angles; 10 kts; Line 208	15.86483	144.80067
0703	2103	EM302 cont. Z=4454; 8076 across; 50/41 angles; 10 kts; Line 209	15.69350	144.76102
0745	2146	EM302 logging stopped. Evaluated weather for *Sentry*.		
0800	2200	EM302 start logging while transit to CTD M15B-15 site.		
1000	0000 Dec 11	EM302 cont. Z=3637; 6917 across; 49/46 angles; 11.5 kts; Line 212	15.24167	144.81717
1213	0213	EM302 cont. Z=2656; 6887 across; 60/56 angles; 11.5 kts; Line 215	14.85450	144.99867
1326	0326	EM302 cont. Z=2161; 5958 across; 60/60 angles; 9 kts; Line 216	14.63417	145.10017
1341	0341	EM302 logging stopped.		
1411	0411	**M15B-15** Trace metal CTD cast in water.	14.60015	145.11692
1510	0510	M15B-15 CTD on deck.		
1518	0518	EM302 start logging. Z=2098; 7090 across; 63/65 angles; 6 kts; Line 217; transit to NW Rota	14.60367	145.11317
1703	0703	EM302 cont. Z=2528; 3240/3165 coverage; 55/57 angles; 382/432 beams	14.59983	144.87183
1724	0724	EM302 cont. Z=2041; 3140/3333 coverage; 57/62 angles	14.59975	144.81150
1739	0739	**V15B-05** CTD cast. EM302 multibeam logging stopped; Line 219.	14.59840	144.77643
1808	0808	EM302 Water Column start logging; Line 220. Summit of NW Rota-1.		
1856	0856	V15B-05 CTD on deck.		
1858	0858	EM302 cont. Line 221 WCD.		
1902	0902	EM302 cont. Logging WCD and bathy; Line 221; turning NW		
1907	0907	EM302 cont. Line 222		
1916	0916	EM302 cont. Line 223; Z=1310; stopped logging WCD; logging bathy.		

Local time / date	**UTC time / date**	**R/V *Falkor* (FK151121) Event**	Latitude °N	Longitude °E
1954	0954	EM302 cont. Z=3318; 3920/3790 coverage; 422/432 beams; 50/52 angles; 9.8 kts.	14.68550	144.72267
2230	1230	EM302 cont. Z=3740; 4525/3600 coverage; 414/432 beams; Line 226; 11.7 kts.	15.13300	144.60867
2256	1256	EM302 cont. Z=3675; 4440/3700 coverage; 52/50 angles; 11.3 kts.	15.20810	144.58967
0015 Dec 12	1415	EM302 cont. Z=4413; 3930/3265 coverage; 51/46 angles; Line 227	15.45417	144.52717
0017	1417	EM302 logging stopped; Line 228		
0055	1455	**S369 *Sentry* dive** begin. Site of high particles north of S367. Z=4143	15.51000	144.64667
0856	2256	Ship moving south for trace metal CTD during *Sentry* dive.		
0914	2314	**M15B-16** Trace metal CTD in water.	15.47991	144.50266
0959	2359	M15B-16 on deck.		
1237	0237 Dec 12	**M15B-17** Trace metal CTD in water.	15.49933	144.50727
1323	0323	M15B-17 CTD on deck.		
1505	0505	**V15B-06** CTD cast at ORP anomaly site of *Sentry* dive S-367.	15.42442	144.50295
1835	0835	V15B-06 CTD on deck. (Bottle #N26 leaking)	15.42380	144.50368
0315 Dec 13	1715	*Sentry* on deck; end dive S-369; Z=4035	15.51117	144.52350
0353	1753	EM302 start logging. Line 229; Z=4426; 413/432 beams; 12.2 kts; mapping to start of tow-yo after *Sentry* recovery.	15.56917	144.53833
0511	1911	EM302 cont. Z=3722; Line 230; 6886 across; 45/52 angles; 12 kts.	15.82917	144.58717
0700	2100	EM302 cont. Z=3502; Line 232; 7751 across; 51/52 angles; 12 kts	16.19367	144.65500
0810	2210	EM302 cont. Z=3471; Line 233; 7580 across; 49/48 angles; 12 kts	16.42683	144.69867
0951	2351	EM302 cont. Z=3443; Line 234; 7485 across; 49/49 angles; 12 kts	16.75867	144.76067
1127	0127 Dec 13	EM302 cont. Z=3891; Line 236; 8433 across; 50/52 angles; 12 kts.	17.07333	144.81950
1219	0219	EM302 cont. Z=3649; Line 237; 8015 across; 47/52 angles; 12 kts.	17.24483	144.85167
1317	0317	EM302 cont. Z=3866; Line 238; 8208 across; 45/52 angles; 12 kts.	17.44300	144.88883
1420	0420	EM302 cont. Z=4190; Line 239; 7254 across; 43/45; 9 kts.		
1443	0443	**T15B-11** CTD in water (Map 9).	17.67238	144.93178
0550 Dec 14	1950	T15B-11 CTD on deck.	17.88582	144.89585
0553	1953	EM302 start logging. 56nm transit south to Map 8 CTD tow-yo. Z=4079; Line 240; 8351 across; 52/48 angles; 8 kts.	17.88183	144.89667
0637	2037	EM302 cont. Z=4018; Line 240; 8104 across; 51/52 angles; 12 kts.	17.76383	144.89617
0805	2205	EM302 cont. Z=3695; Line 242; 6998 across; 47/41 angles; 12 kts.	17.47017	144.89433
1025	0025 Dec 14	EM302 cont. Z=3233; Line 244; 7341 across; 51/52 angles; 12 kts.	17.00017	144.89117
1052	0052	EM302 cont. Z=3370; Line 244; 7971 across; 52/52 angles; 10 kts.	16.90583	144.88867
1101	0101	EM302 logging stopped.		
1120	0120	**T15B-12** CTD tow in water (map 8).	16.88955	144.89073

Local time / date	**UTC time / date**	**R/V *Falkor* (FK151121) Event**	Latitude °N	Longitude °E
2333	1333	T15B-12 CTD on deck (large plume found).	17.04811	144.84574
0033 Dec 15	1433	***Sentry* 370** dive in water to map area of large plume and to conduct photo survey.	16.95822	144.86490
1555	0555 Dec 15	**V15B-07** CTD cast in water.	16.96580	144.86744
1852	0852	V15B-07 CTD on deck.		
0731 Dec 16	2131	*Sentry* off bottom.		
0900	2300	End S-370. *Sentry* on deck.	16.95941	144.87262
0912	2312	EM302 start logging. Mapping edge back to Guam. Line 246.		
1050	0050 Dec 16	EM302 cont. Z=3854; Line 247; 8792 across; 52/52 angles; 10 kts.	16.74717	144.95600
1214	0214	EM302 cont. Z=3640; Line 249; 7223 across; 43/50 angles; 10 kts.	16.53033	144.96567
1406	0406	EM302 cont. Z=3665; Line 250; 7811 across; 52/52 angles; 11 kts.	16.25233	144.94133
1611	0611	EM302 cont. Z=3684; Line 252; 7570 across; 50/51 angles; 10 kts.	15.93750	144.86350
1032 Dec 17	2232	EM302 logging stopped. EOL 269		
1800 Dec 17	0800 Dec 17	Arrived in Guam.		

Mariana Back-arc Segment Nomenclature

Bill Chadwick and Susan Merle

There was no previous naming convention for the segments of the Mariana back-arc. Before the 2015 *Falkor* expedition, we created a series of maps that were numbered 1 through 10, from south to north in our survey area, that showed bathymetry and depth profiles along the axis of the back-arc to aid in planning our at-sea operations. The boundaries of these maps were somewhat arbitrary, but the map names became a quick shorthand for communicating specific locations along the back-arc during the cruise (and also on the Schmidt cruise web site). However, after the cruise we realized that a better naming scheme was needed that related to the physical segmentation of the back-arc spreading axis and referred to real-world coordinates. We also refined our drawing of where the back-arc spreading axis is located and how it is segmented after the cruise. We decided to name the major back-arc segments by latitude, based on either their geographic or magmatic centers (the latter referring to the shallowest parts of back-arc segments). For example, what we referred to previously as "Map 1" would now be called "the segment centered at 12.8°N" (long version), or "12.8°N Segment", for short.

Geological Feature Nomenclature		
Mariana Back-Arc Ridge Segments		
Old Map Name	**Short Segment Name**	**Long Segment Name**
Map 1	12.8°N Segment	Segment centered at 12.8°N
Map 2	13.3°N Segment	Segment centered at 13.3°N
Map 3	13.9°N Segment	Segment centered at 13.9°N
Map 4	14.5°N Segment	Segment centered at 14.5°N
Map 5 (two segments)	15.1°N Segment	Segment centered at 15.1°N
	15.5°N Segment	Segment centered at 15.5°N
Map 6	16.1°N Segment	Segment centered at 16.1°N
Map 7	16.5°N Segment	Segment centered at 16.5°N
Map 8	17.0°N Segment	Segment centered at 17.0°N
Map 9	17.8°N Segment	Segment centered at 17.8°N
Map 10	18.2°N Segment	Segment centered at 18.2°N
Mariana Back-Arc Vent Fields and Features		
Old Site Name	**New Site Name**	**Long Site Name**
Map 1 Vent Fields also known as Snail Vent	Snail Vent	-
Map 4 vent field	Vent field at 14.5°N	-
Map 5 vent field	Vent field at 15.5°N	-
Map 5 lava flows	Lava flows at 15.4°N	-
Map 7 vent field	Vent field at 16.5°N	-
Map 8 vent field	Vent field at 17.0°N	-
Map 10 vent field (Alice Springs)	Alice Springs vent fields at 18.2°	Alice Springs vent fields at 18.2°N (Alice Springs, Illium, and Burke – see below)
Map 10 vent field (Central Trough)	Central Trough vent field at 18.0°N	Central Trough vent field at 18.0°N

In the future, the long version of the segment names could be used for clarity, or at first to define and explain the naming scheme. Thereafter, the short version of the segment names could be used for brevity. According to this new naming scheme, the "Geological Feature Nomenclature" table shows old/new names for the major segments of the Mariana back-arc, tentative names for the vent fields and lava flows that were discovered during the cruise, and some previously known vent sites. We may come up with better vent field names after our ROV dives in the fall of 2016.

Alice Springs vent field nomenclature

The Alice Springs vent field was discovered in 1987 during a series of Alvin dives. It is located near the crest of the 18.2°N segment. However, there is potential confusion because "Alice Springs" is both the name of one specific vent field and a collection of three vents within a radius of several km. The following nomenclature and locations come from two published papers by Hessler and Martin (1989) and Hessler et al. (1991). There are the 3 separate vent fields commonly lumped together under the name "Alice Springs", and a fourth vent field "Central Trough" located ~20 km to the south.

Long	Lat	LonDeg	LonMin	LatDeg	Latmin	Vent site name
144.707183	18.209983	144	42.431	18	12.599	Alice Springs vent field
144.720067	18.182467	144	43.204	18	10.948	Snail Pits - part of Burke vent field
144.720167	18.181950	144	43.210	18	10.917	Anemone Heaven - part of Burke vent field
144.707083	18.213417	144	42.425	18	12.805	Illium vent field
144.753333	18.046667	144	45.200	18	02.800	Central Trough

For example, the Mariana Trench Marine National Monument (MTMNM) lists "Alice Springs" as one of the Vents Unit sites located at 18° 12.0'N, 144° 30.0'E (which is clearly an erroneous longitude). "Central Trough" is listed as a separate MTMNM Vents Unit site located on the same back-arc segment. The location of the Central Trough vent field is listed as 18° 01'N, 144 45.0'E in the MTMNM, but Hessler et al., (1991) list the vent field location as 18° 02.8'N, 144° 45.2'E.

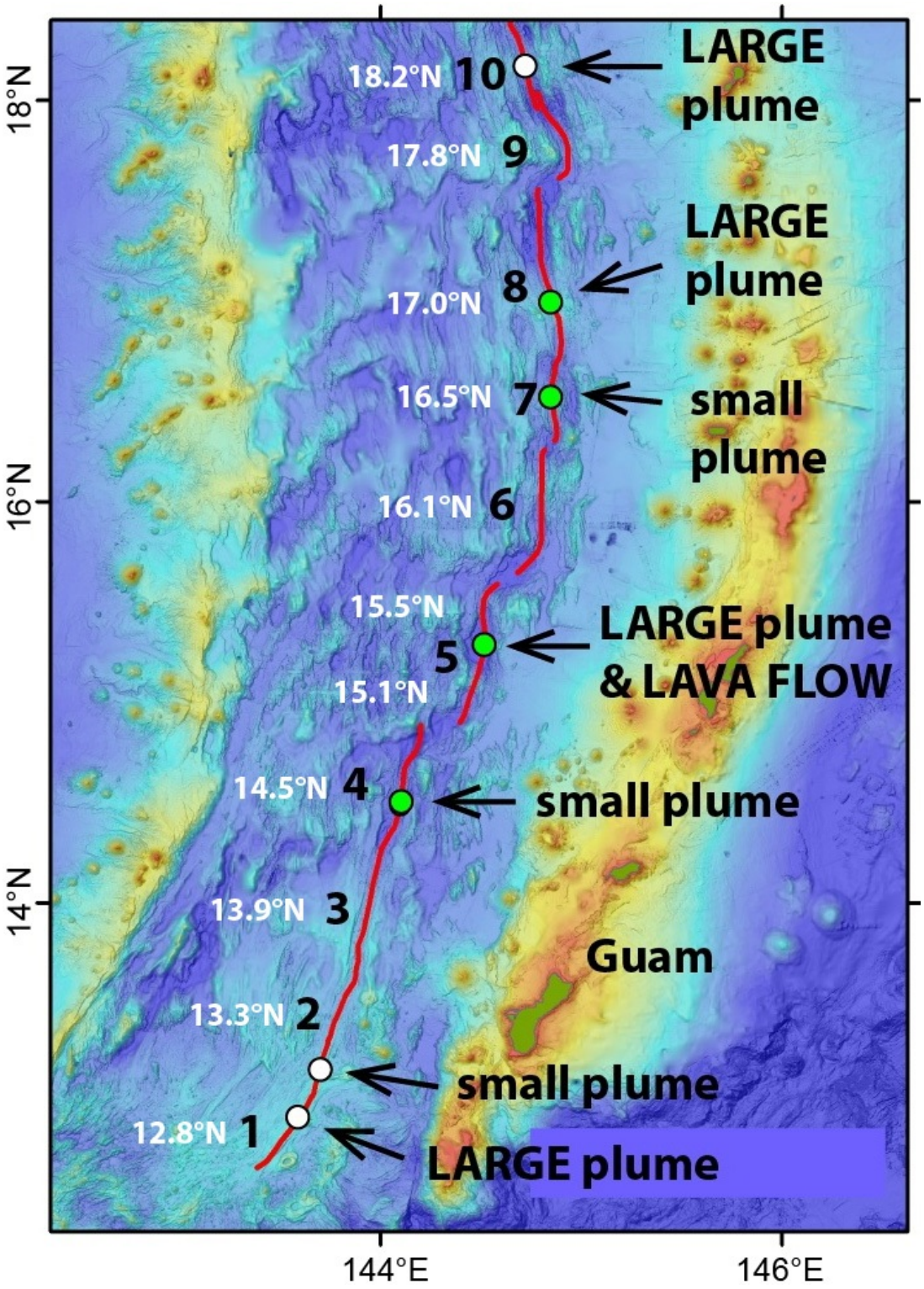

Figure relating arbitrary map designations (Maps 1-10) and new back-arc segment nomenclature, and summarizing where we found new hydrothermal sites along the Mariana back-arc spreading center. New areas of hydrothermal venting discovered during the expedition are shown by green dots; white dots are previously known sites in the south and north of the area.

Maps showing designations used at sea and new back-arc segment nomenclature

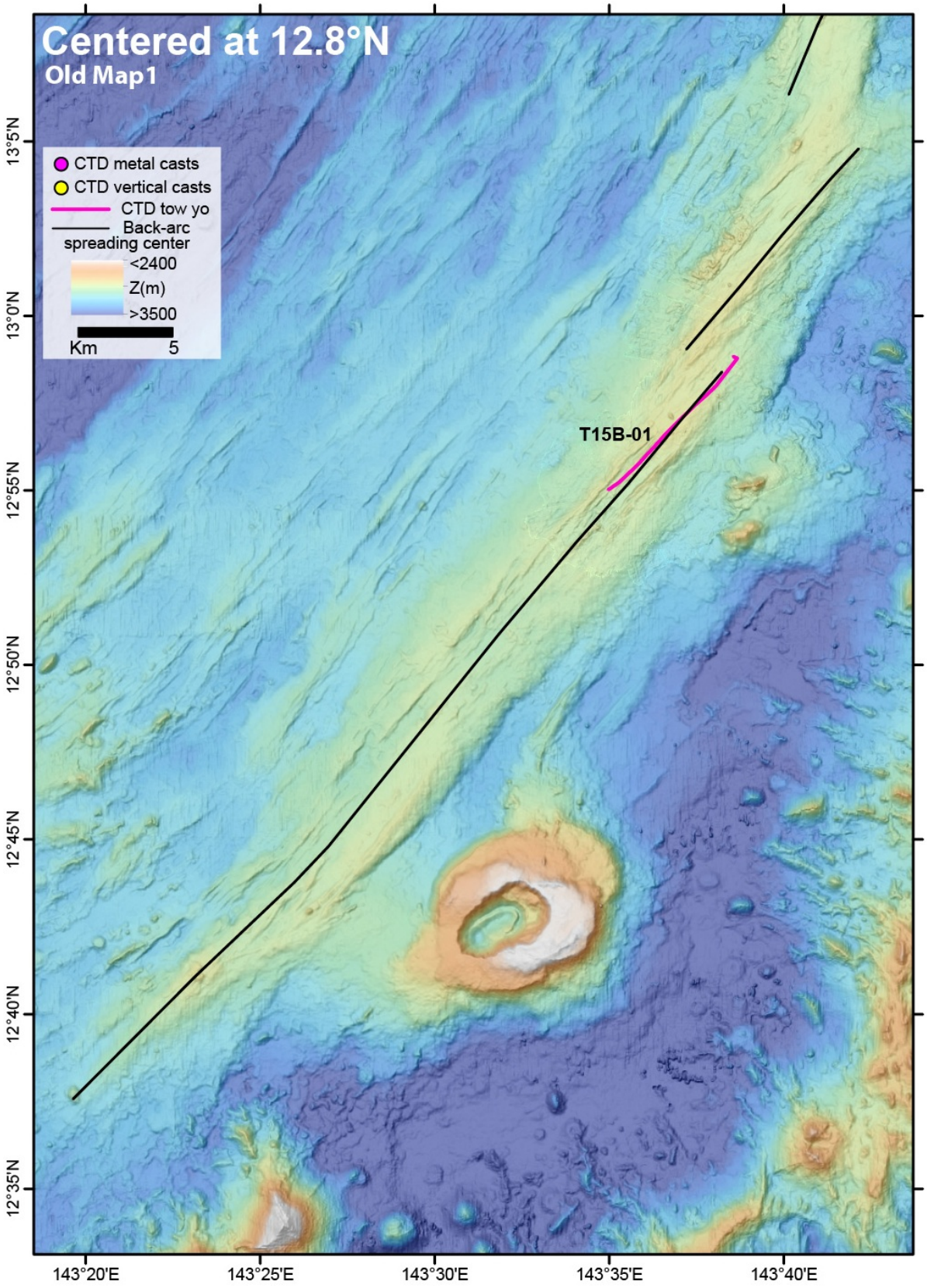

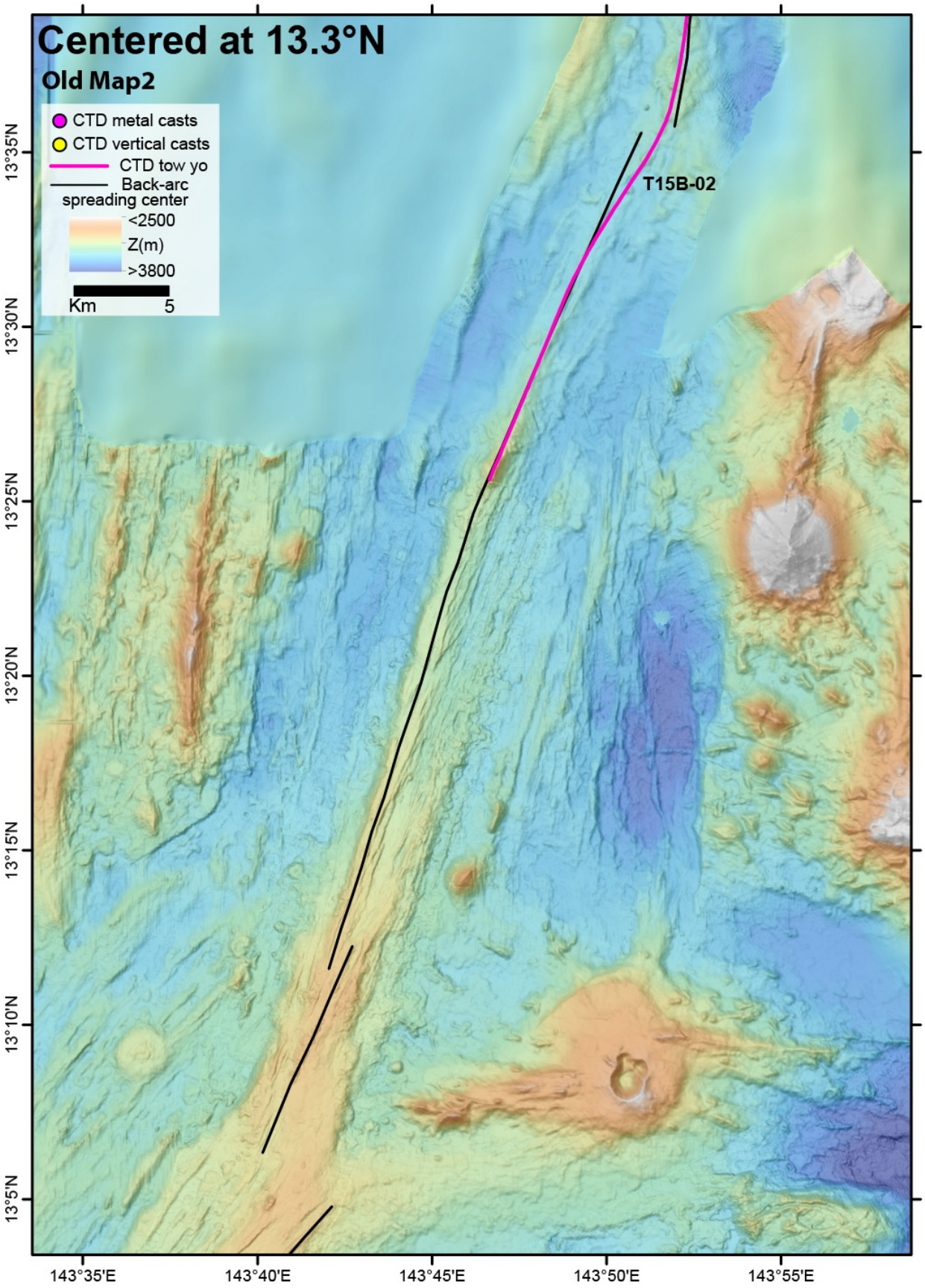
Centered at 13.3°N
Old Map2
CTD metal casts
CTD vertical casts
CTD tow yo
Back-arc spreading center
<2500
Z(m)
>3800
Km
5
T15B-02
13°35'N
13°30'N
13°25'N
13°20'N
13°15'N
13°10'N
13°5'N
143°35'E
143°40'E
143°45'E
143°50'E
143°55'E

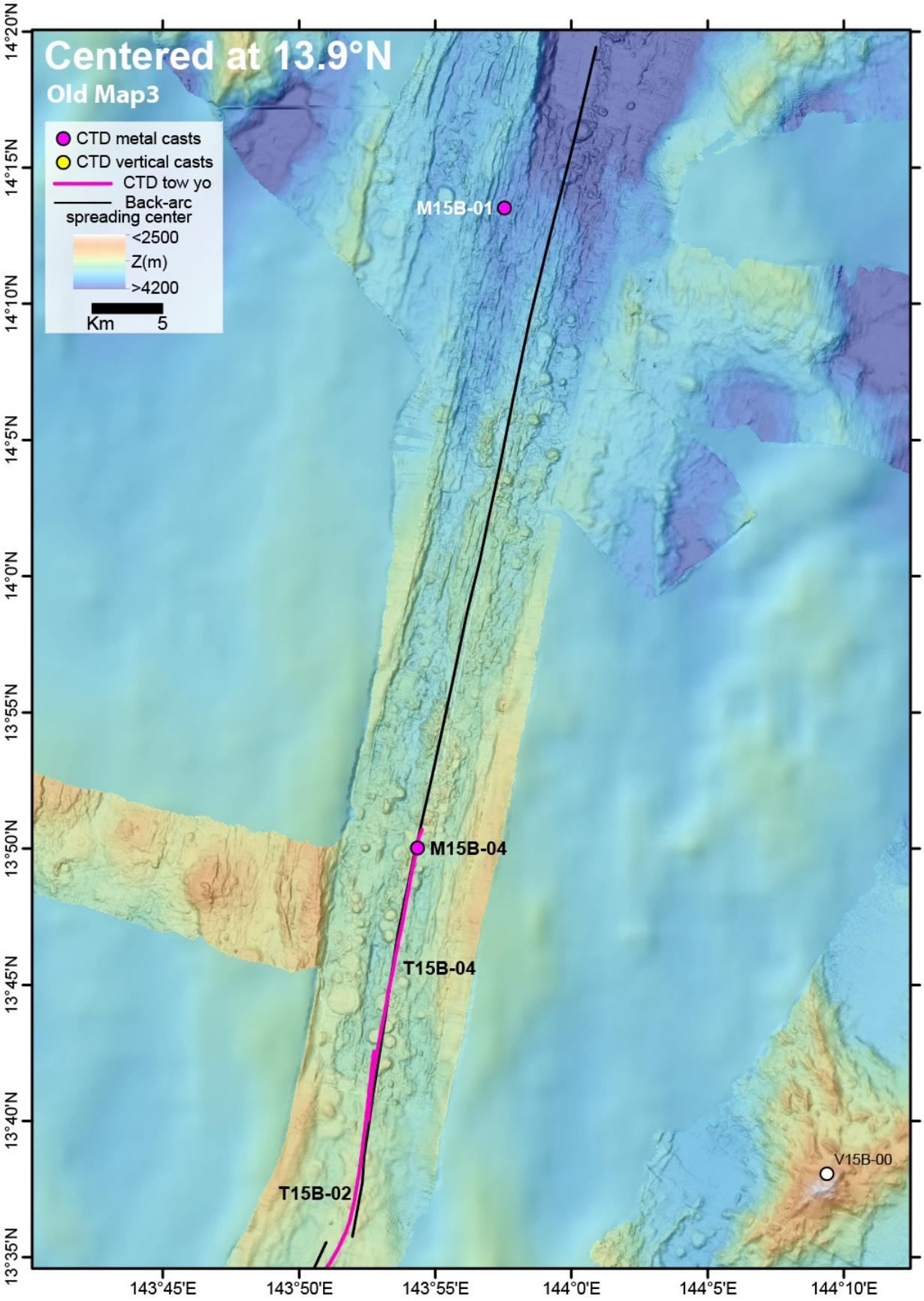
Centered at 13.9°N
Old Map3
CTD metal casts
CTD vertical casts
CTD tow yo
Back-arc spreading center
<2500
Z(m)
>4200
Km 5
M15B-01
M15B-04
T15B-04
T15B-02
V15B-00
14°20'N
14°15'N
14°10'N
14°5'N
14°0'N
13°55'N
13°50'N
13°45'N
13°40'N
13°35'N
143°45'E
143°50'E
143°55'E
144°0'E
144°5'E
144°10'E

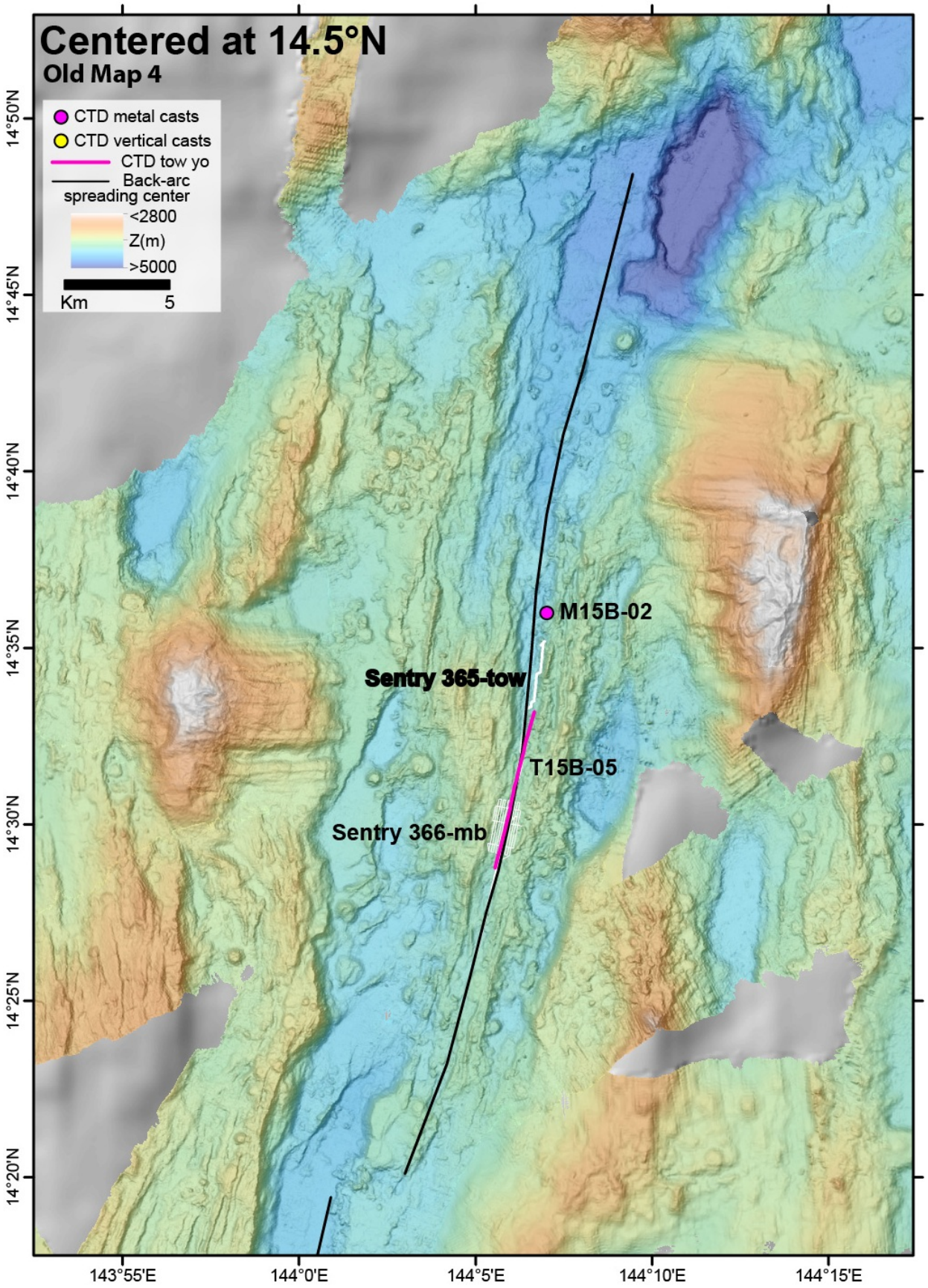
Centered at 14.5°N
Old Map 4
CTD metal casts
CTD vertical casts
CTD tow yo
Back-arc spreading center
<2800
Z(m)
>5000
Km
5
M15B-02
Sentry 365-tow
T15B-05
Sentry 366-mb
14°50'N
14°45'N
14°40'N
14°35'N
14°30'N
14°25'N
14°20'N
143°55'E
144°0'E
144°5'E
144°10'E
144°15'E

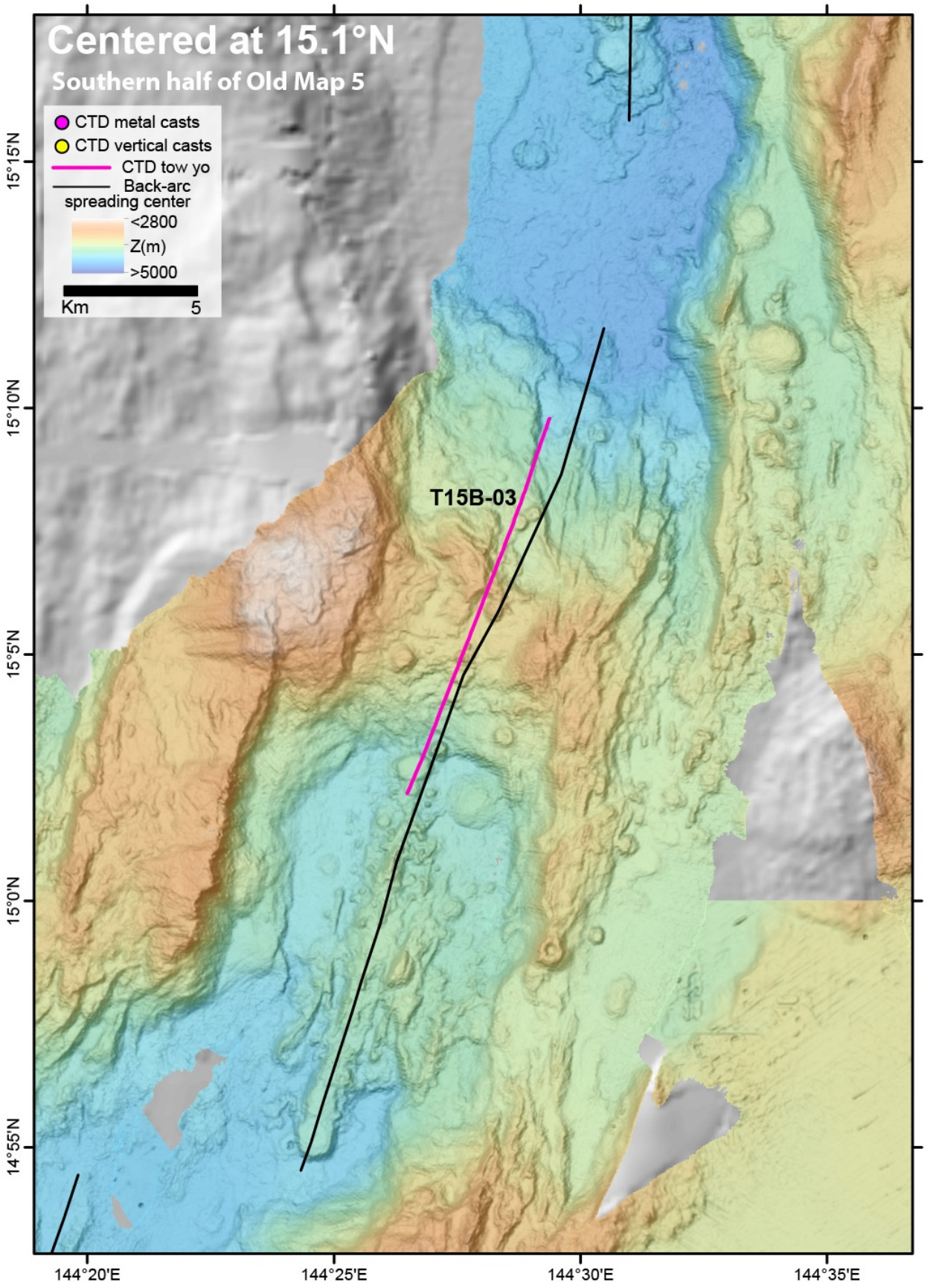
Centered at 15.1°N
Southern half of Old Map 5
CTD metal casts
CTD vertical casts
CTD tow yo
Back-arc spreading center
<2800
Z(m)
>5000
Km
5
T15B-03
15°15'N
15°10'N
15°5'N
15°0'N
14°55'N
144°20'E
144°25'E
144°30'E
144°35'E

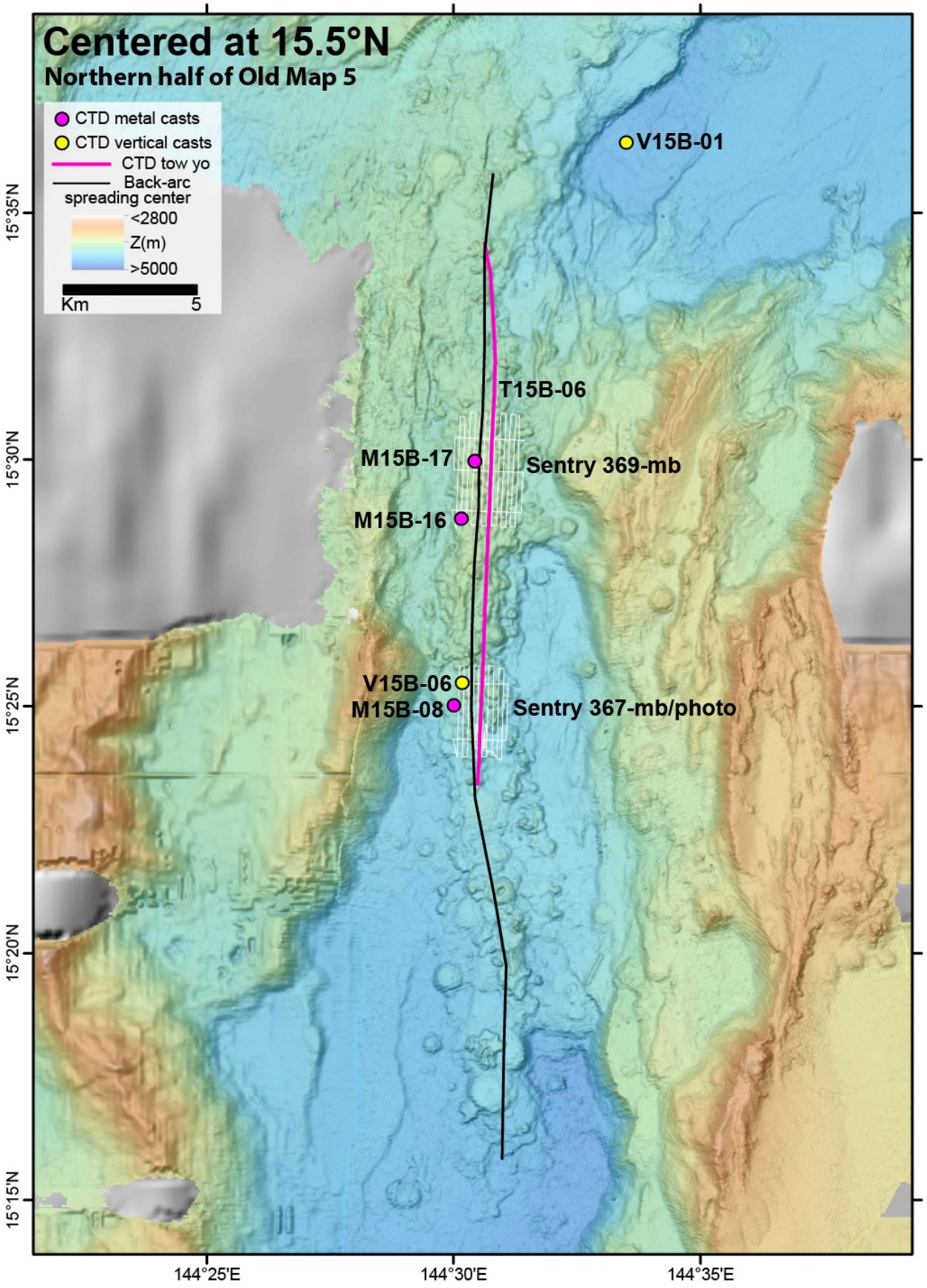
Centered at 15.5°N
Northern half of Old Map 5
CTD metal casts
CTD vertical casts
CTD tow yo
Back-arc spreading center
<2800
Z(m)
>5000
Km
5
V15B-01
T15B-06
M15B-17
Sentry 369-mb
M15B-16
V15B-06
M15B-08
Sentry 367-mb/photo
15°35'N
15°30'N
15°25'N
15°20'N
15°15'N
144°25'E
144°30'E
144°35'E

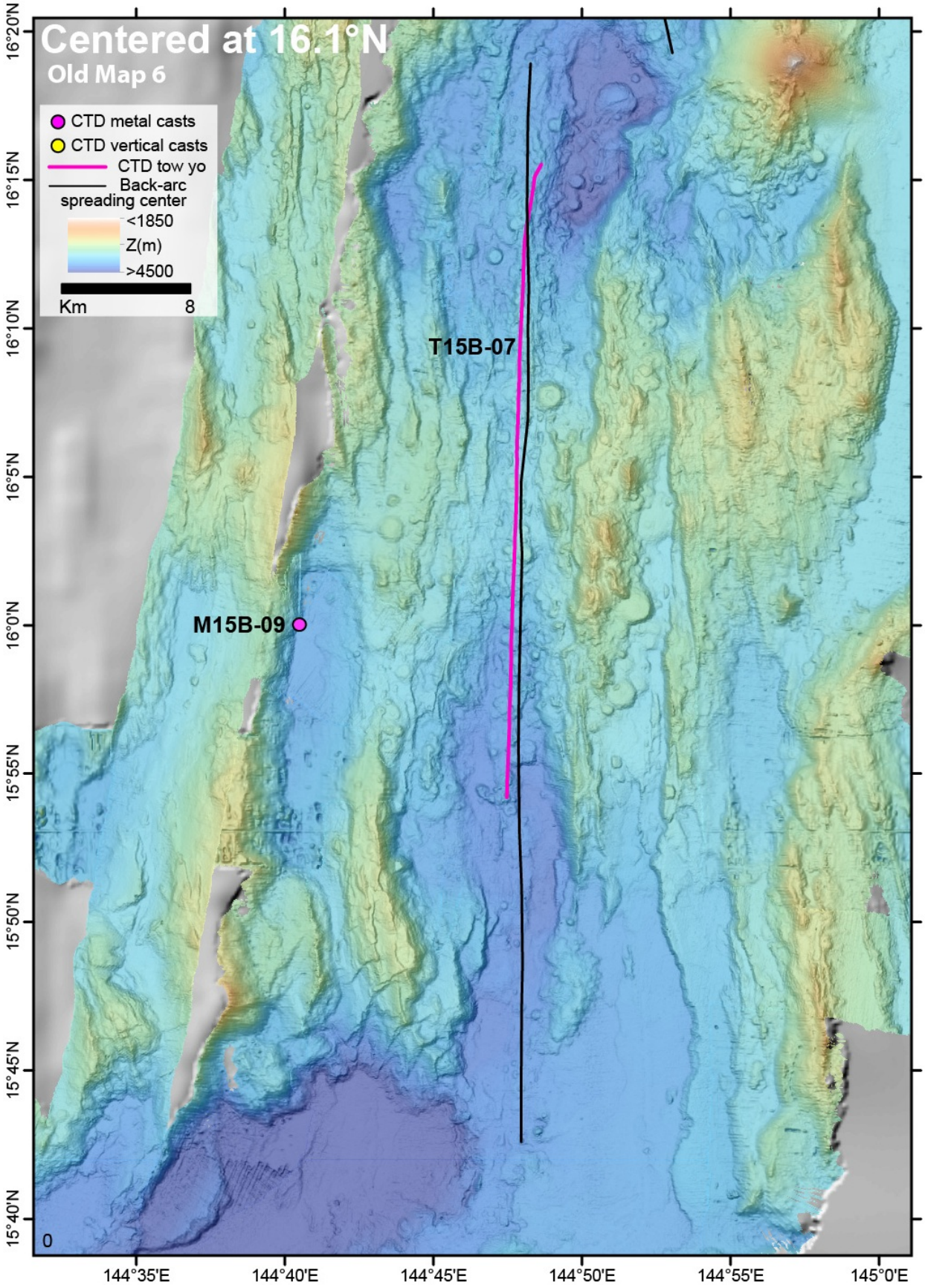
Centered at 16.1°N
Old Map 6
CTD metal casts
CTD vertical casts
CTD tow yo
Back-arc spreading center
<1850
Z(m)
>4500
Km
8
T15B-07
M15B-09
0
16°20'N
16°15'N
16°10'N
16°5'N
16°0'N
15°55'N
15°50'N
15°45'N
15°40'N
144°35'E
144°40'E
144°45'E
144°50'E
144°55'E
145°0'E

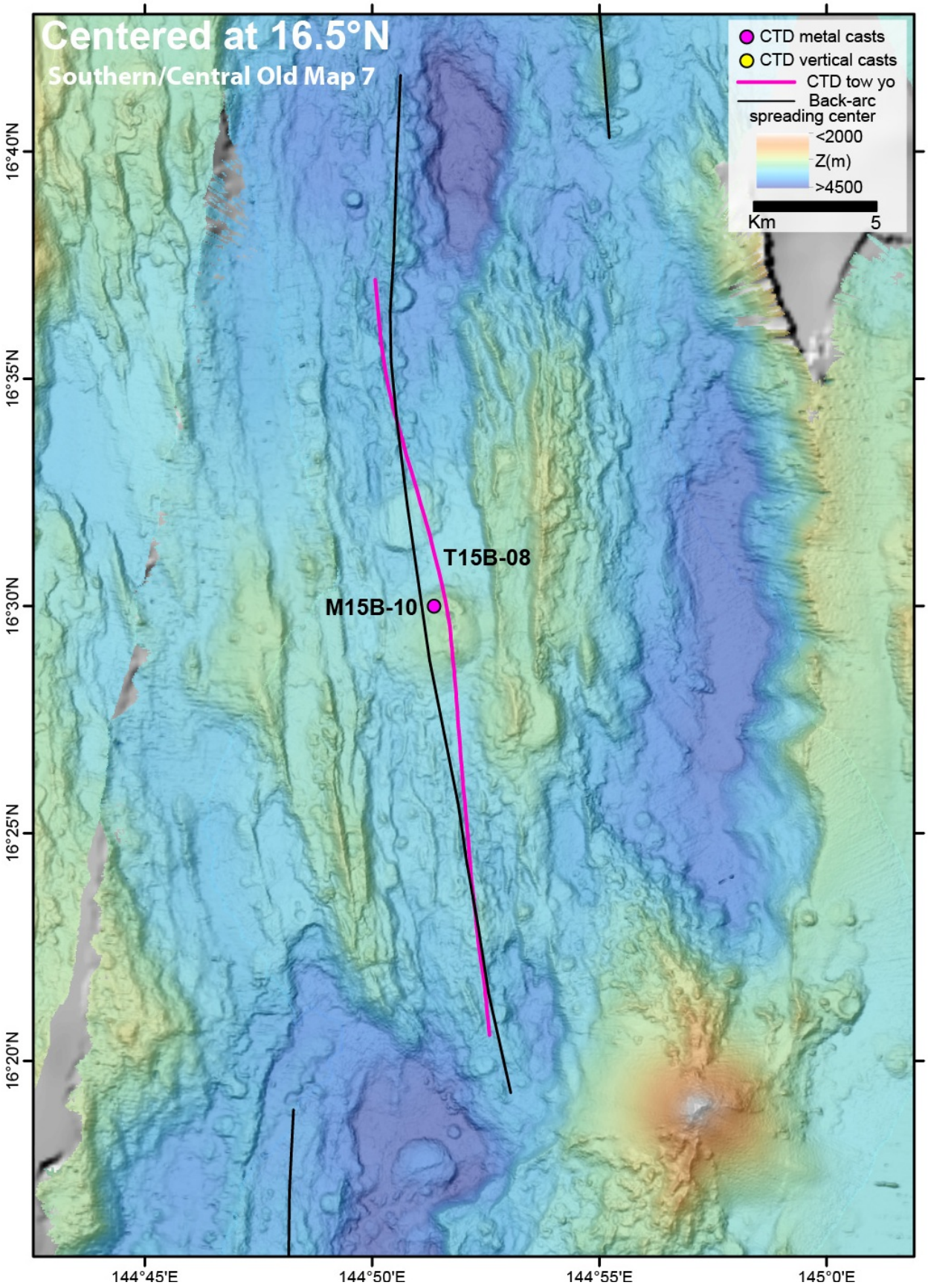
Centered at 16.5°N
Southern/Central Old Map 7
CTD metal casts
CTD vertical casts
CTD tow yo
Back-arc spreading center
<2000
Z(m)
>4500
Km
5
T15B-08
M15B-10
16°40'N
16°35'N
16°30'N
16°25'N
16°20'N
144°45'E
144°50'E
144°55'E
145°0'E

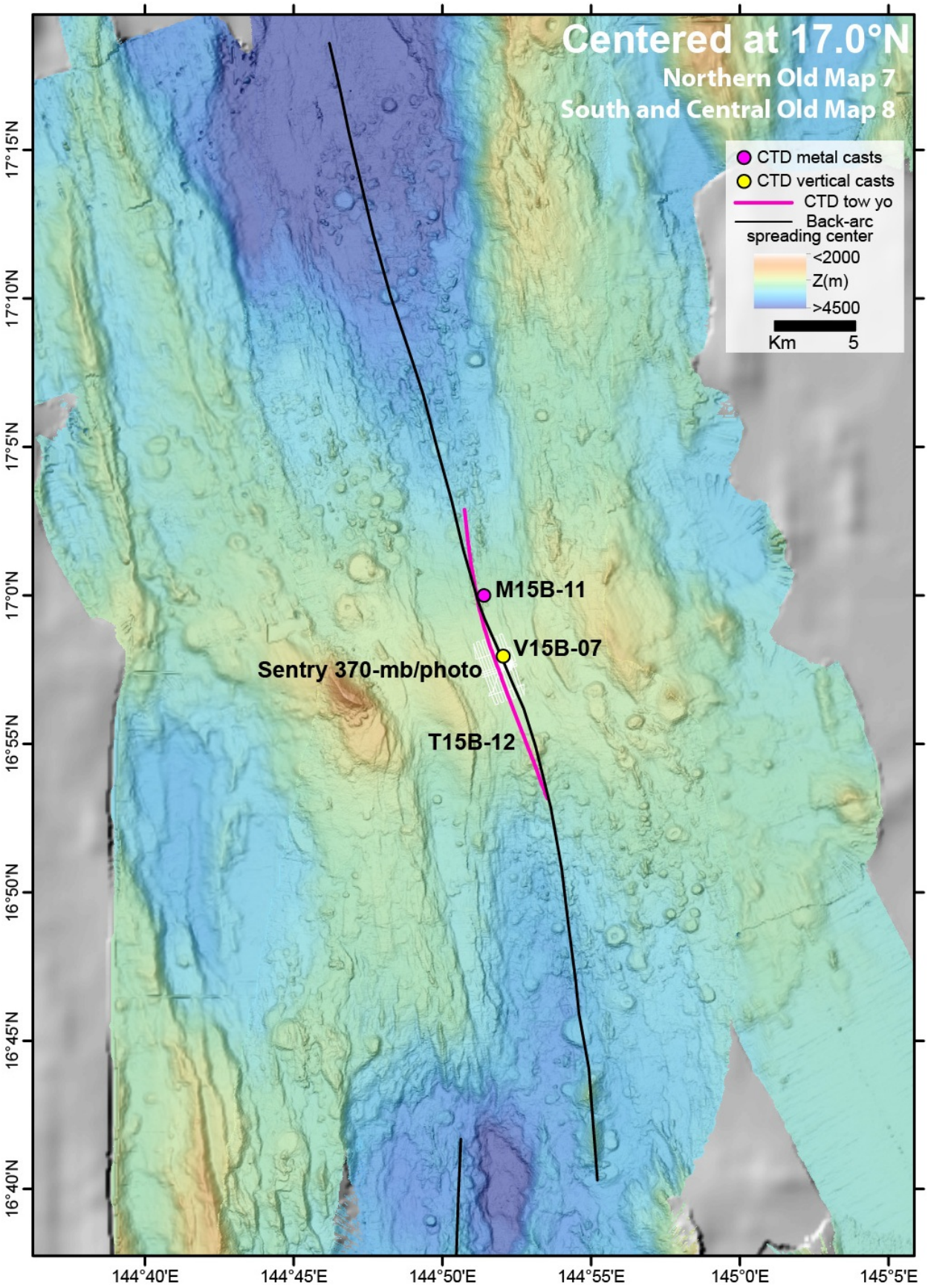
Centered at 17.0°N
Northern Old Map 7
South and Central Old Map 8
CTD metal casts
CTD vertical casts
CTD tow yo
Back-arc spreading center
<2000
Z(m)
>4500
Km 5
M15B-11
V15B-07
Sentry 370-mb/photo
T15B-12
17°15'N
17°10'N
17°5'N
17°0'N
16°55'N
16°50'N
16°45'N
16°40'N
144°40'E
144°45'E
144°50'E
144°55'E
145°0'E
145°5'E

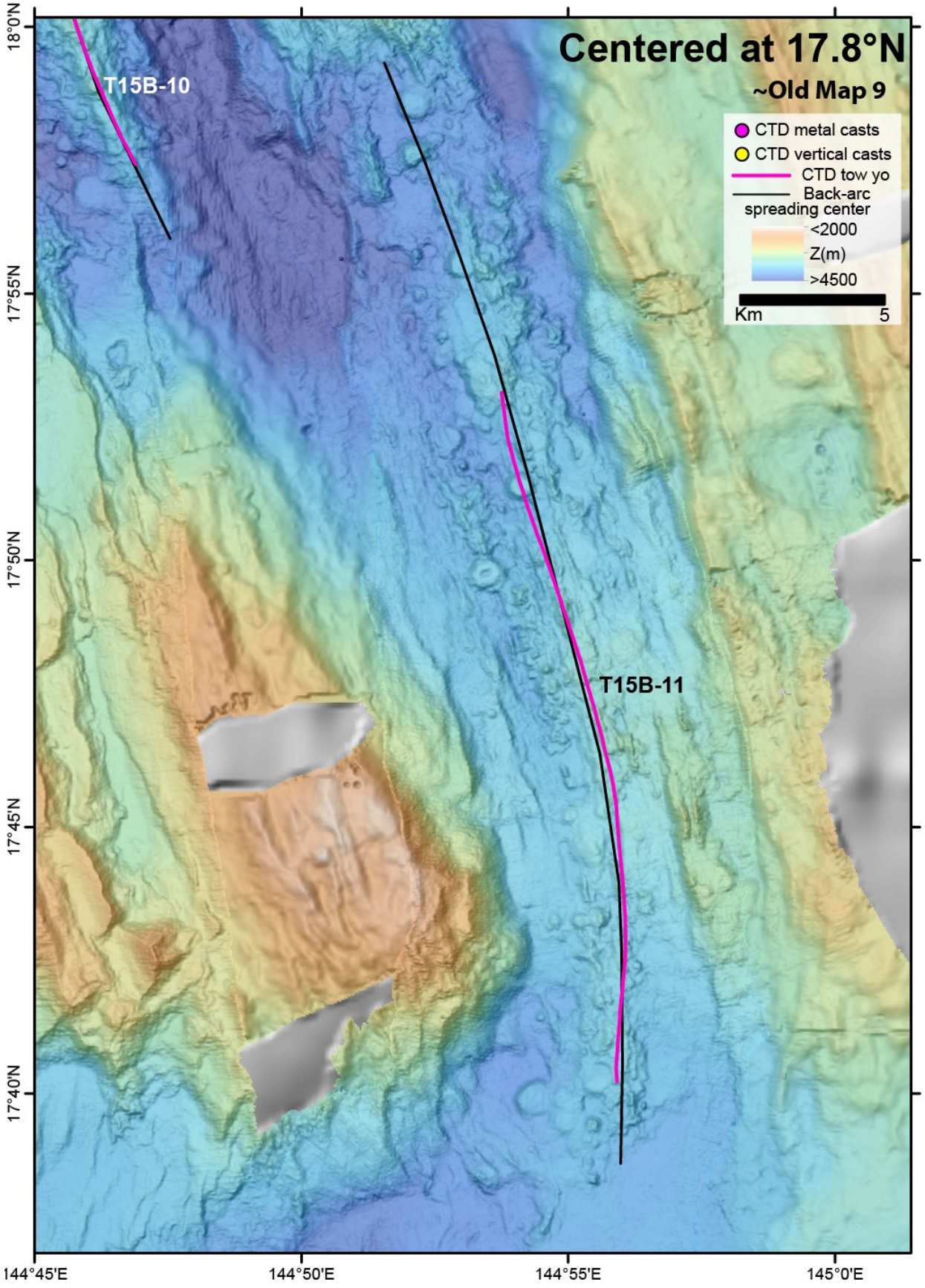
Centered at 17.8°N
~Old Map 9
T15B-10
T15B-11
CTD metal casts
CTD vertical casts
CTD tow yo
Back-arc spreading center
<2000
Z(m)
>4500
Km
5
18°0'N
17°55'N
17°50'N
17°45'N
17°40'N
144°45'E
144°50'E
144°55'E
145°0'E

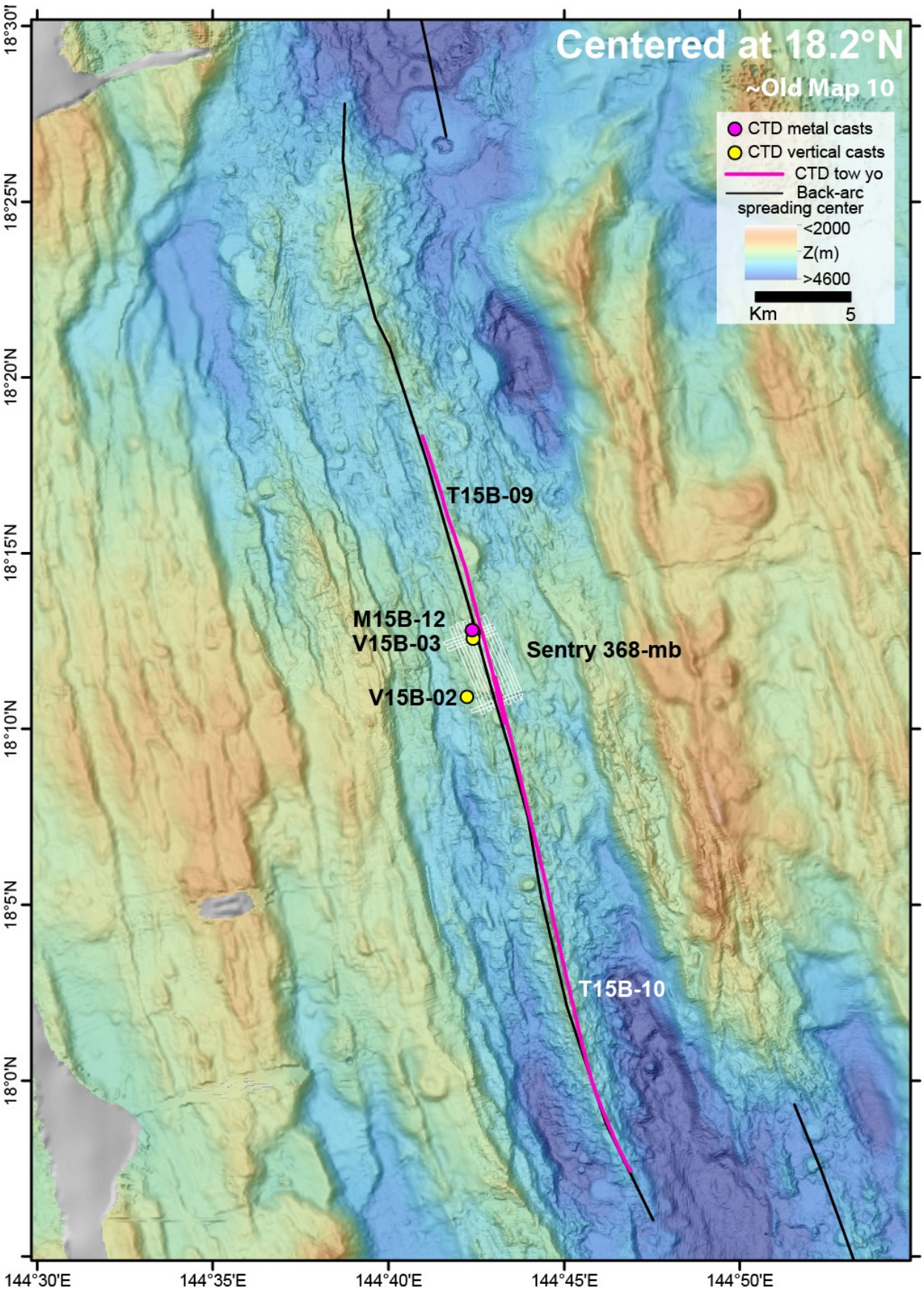
Centered at 18.2°N
~Old Map 10
CTD metal casts
CTD vertical casts
CTD tow yo
Back-arc spreading center
<2000
Z(m)
>4600
Km
5
T15B-09
M15B-12
V15B-03
Sentry 368-mb
V15B-02
T15B-10
18°30'N
18°25'N
18°20'N
18°15'N
18°10'N
18°5'N
18°0'N
144°30'E
144°35'E
144°40'E
144°45'E
144°50'E

CTD Operations Summary – Hydrothermal Plume Exploration

Sharon Walker and Edward Baker

The southern and central portions of the Mariana back-arc were explored for hydrothermal activity using a Seabird 9*plus* CTD with auxiliary sensors for optical backscatter, oxidation-reduction potential (ORP), and altitude above the seafloor. The system included two high sensitivity Seapoint turbidity meters (0-5 NTU), two PMEL ORP sensors (-500 to +500 mv), and one Valeport VA-500 altimeter (0-100 m range). Twelve (12) along-axis CTD tows were completed and followed up with four (4) vertical casts to more thoroughly characterize plume chemistry. Two (2) additional vertical casts were done in deep basins along-axis between axial highs and did not detect hydrothermal plumes (V15B-01 and V15B-04). Finally, one (1) vertical cast (V15B-05) was done over the summit of NW Rota-1 volcano. No significant plume signals were identified indicating that it was not erupting and at a low-level of hydrothermal activity. Hydrothermal anomalies were detected at 5 separate locations along the southern and central Mariana back-arc (including two previously known sites), and possibly 3 other sites:

1) Mariana back-arc segment centered at 12.8°N (Map 1): Tow T15B-01 revisited the previously known "Snail" site on the southern Mariana back-arc. Particle and ORP anomalies extended from ~2550 m to the seafloor in multiple layers from the southern end of the tow to the latitude of the Snail vent (12°57.2'N = 12.9533°N). The most intense particle anomaly ($dNTU_{max}$ = 0.030) was located at ~2590 m near 12°55.9'N (12.9317°N; sample Niskin#2). ORP anomalies were generally correlated with particle anomalies, however the most intense ORP anomaly (ΔE_{max} = -23 mv; dE/dt_{max} = -3.4 mv/5sec) was located 170 m deeper (~2760 m) and offset slightly to the north (12°56.06'N = 12.9343°N; ; sample Niskin#3) of the maximum particle anomaly. Figure 1_{CTD} shows results for T15B-01 along with the corresponding portion of T03A-01 (2003 R/V Thompson cruise) for comparison.

2) Mariana Back-arc Segment centered at 14.5°N (Map 4): AUV *Sentry* was used in "tow-yo" mode during *Sentry*-365 for an along-axis survey of this segment. A weak particle anomaly ($dNTU_{max}$ = 0.012) with associated ORP signals (ΔE_{max} = -1.7 and -2.3 mv) occurred between 14°29.64'N and 14°30.18'N (14.4440-14.5030°N) at 3750-3800 m water depth. Two days later, CTD tow T15B-05 sampled the plume maximum at a depth of 3720 m between 14°28.80'N and 14°29.34'N (14.4800-14.4890°N), about 1.5-2 km south of the *Sentry*-365 location ($dNTU_{max}$ = 0.008; no significant ORP anomaly). *Sentry*-366 mapped an area of the seafloor in the region of this plume at an altitude of ~70 mab, but no significant particle or ORP anomalies were identified. Additional analyses will need to be done to see if there were any temperature anomalies. Figure 2_{CTD} shows data from both *Sentry*-365 and CTD tow T15B-05.

3) Mariana Back-arc Segment centered at 15.5°N (Map 5): Two distinct regions of hydrothermal activity were mapped by CTD tow T15B-06. The southern half of the tow (south

of 15°28'N (15.4667°N) was characterized by a weak particle anomaly (dNTU < 0.005) but strong ORP anomalies (ΔE_{max} = -39 mv). The northern half of the tow mapped more intense particle plumes ($dNTU_{max}$ = 0.032), but only the southern section had concurrent ORP anomalies (ΔE_{max} = -14 mv), see Figure 3_{CTD}. The tow was followed by dives *Sentry*-367, for high-resolution mapping (70 mab) and a near-bottom (~5 mab) photo survey in the area of the particle-poor/ORP-intense plume, and *Sentry*-369 for a mapping survey (70 mab) in the area of the particle-enriched plumes. MAPR data from these dives, combined with the CTD tow, provide a 3-dimensional view of the plumes in the water column (see MAPR data section and Fledermaus scene file). Vertical cast V15B-06 was located in the area of the new lava flow.

4) Mariana Back-arc Segment centered at 18.2°N (Map 10): This segment is host to the previously known (listed from north to south) Ilium, Alice Springs, Burke and Central Trough vent sites, first discovered in 1987 (Hessler, et al., 1989). CTD tows T15B-09 and T15B-10 systematically surveyed the axial high of this segment from 17°57.5'N to 18°19.3'N (17.9583-18.3217°N). Hydrothermal signals were limited to the areas of the previously-known vents, confirming these sites are still active nearly 30 years later. Plumes over the Central Trough and northernmost Alice Springs and Ilium locations were particle-poor (virtually no noticeable dNTU) but had significant ORP anomalies (ΔE_{max} = -4 mv). The plume over the Burke vent site location (18°10.9'N = 18.1817°N) was defined by both particle and ORP anomalies ($dNTU_{max}$ = 0.010; ΔE_{max} = -11 mv) at 3000-3300 m (600-700 m above the seafloor), with the ORP signal persisting to within 120 m of the seafloor (Figure 4_{CTD}). Dive *Sentry*-368 conducted a mapping survey (70 mab) in this area. Temperature spikes and ORP anomalies correspond very closely to the previously known vent site locations (see MAPR data section and Fledermaus scene file). Vertical cast V15B-02 sampled the plume over the Burke vent site; V15B-03 obtained profiles over the Alice Springs and Ilium vents.

5) Mariana Back-arc Segment centered at 17.0°N (Map 8): A relatively intense plume was found at 16°57.72'N (16.9620°N) during CTD tow T15B-12 where particle and ORP anomalies ($dNTU_{max}$ = 0.023; ΔE_{max} = -88 mv) extended from ~2900 m to the seafloor (Figure 5_{CTD}). The plume core was at a depth of ~3000-3100 m. A separate, particle-only anomaly (no ORP) was detected about 2 km south of this plume (at 16°56.57'N (16.9428°N); $dNTU_{max}$ = 0.006; depth = 3075-3175 m). AUV dive *Sentry*-370 conducted both a mapping survey (70 mab) and a photo survey (5 mab) in the area of these plumes, again providing a 3-d view of the water column plume distribution and estimate of seafloor targets for the 2016 expedition (see MAPR data section and Fledermaus scene file). Vertical cast V15B-07 sampled the larger plume.

In addition to the 5 sites summarized above, there were three tows with very weak particle anomalies (with no detectable ORP anomalies >1 mv) that might be significant, but will require additional information and sample analysis to confirm (or not) hydrothermal origin:

1) T15B-03 (Map 5): There is a broad area to the south of the axial high (south of ~15.08°N) with $dNTU_{max}$ = 0.004-0.006. Unfortunately, no samples were taken during this part of the tow in anticipation that there would be more interesting samples to take over the axial high (Figure 6_{CTD}).

2) T15B-08 (Map 7): A weak particle maximum ($dNTU_{max}$ = 0.008) at 16.40°N about 350 m above bottom (3380 m water depth) looks to be significant, however, there may have been some sensor issues in the early part of this tow that need further evaluation. One sample was taken in this particle maximum (bottle N#2; Figure 7_{CTD}).

8) T15B-11 (Map9): There was a slight increase in dNTU ($dNTU_{max}$ = 0.007) only near bottom between 17.68-17.71°N. Bottle N#1 was tripped within this area. For comparison, other bottles were tripped near the bottom where no dNTU increase was observed (Figure 8_{CTD}).

NOTE: Contact Sharon Walker for Fledermaus scene files discussed in this summary. sharon.l.walker@noaa.gov Fledermaus scenes can be viewed with free software (iView4D) downloadable at: http://www.qps.nl/display/fledermaus/iview

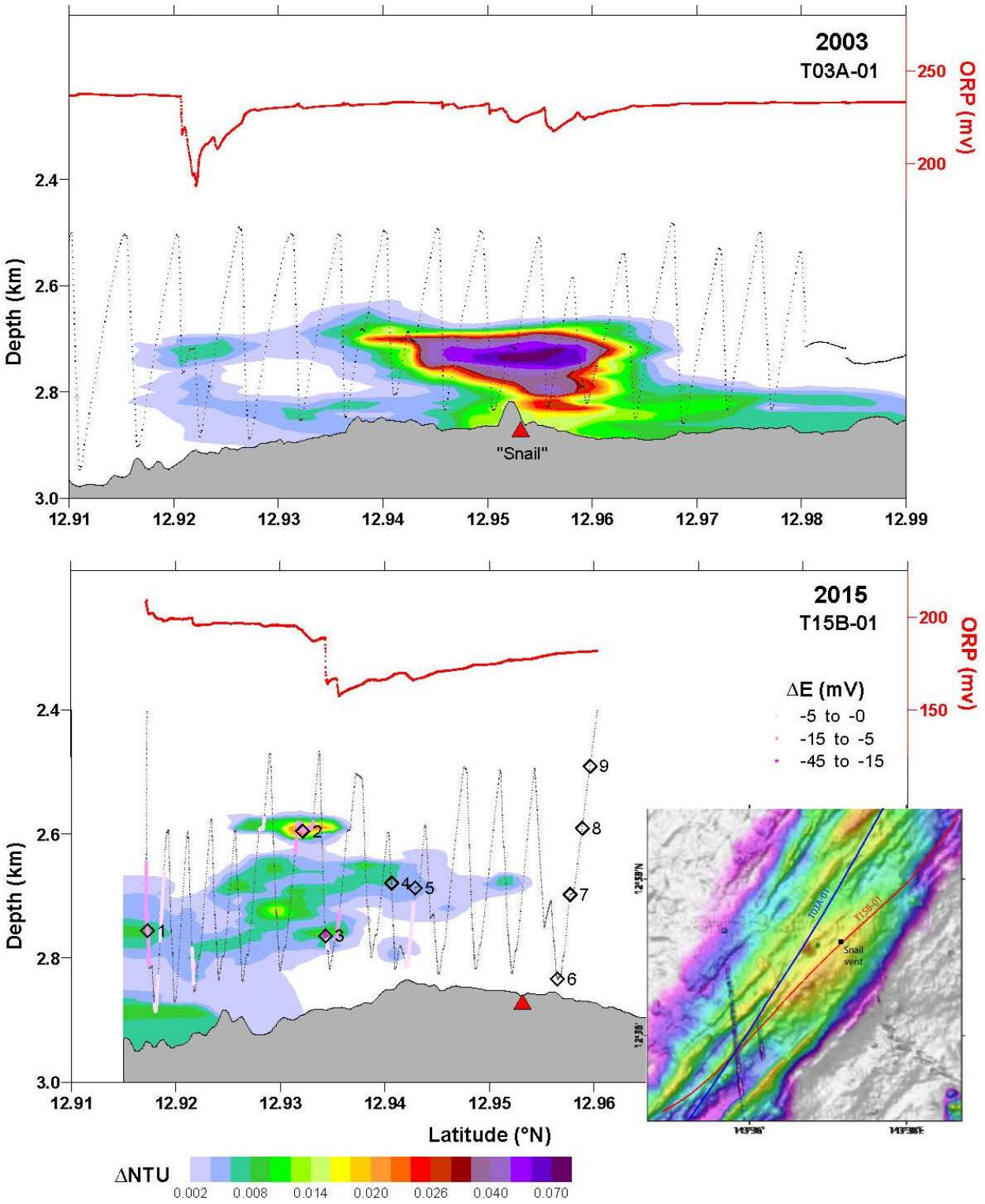

Figure 1_{CTD}: Color contours map the particle plume (ΔNTU) distribution above the Mariana back-arc segment centered at 12.8°N (Map 1) : CTD tow T15B-01 (bottom panel), along with 2003 CTD tow T03A-01 (top) for comparison. Black dots show tow tracklines; open diamonds are bottle sample locations (shown only for T15B-01) with labels indicating Niskin bottle number. Red line above color contours is ORP voltage; pink dots along trackline indicate duration and magnitude of ORP anomalies (dE/dt < 0; color indicates ΔE for each signal). Red triangle on bathymetry profile shows location of the "Snail" vent site. Inset: map of tracklines for each tow and location of Snail vent.

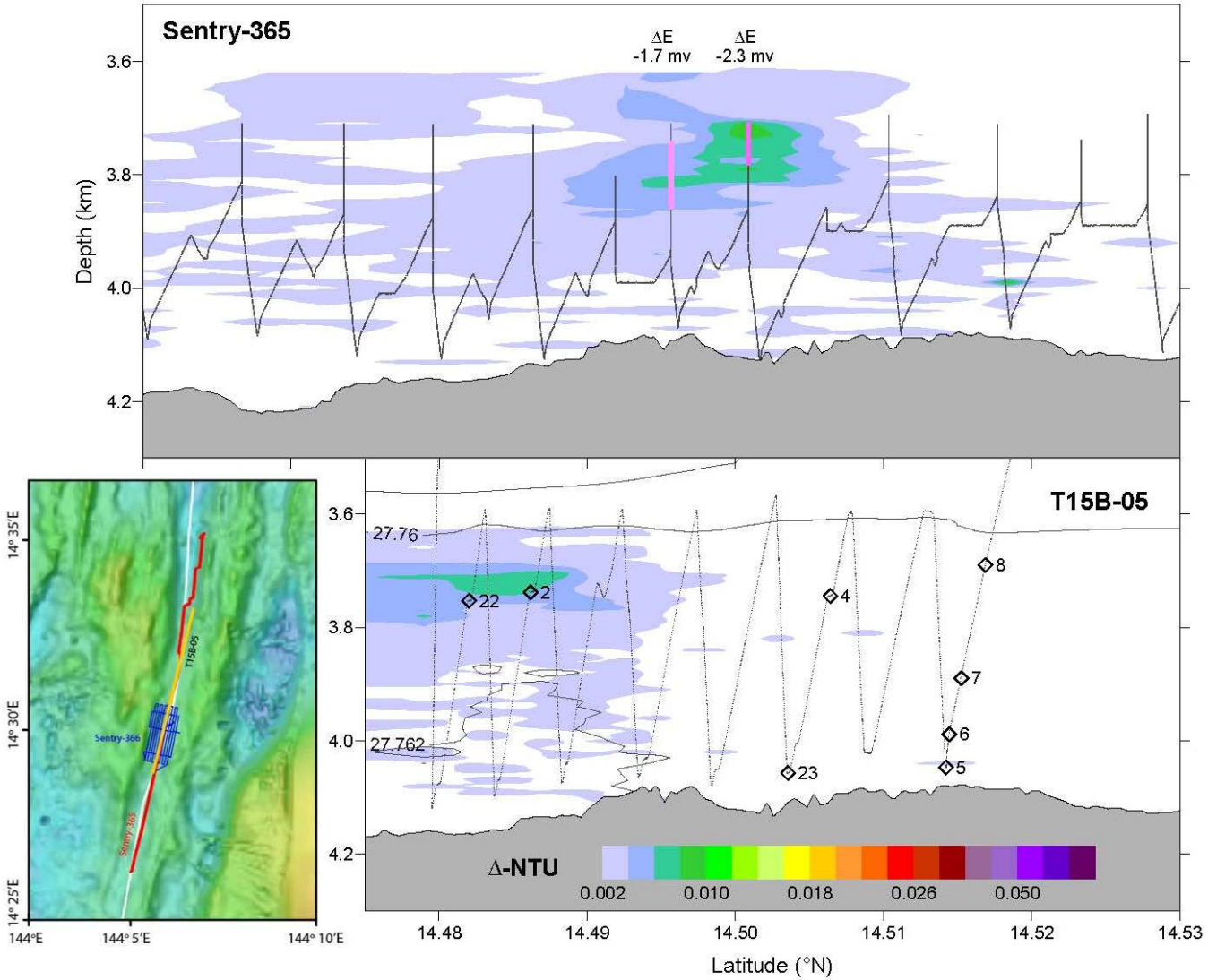

Figure 2$_{CTD}$: Color contours map the particle plume (ΔNTU) distribution above the Mariana back-arc segment centered at 14.5°N (Map 4): AUV dive *Sentry*-365 (top panel) and CTD tow T15B-05 (bottom panel). Black dots show tow tracklines; open diamonds are bottle sample locations with labels indicating Niskin bottle number. Pink dots along *Sentry*-365 trackline indicate duration and magnitude of ORP anomalies (dE/dt < 0; color indicates ΔE for each signal and is labeled above each anomaly). No ORP data are shown for T15B-05 because no anomalies were detected during the tow. Inset: map of tracklines for *Sentry*-365 (red), T15B-05 (yellow), and the *Sentry* mapping mission (*Sentry*-366; blue).

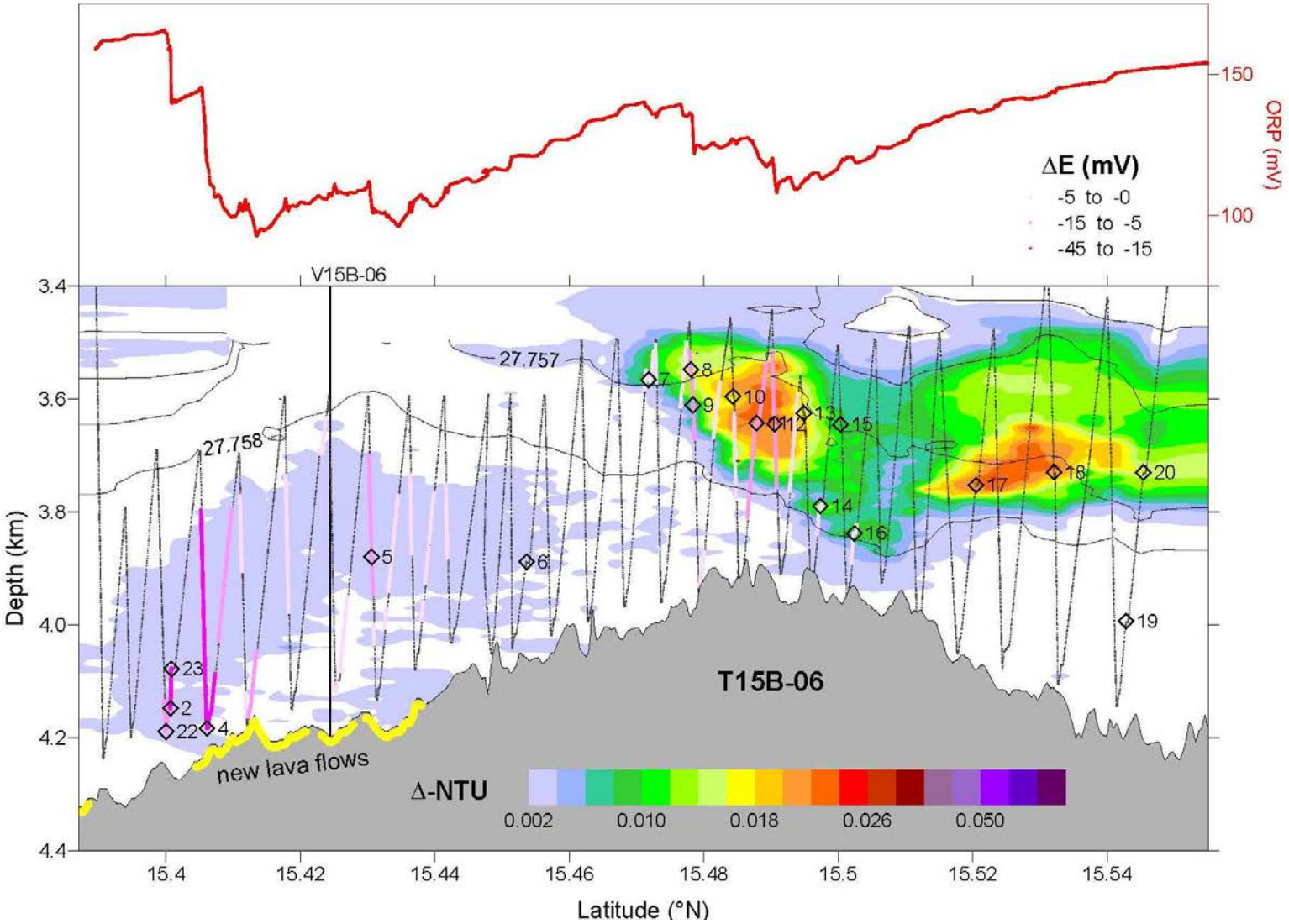

Figure 3_{CTD}: Color contours map the particle plume (ΔNTU) distribution above the Mariana back-arc segment centered at 15.5°N (Map 5): CTD tow T15B-06. Black dots show tow trackline; open diamonds are bottle sample locations with labels indicating Niskin bottle number. Red line above color contours is ORP voltage; pink dots along trackline indicate duration and magnitude of ORP anomalies (dE/dt < 0; color indicates ΔE for each signal). Yellow line along bathymetry shows extent of new lava flow along the tow trackline. Location of vertical cast V15B-06 is shown with a black line.

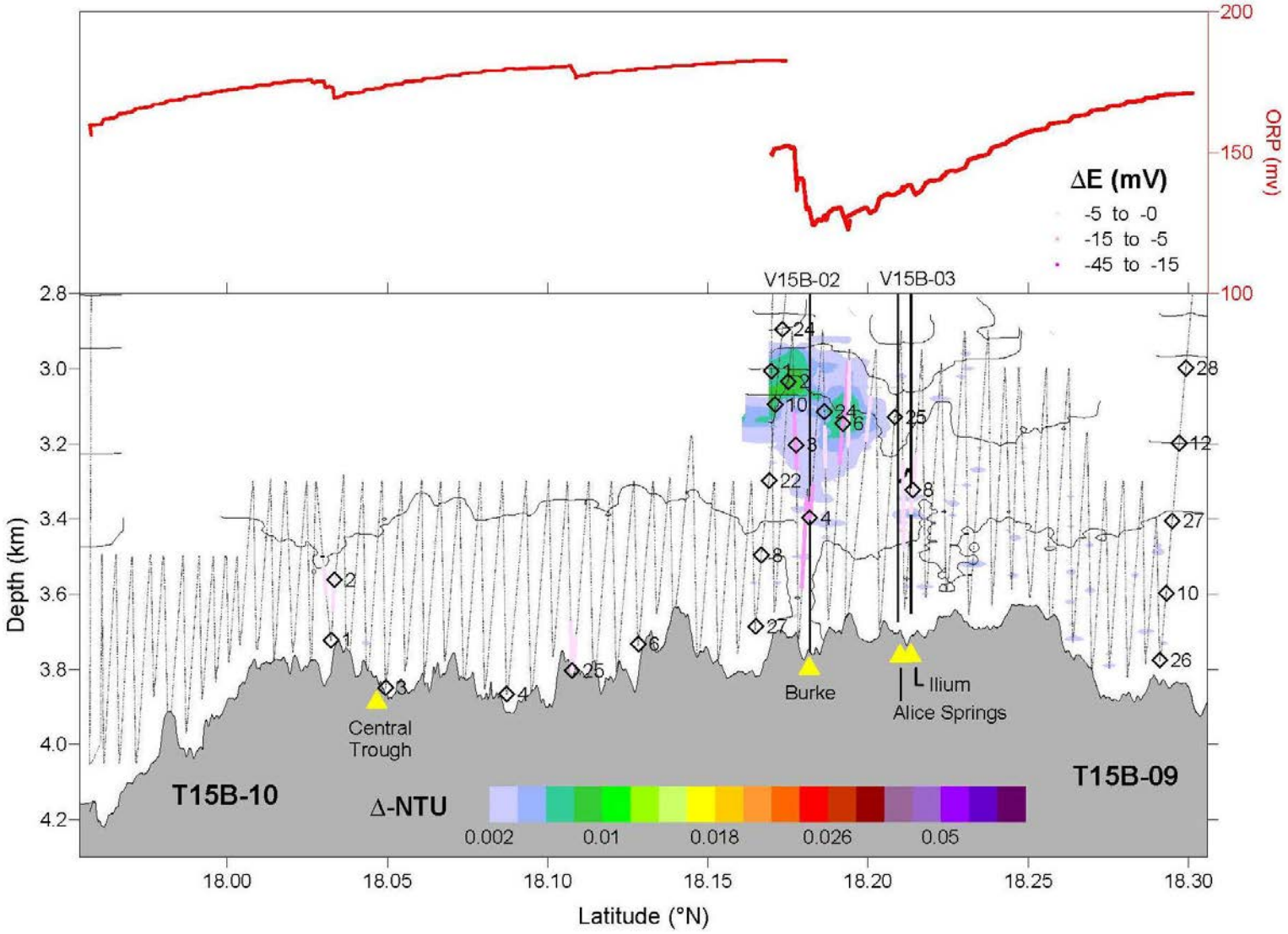

Figure 4$_{CTD}$: Color contours map the particle plume (ΔNTU) distribution above the Mariana back-arc segment centered at 18.2°N (Map 10): CTD tow T15B-09 and T15B-10. Black dots show tow trackline; open diamonds are bottle sample locations with labels indicating Niskin bottle number. Red line above color contours is ORP voltage; pink dots along trackline indicate duration and magnitude of ORP anomalies (dE/dt < 0; color indicates ΔE for each signal). Yellow triangles along bathymetry show locations of previously known vent sites. Location of vertical casts V15B-02 (light black line) and V15B-03 (heavy black line) are included.

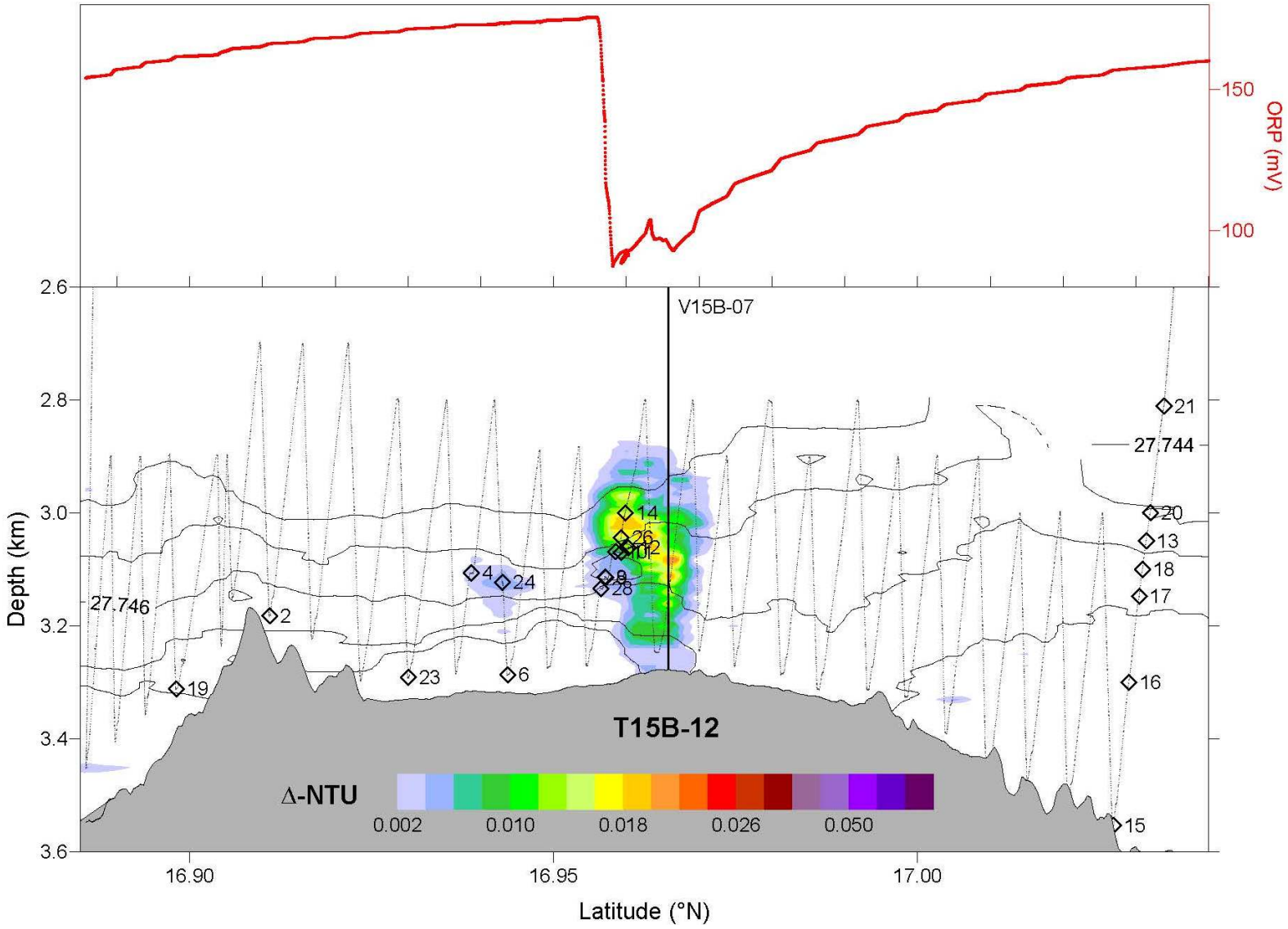

Figure 5$_{CTD}$: Color contours map the particle plume (ΔNTU) distribution above the Mariana back-arc segment centered at 17.0°N (Map 8): CTD tow T15B-12. Black dots show tow trackline; open diamonds are bottle sample locations with labels indicating Niskin bottle number. Red line above color contours is ORP voltage. Location of vertical cast V15B-07 is shown with a black line.

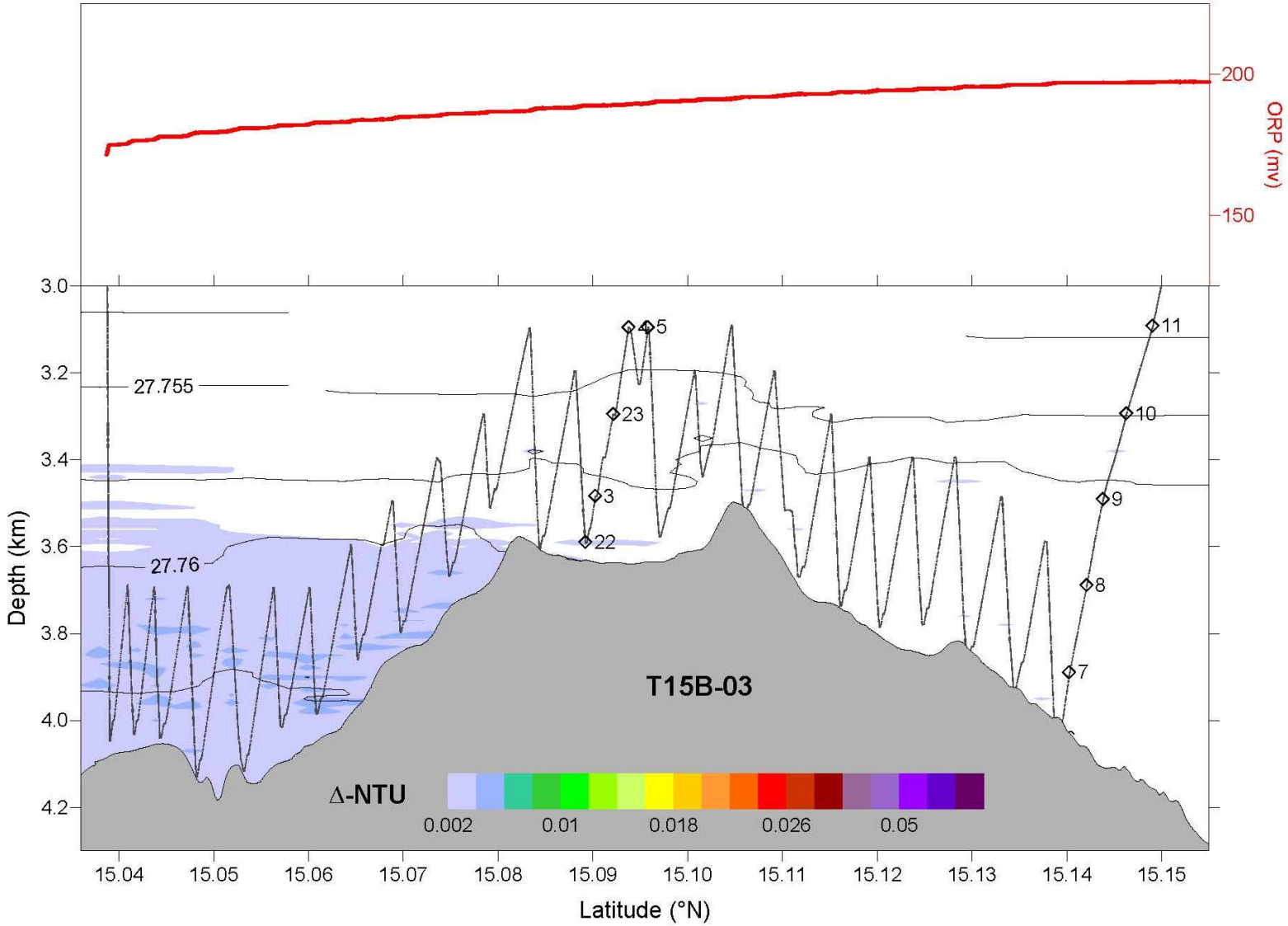

Figure 6_{CTD}: Color contours map the particle plume (ΔNTU) distribution above the Mariana back-arc segment centered at 15.1°N (Map 5): CTD tow T15B-03. Black dots show tow trackline; open diamonds are bottle sample locations with labels indicating Niskin bottle number. Red line above color contours is ORP voltage.

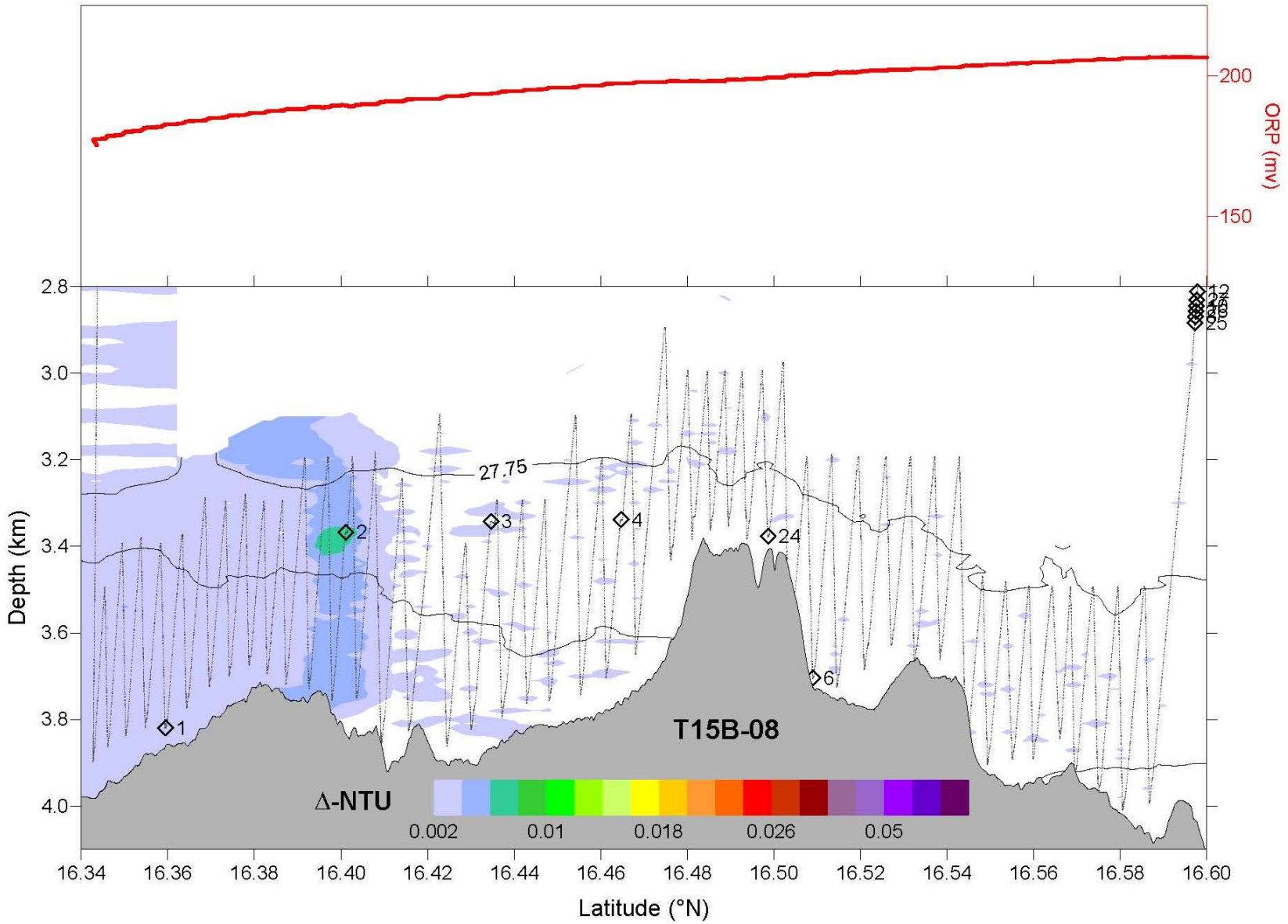

Figure 7$_{CTD}$: Color contours map the particle plume (ΔNTU) distribution above the Mariana back-arc segment centered at 16.5°N (Map 7): CTD tow T15B-08. Black dots show tow trackline; open diamonds are bottle sample locations with labels indicating Niskin bottle number. Red line above color contours is ORP voltage.

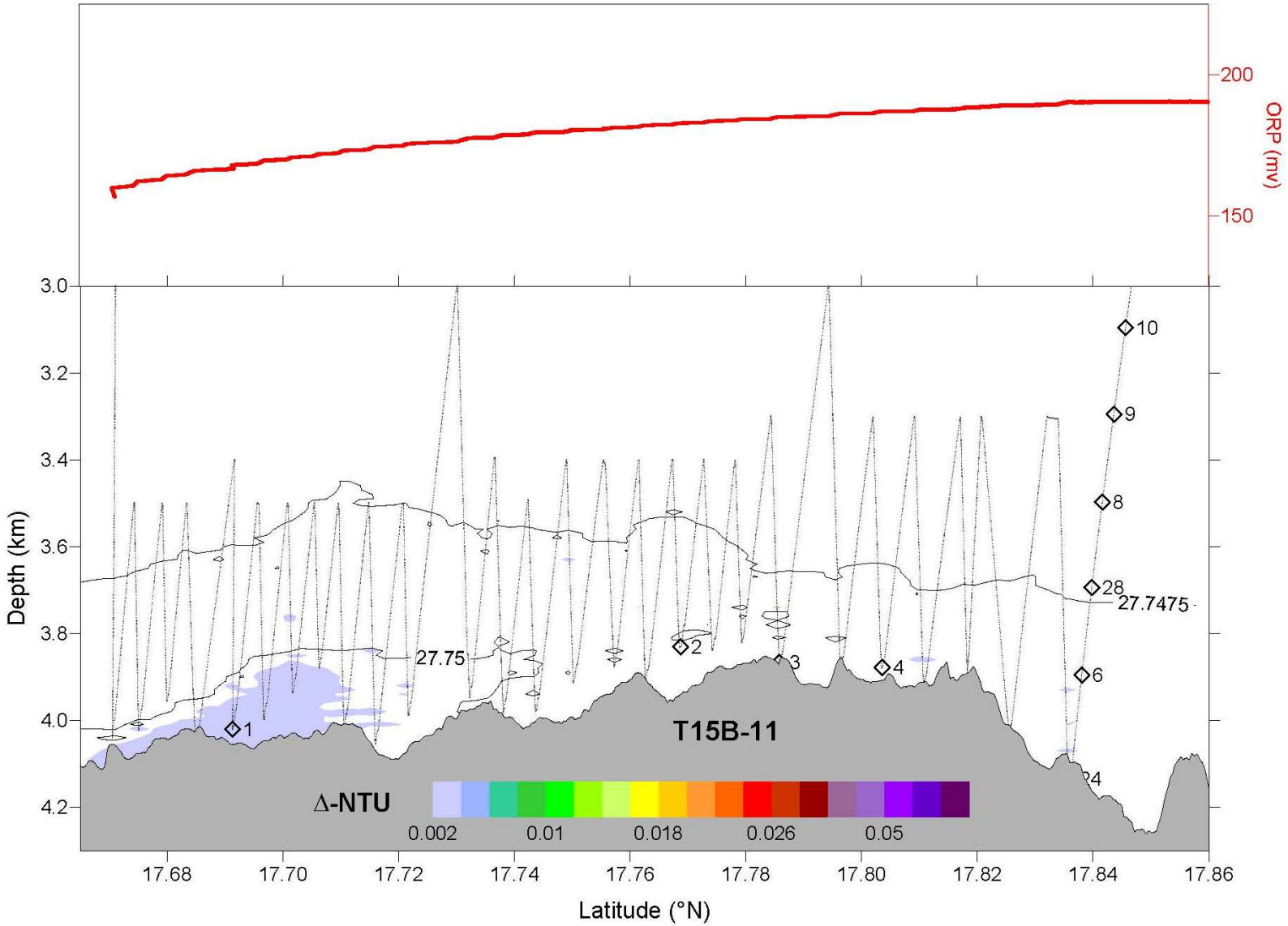

Figure 8$_{CTD}$: Color contours map the particle plume (ΔNTU) distribution above the Mariana back-arc segment centered at 17.8°N (Map 9): CTD tow T15B-11. Black dots show tow trackline; open diamonds are bottle sample locations with labels indicating Niskin bottle number. Red line above color contours is ORP voltage.

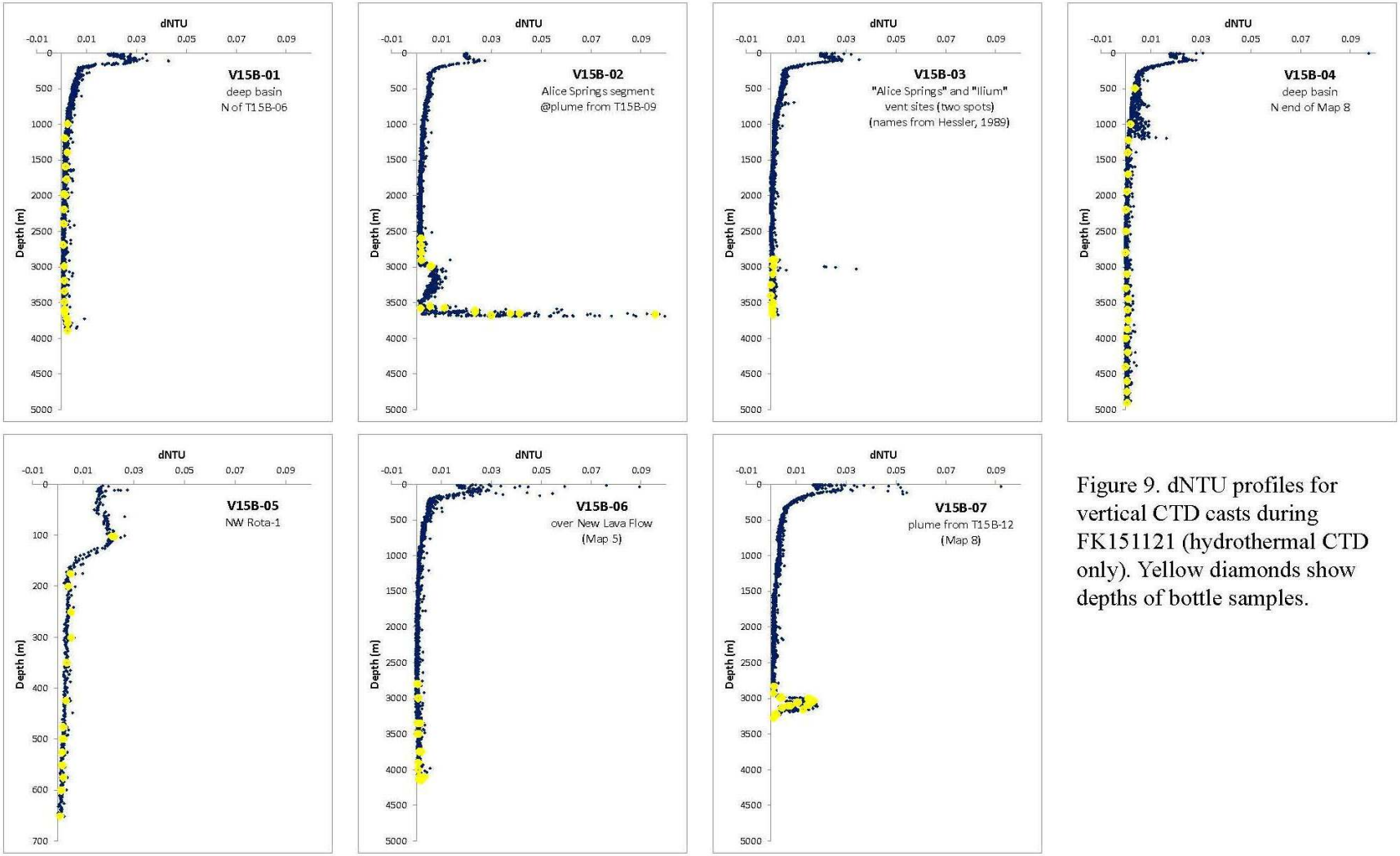

Figure 9. dNTU profiles for vertical CTD casts during FK151121 (hydrothermal CTD only). Yellow diamonds show depths of bottle samples.

Table Summarizing CTD vertical casts and tows

Cast	Sta Name	LatDDN	LongDDE	Start time (UTC)	End time (UTC)	pH	3He	H2& CH4	CO 2	Nuts	TDMe	DMe	Libr ary	XR F	SEM	Cell count	Fe iso	liga nds
						712	515	479	11	199	480	284	197	244	0	11	45	142
0-A	V15B-00	13.634067	144.156550	22-Nov-2015 06:05	22-Nov-2015 06:58													
		test CTD - vertical cast to ~1000 m just west of Guam (Tamara wants some surface water)																
0-B	T15B-00 (start)	13.813917	144.480833	22-Nov-2015 09:02														
	T15B-00 (end)	13.839883	144.478117		22-Nov-2015 13:00													
		test CTD tow just west of Guam - to observe winch tension and wire angle. Look like limits of operations in ~1 kt																
1	T15B-01(start)	12.917128	143.582962	23-Nov-2015 14:18		28	19	19			14	2		2				
	T15B-01(end)	12.980607	143.642562		23-Nov-2015 20:55													
		southern Mariana bark-arc - Snail segment																
2	T15B-02(start)	13.426833	143.777417	24-Nov-2015 07:00		28	21	21			21							
	T15B-02(end)	13.709292	143.879122		25-Nov-2015 02:52													
		southern Mariana back-arc																
3	M15B-01	14.225267	143.959167	25-Nov-2015 06:51	25-Nov-2015 07:55	12	11			11	11	11	11	11				22
		trace metal cast to 1050 m																
4	T15B-03(start)	15.037575	144.442022	26-Nov-2015 15:13		28	21	21			21	21						21
	T15B-03(end)	15.163563	144.490037		27-Nov-2015 02:01													
		central Mariana back-arc (over high in map 5)																
5	M15B-02	14.599643	144.117023	27-Nov-2015 07:06	27-Nov-2015 08:02	18	12	12		12	12	11	11	11				
		trace metal cast to 950 m																
6	M15B-03	14.599680	144.465945	28-Nov-2015 13:43	28-Nov-2015 15:02	16	12	12		12	12	12	12	12			12	4
		trace metal cast to 950 m																
7	T15B-04(start)	13.682295	143.875483	29-Nov-2015 00:17		18	17	10			11							
	T15B-04(end)	13.845053	143.908555		29-Nov-2015 13:27													
		southern Mariana back-arc (map 3; to close gap between T15B-02 and *Sentry*-364)																
8	M15B-04	13.833658	143.905792	29-Nov-2015 14:16	29-Nov-2015 15:36	16	10	10		11	11	11	11	11				
		trace metal cast to 1000 m																
9	M15B-05	14.599990	143.466785	30-Nov-2015 00:14	30-Nov-2015 01:18	16	12	12		12	12	12	12	12			12	
		trace metal cast to 950 m																
10	T15B-05(start)	14.482013	144.093232	30-Nov-2015 07:05		25	18	10			9							3
	T15B-05(end)	14.553108	144.111057		30-Nov-2015 13:07													
		short tow to define plume seen during *Sentry*-365 (map 4)																
11	M15B-06	14.599793	143.800153	01-Dec-2015 07:57	01-Dec-2015 09:00	16	12	12		12	12	12	12	12				
		trace metal cast to 1050 m																

Cast	Sta Name	LatDDN	LongDDE	Start time (UTC)	End time (UTC)	pH	3He	H2& CH4	CO 2	Nuts	TDMe	DMe	Library	XRF	SEM	Cell count	Fe iso	ligands
12	M15B-07	14.999968	144.283207	01-Dec-2015 13:47	01-Dec-2015 14:50	16	12	12		12	12	12	12	12				
		trace metal cast to 1000 m																
	T15B-06(start)	15.391483	144.508227	01-Dec-2015 20:01		26	20	20			20	11		9				42
13	T15B-06(end)	15.572902	144.510405		02-Dec-2015 09:30													
		tow north along axis (map 5)																
14	M15B-08	15.416833	144.500307	02-Dec-2015 12:13	02-Dec-2015 13:16	16	12	12		12	12	12	12	12				
		trace metal cast to 1025 m																
15	V15B-01	15.606959	144.558378	03-Dec-2015 00:51	03-Dec-2015 03:48	25	18	18			9	6						
		deep basin N of T15B-06																
16	M15B-09	16.000109	144.674787	04-Dec-2015 02:57	04-Dec-2015 03:52	16	11	11		12	12	12	12	12				
		trace metal cast to 950 m																
	T15B-07(start)	15.908923	144.791405	04-Dec-2015 05:14		28	21	21			15	5						
17	T15B-07(end)	16.258783	144.810515		05-Dec-2015 08:57													
		tow north along axis (map 6)																
18	M15B-10	16.499828	144.856173	05-Dec-2015 12:05	05-Dec-2015 12:58	16	11	12		12	12	12	12	12				
			trace metal cast to 975 m															
	T15B-08(start)	16.346220	144.875950	05-Dec-2015 14:47		9	6	6			6	1						
19	T15B-08(end)	16.619652	144.834378		06-Dec-2015 11:12													
		tow north along axis (map #7)																
20	M15B-11	16.999772	144.856937	06-Dec-2015 14:52	06-Dec-2015 15:51	11	11	15		11	11	11	11	11				
		trace metal cast to 1050 m																
	T15B-09(start)	18.173317	144.721200	05-Dec-2015 14:47		28	21	21			21	4		4				
21	T15B-09(end)	18.321628	144.677707		06-Dec-2015 11:12													
		tow north along axis (map #10) - Alice Springs Segment																
22	V15B-02	18.181750	144.704083	07-Dec-2015 23:31	08-Dec-2015 02:13	27	21	21	11		20	10		10				11
		Alice Springs segment - site near signal seen during T15B-09																
23	M15B-12	18.212408	144.707143	08-Dec-2015 05:52	08-Dec-2015 06:46	15	11	11		11	11	11	11	11				
		trace metal cast to 1000 m																
	V15B-03(a)	18.209433	144.706820	08-Dec-2015 09:16		18	12	12			12	4		1				
24	V15B-03(b)	18.213418	144.706527		08-Dec-2015 13:03													
		vertical cast at northmost Alice Springs locations - modified to go to the bottom at two different locations ~400 m apart. Moved ship with CTD at 2900 m																
25	M15B-13	18.583433	144.670383	08-Dec-2015 22:16	08-Dec-2015 23:13	15	11	11		11	11	11	11	11				13
		trace metal cast to 975 m.																
	T15B-10(start)	17.958650	144.780667	09-Dec-2015 04:36		25	19	19			17	4		4				

Cast	Sta Name	LatDDN	LongDDE	Start time (UTC)	End time (UTC)	pH	3He	H2& CH4	CO 2	Nuts	TDMe	DMe	Library	XRF	SEM	Cell count	Fe iso	ligands
26	T15B-10(end)	18.191667	144.717200		09-Dec-2015 21:25													
		tow along south end of Alice Springs segment ("Central Trough" area - map 10)																
27	V15B-04	17.431853	144.789917	10-Dec-2015 04:05	10-Dec-2015 07:51	28	20	20			20	1					9	
		deep basin a N end of map 8																
28	M15B-14	17.431902	144.799568	10-Dec-2015 08:32	10-Dec-2015 09:18	16	12	12		12	11	11	11	11				15
		trace metal cast to 700 m																
29	M15B-15	14.600150	145.116917	11-Dec-2015 04:09	11-Dec-2015 05:06	15	12	12		12	12	12	12	12			12	
		trace metal cast to 950 m - NW Rota transect																
30	V15B-05	14.598398	144.776433	11-Dec-2015 07:57	11-Dec-2015 08:54	28	14	11			15	5		5				
		NW Rota-summit																
31	M15B-16	15.479908	144.502658	11-Dec-2015 23:15	11-Dec-2015 23:58	16	12	6		12	12	12	12	12				
		trace metal cast to 900 m (replicate bottles tripped at 850 m)																
32	M15B-17	15.499333	144.507267	12-Dec-2015 03:11	12-Dec-2015 03:24	16	12	6		12	12	12	12	12				
		trace metal cast to 200 m (replicate bottles tripped at FLU max =105-95 m)																
33	V15B-06	15.424418	144.502950	12-Dec-2015 05:07	12-Dec-2015 08:33	25	10	10			10	5		5				
		over new lava flow area (map 5)																
	T15B-11(start)	17.672383	144.931783	13-Dec-2015 04:43		28	20	20			20	3		2				
34	T15B-11(3nd)	17.885817	144.895850		13-Dec-2015 19:46													
		along-axis tow (map 9)																
	T15B-12(start)	16.889550	144.890733	14-Dec-2015 01:21		28	21	21			21	5		5		11		11
35	T15B-12(end)	17.048113	144.845737		14-Dec-2015 13:30													
		along-axis tow (map 8)																
36	V15B-07	16.965800	144.867438	15-Dec-2015 05:55	15-Dec-2015 08:47													
		vertical cast at plume location in V15B-12 (map 8)																

Trace Metal Sampling

Susanna Michael, Pam Barrett, Joseph Resing, Nathan Buck

Trace-Metal-clean surface water CTD operations were conducted aboard the R/V *Falkor* during the November-December 2015 cruise to the Mariana Back-Arc. There are seven known shallow vent sites (<1000 m) along the Mariana Arc that are sources of iron and other trace metals to the upper water column. The North Equatorial Current (NEC) flows west at about 200 m deep, from the Mariana Arc to the Back-Arc and continuing west, transporting potential nutrients towards the Mindanao and Kuroshio currents. Our primary objective was to sample a shallow (<1000 m) north-south transect to the west of, and roughly parallel to, the Mariana Arc for total, dissolved (filtrate from <0.4 µm filter), and particulate (particles >0.4 µm) aluminum, iron, manganese, as well as ^{3}He. This effort aims to determine if there is long-range metal transport from the shallow volcanoes of the Mariana Arc via the NEC. We also conducted an east-west transect at14.6°N to capture potential north-south transport suggested by the CNMI regional scale model of currents in the region (personal communication, James Potemera). We initially selected 14.6°N because this is the latitude of Northwest Rota submarine volcano, a volcano that had been erupting for more than 10 years. We believe that eruptive arc volcanoes likely export more Fe to the ocean than ones that are merely hydrothermal in their output. Although the cessation of eruptive activity was noted during SROF14-Ironman cruise in 2014, its latitudinal location was centrally located within our study area and therefore represented a prime latitude to place our east-west section.

Samples were collected from the top ~1000 m using an epoxy-coated rosette and twelve General Oceanics, Teflon coated, 10-L Go-Flo bottles. When not in use, Go-Flos were kept on plastic racks in a positively pressurized, trace-metal clean bubble. Go-Flo openings were kept covered with shower caps until deployment to prevent contamination. Upon return to the surface, nontrace-metal samples for Helium-3, dissolved gases (CH_4, CO_2), and pH, were collected on deck using a separate non-trace metal spigot. The Go-Flo bottles were moved to the clean lab for trace metal sampling. In the clean lab, the Go-Flo bottles were hooked up to an air filtration system, which positively pressurized the bottles, and samples were taken through a separate trace metal clean spigot. Water samples were collected in 100 mL LDPE bottles for trace metal analysis and 30 mL HDPE bottles for nutrient analysis. A whole water fraction was collected directly from each Go-Flo bottle. Then, filters (Milipore Isopore Membrane filters, 0.4 µm Polycarbonate) were loaded onto filter cartridges and attached to the TM-clean spigots. Two-100 mL bottles were taken of the dissolved fraction. Iron ligand (filtered, 1L, HDPE) and iron isotope (filtered, 1L, LDPE) samples were taken at sites of interest. The filters were processed for XRF analysis.

Continuous data were collected using a Seabird electronics instrument package consisting of a SBE911 plus CTD and included a SEBE03 temperature sensor, SBE04 conductivity cell, SBE43 oxygen sensor, and a Wet Labs ECO FLNTU fluorometer with turbidity meter.

During this cruise, a total of 17 trace-metal clean CTD casts were conducted (Table 1(tm)), including two reference casts to determine sample variation and bottle effects. A total of 196 Helium samples, 199 nutrient samples, 198 total metal samples, 197 dissolved metal (and library) samples, 197 XFR/filter samples, 36 iron isotope samples, and 22 iron ligand samples were collected for land-based laboratory analysis. In addition, 262 pH and 178 hydrogen and methane samples were collected and analyzed ship-board.

Of these seventeen casts, eleven casts (M15B-04, -01, -02, -07, -08, -09, 10, 11, -14, -12, -13) created the north-south transect that runs parallel to the Mariana Arc, from 13.8°N-18.6°N, and curves slightly from 143.9°W-144.7° W. Five casts (M15B-05, -06, -02, -03, and -15) created the east-west transect along 14.6°N, between 143.4° W and 145.2° W (Figure 1).

Contour plots of the north-south transect show a deepening of the oxygen minimum from north to south (Figure 2). This corresponds to a plume of low-salinity water (Figure 3) that intrudes along the north side of the transect around 400 m. Additionally, this corresponds with a region of anomalously high pH (Figure 4), though it is unclear at this stage if this is a real feature or if it is due to a miss-trip. There is also a region of low pH at station M15B-14, adjacent to this high-pH zone. There are no large changes in the chlorophyll maximum (Figure 5) or temperature profile (Figure 6) across the transect.

The physical parameters of the east-west transect remain fairly constant across the sampling space (Figure 7, Figure 8, Figure 9, Figure 10), and is suggestive of a single water mass. There is a slight anomaly in the T-S plot of station M15B-05, the westernmost station along the transect at about $26\sigma_\theta$ (Figure 10). Additionally, there are some slight variations at stations M15B-01, and M15B-01, the southernmost stations along the N-S transect, at about 26.5 σ_θ.

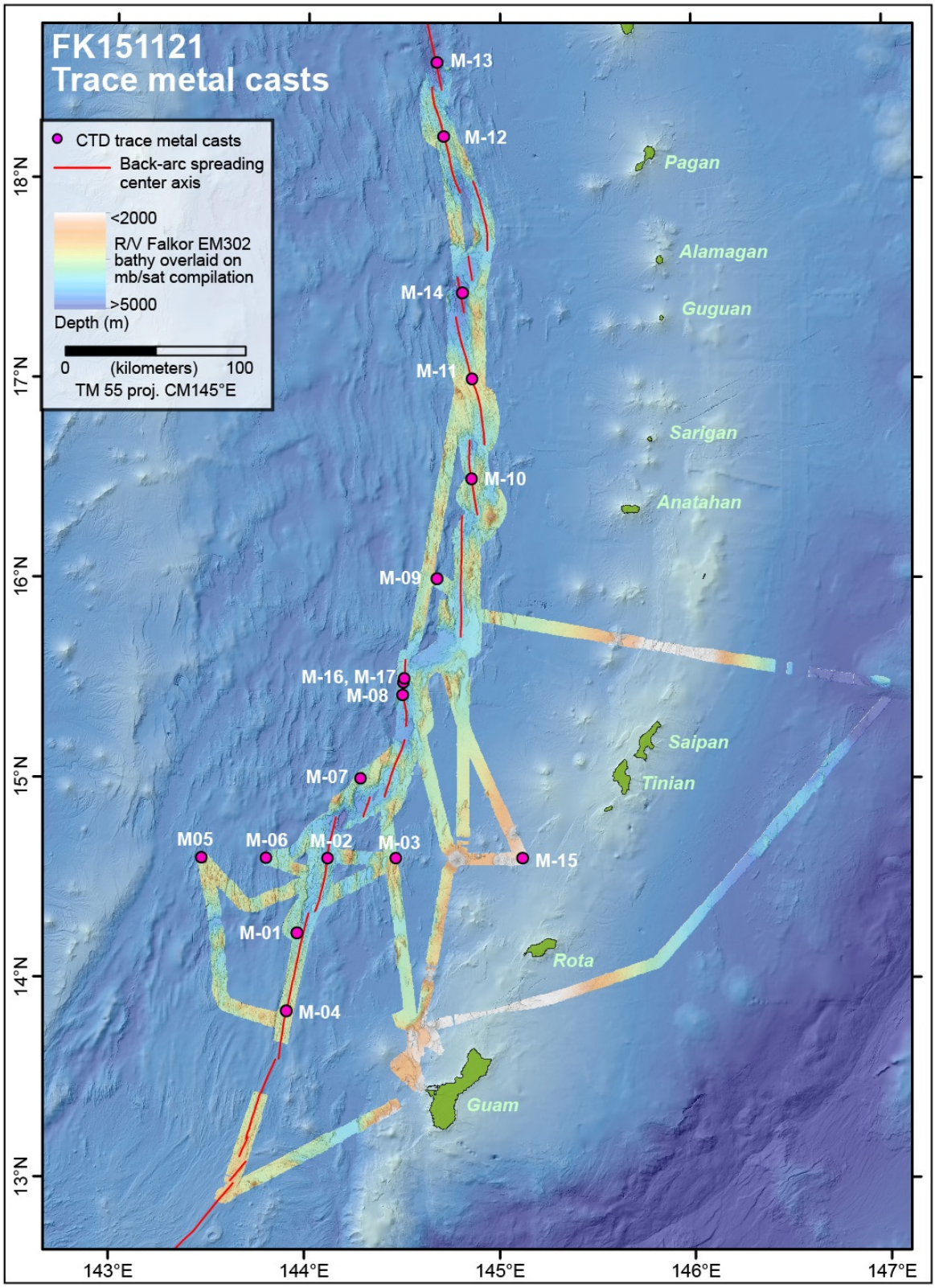

Figure 1_{tm}: Map of trace metal sampling sites, showing north-south and east-west transects.

Cast	Station Name	Latitude (°N)	Longitude (°W)	Start time (UTC)	Number of samples collected									
					pH	^{3}He	H_2&CH_4	Nuts	TDMe	DMe	Library	XRF	Fe isotopes	Ligands
3	M15B-01	14.225267	143.959167	25-Nov-2015 06:51	12	11		11	11	11	11	11		22
5	M15B-02	14.599643	144.117023	27-Nov-2015 07:06	18	12	12	12	12	11	11	11		
6	M15B-03	14.599680	144.465945	28-Nov-2015 13:43	16	12	12	12	12	12	12	12	12	4
8	M15B-04	13.833658	143.905792	29-Nov-2015 14:16	16	10	10	11	11	11	11	11		
9	M15B-05	14.599990	143.466785	30-Nov-2015 00:14	16	12	12	12	12	12	12	12	12	
11	M15B-06	14.599793	143.800153	01-Dec-2015 07:57	16	12	12	12	12	12	12	12		
12	M15B-07	14.999968	144.283207	01-Dec-2015 13:47	16	12	12	12	12	12	12	12		
14	M15B-08	15.416833	144.500307	02-Dec-2015 12:13	16	12	12	12	12	12	12	12		
16	M15B-09	16.000109	144.674787	04-Dec-2015 02:57	16	11	11	12	12	12	12	12		
18	M15B-10	16.499828	144.856173	05-Dec-2015 12:05	16	11	12	12	12	12	12	12		
20	M15B-11	16.999772	144.856937	06-Dec-2015 14:52	11	11	15	11	11	11	11	11		
23	M15B-12	18.212408	144.707143	08-Dec-2015 05:52	15	11	11	11	11	11	11	11		
25	M15B-13	18.583433	144.670383	08-Dec-2015 22:16	15	11	11	11	11	11	11	11		13
28	M15B-14	17.431902	144.799568	10-Dec-2015 08:32	16	12	12	12	11	11	11	11		15
29	M15B-15	14.600150	145.116917	11-Dec-2015 04:09	15	12	12	12	12	12	12	12	12	
31	M15B-16	15.479908	144.502658	11-Dec-2015 23:15	16	12	6	12	12	12	12	12		
32	M15B-17	15.499333	144.507267	12-Dec-2015 03:11	16	12	6	12	12	12	12	12		

Table 1_{tm}: Locations of trace metal sampling and number of samples taken during FK151121

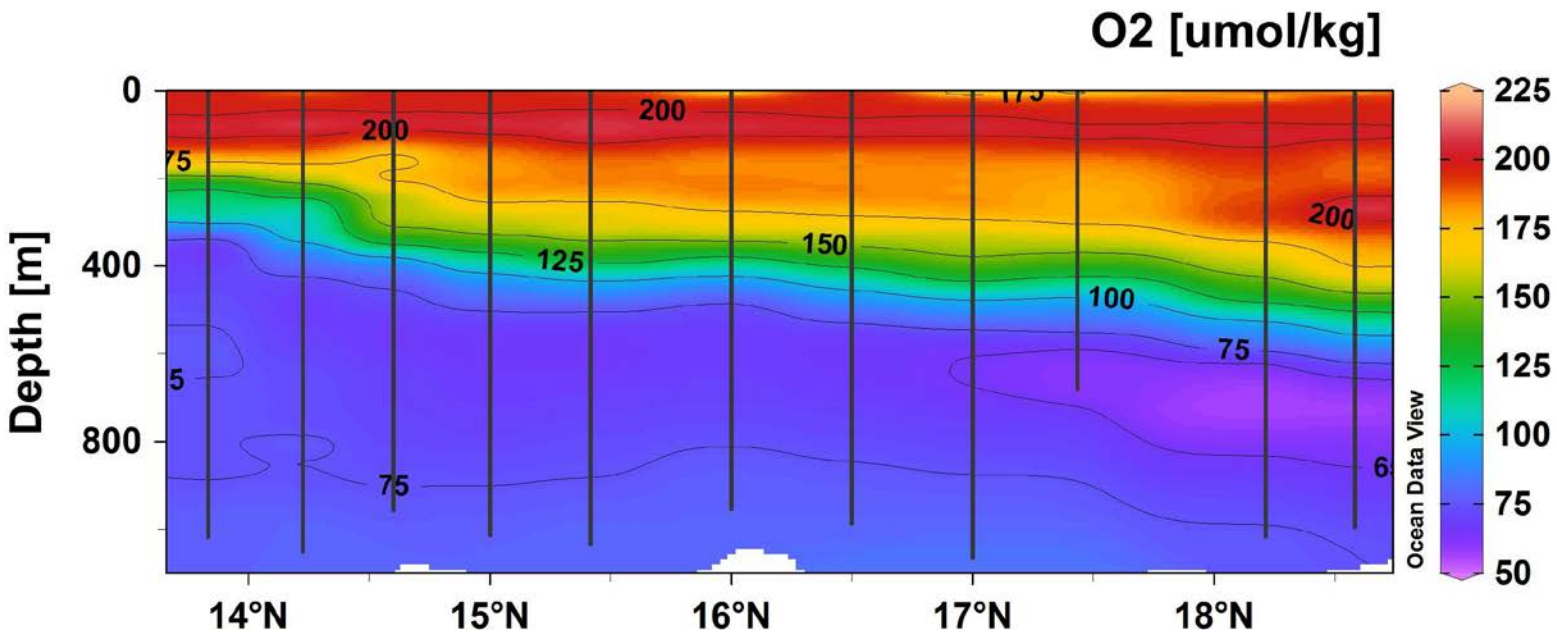

Figure 2$_{tm}$: Oxygen concentrations (µmol/kg) along the N-S transect. Black lines indicate where sampling occurred.

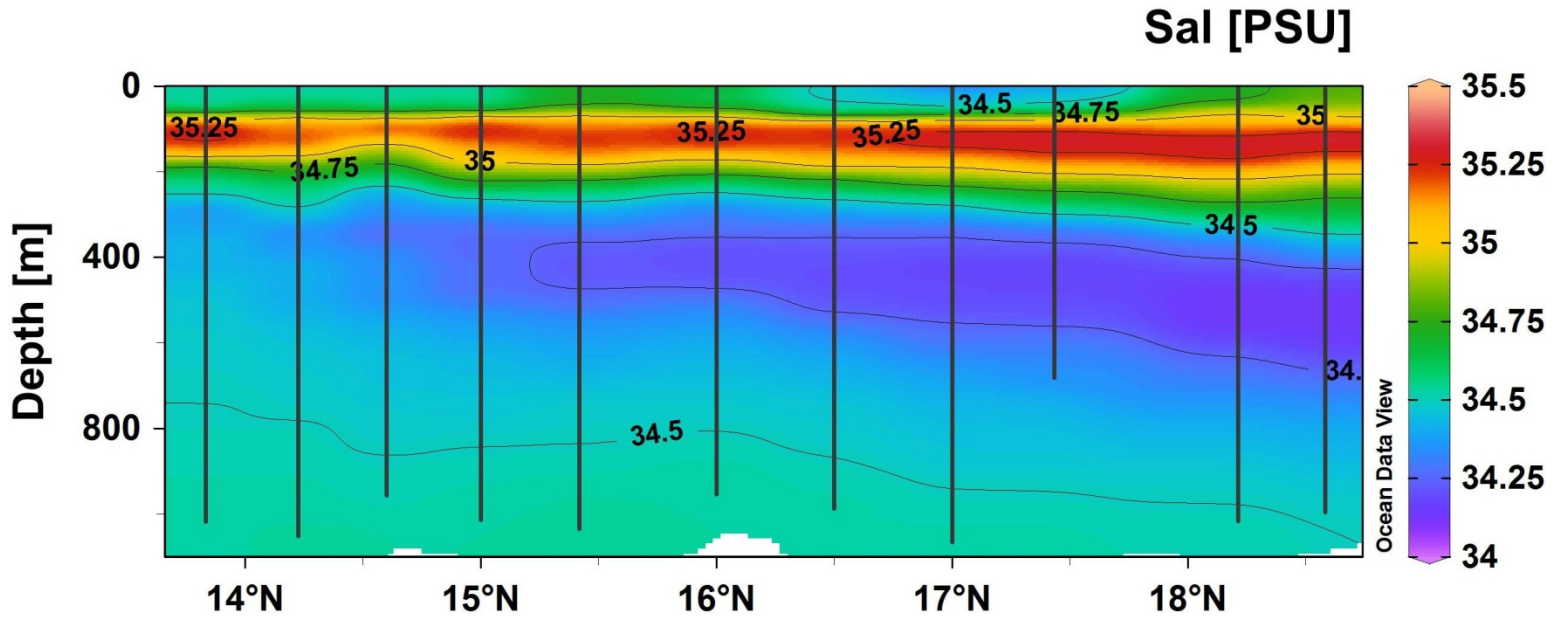

Figure 3$_{tm}$: Salinity (PSU) along the N-S transect. Black lines indicate where sampling occurred.

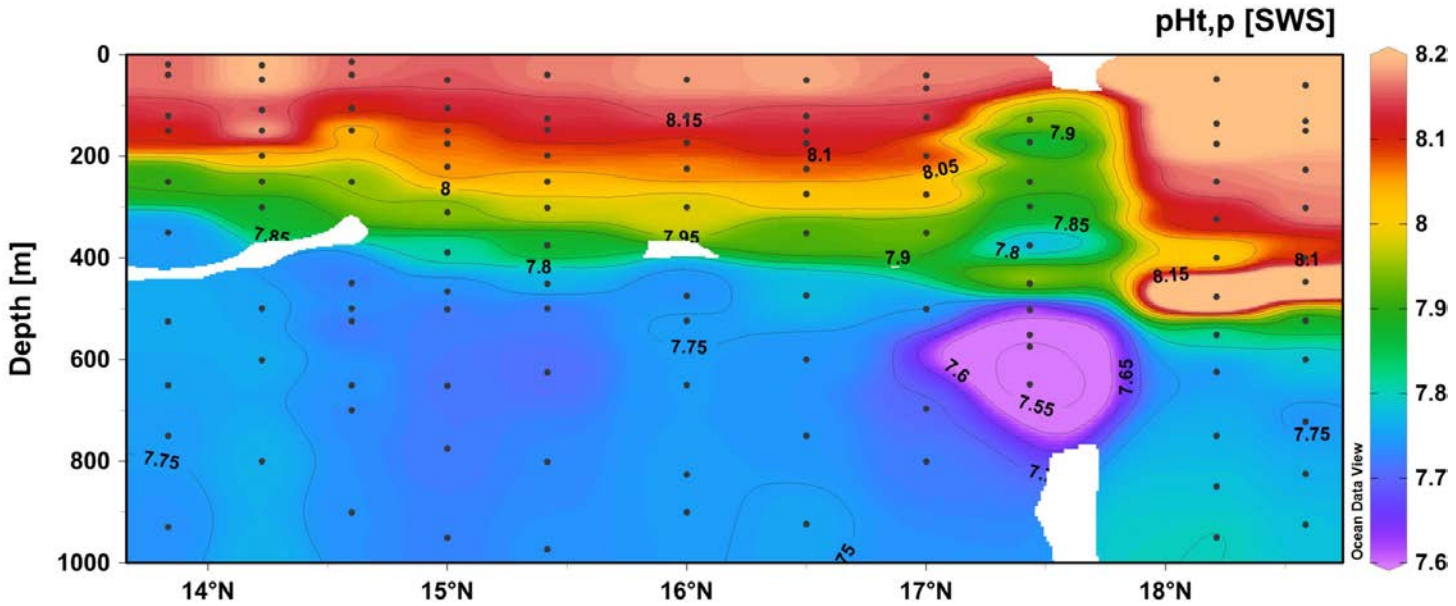

Figure 4$_{tm}$: pH along the N-S transect. Black points indicate samples

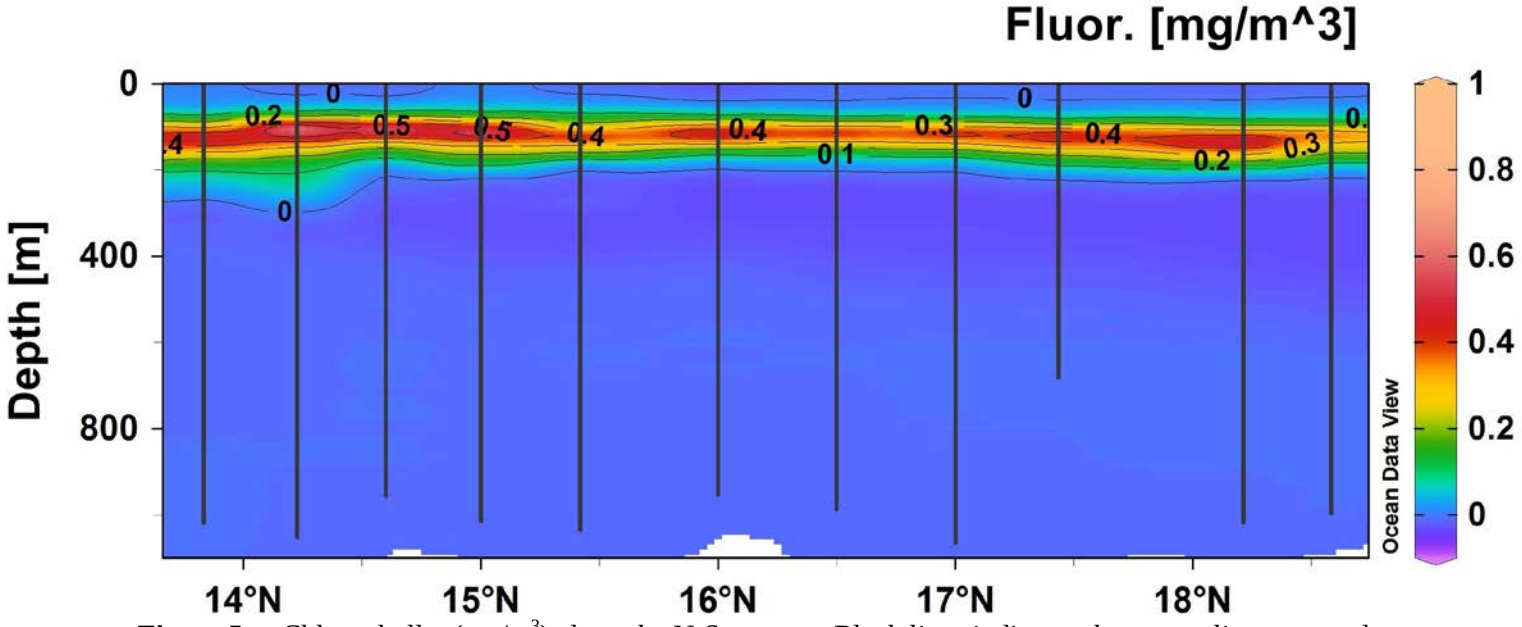

Figure 5$_{tm}$: Chlorophyll *a* (mg/m^3) along the N-S transect. Black lines indicate where sampling occurred.

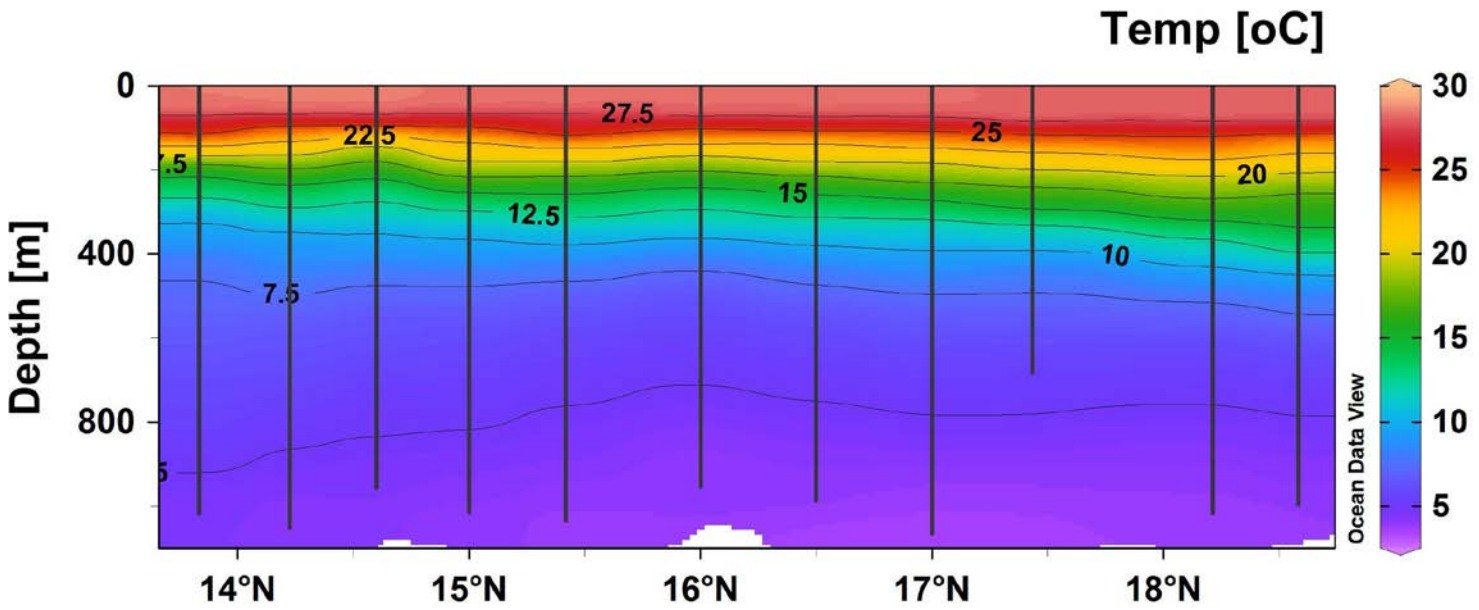

Figure 6$_{tm}$: Temperature along the N-S transect. Black lines indicate where sampling occurred.

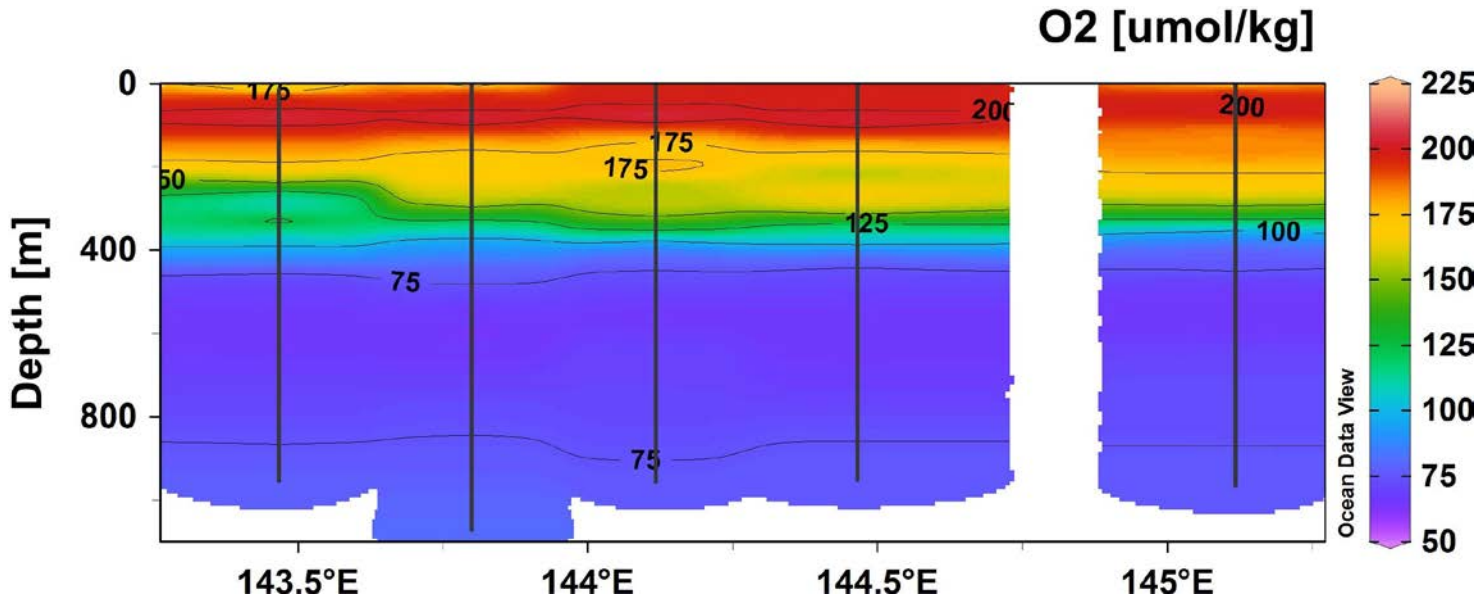

Figure 7$_{tm}$: Oxygen along the E-W transect. Black lines indicate where sampling occurred.

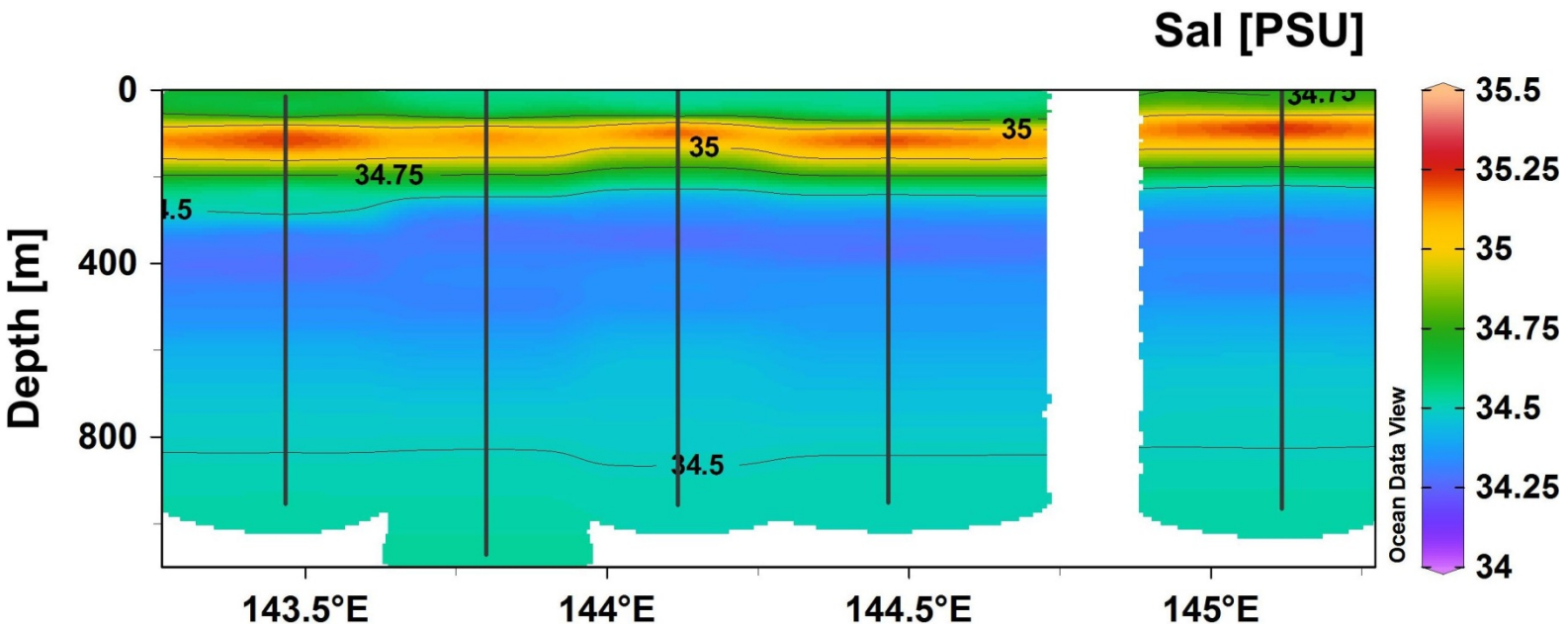

Figure 8$_{tm}$: Salinity along the E-W transect. Black lines indicate where sampling occurred.

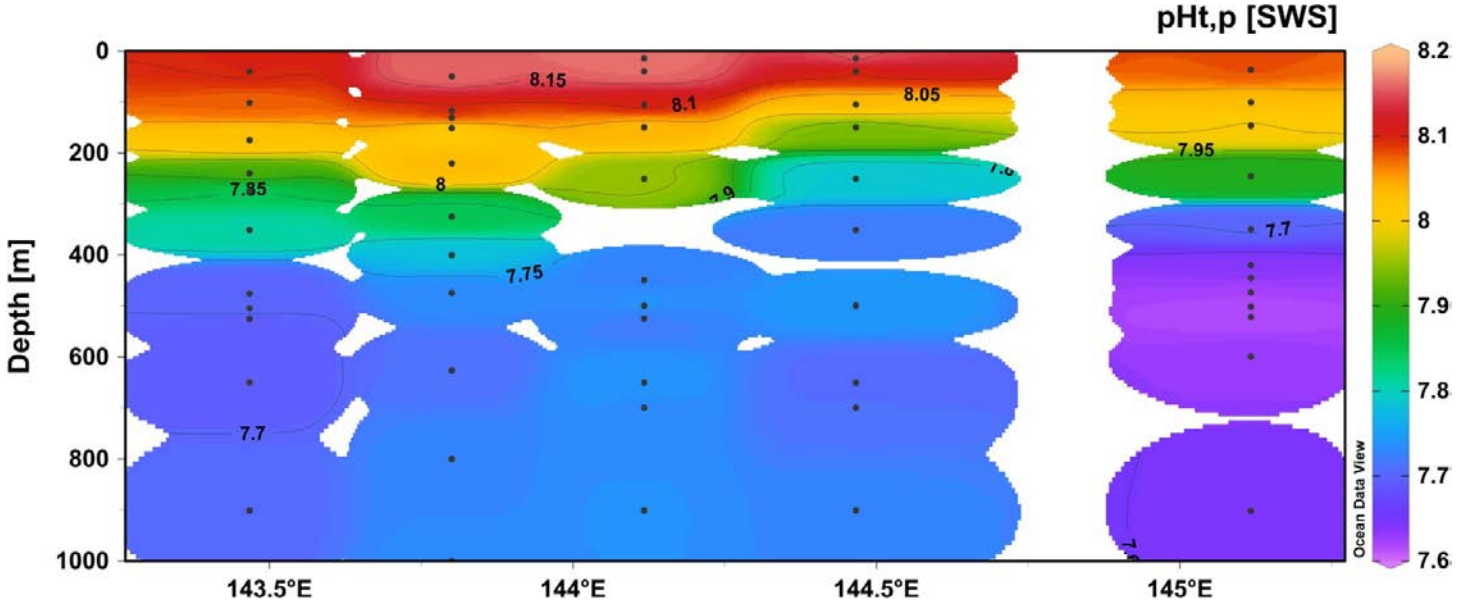

Figure 9$_{tm}$: pH along the E-W transect. Black points indicate samples.

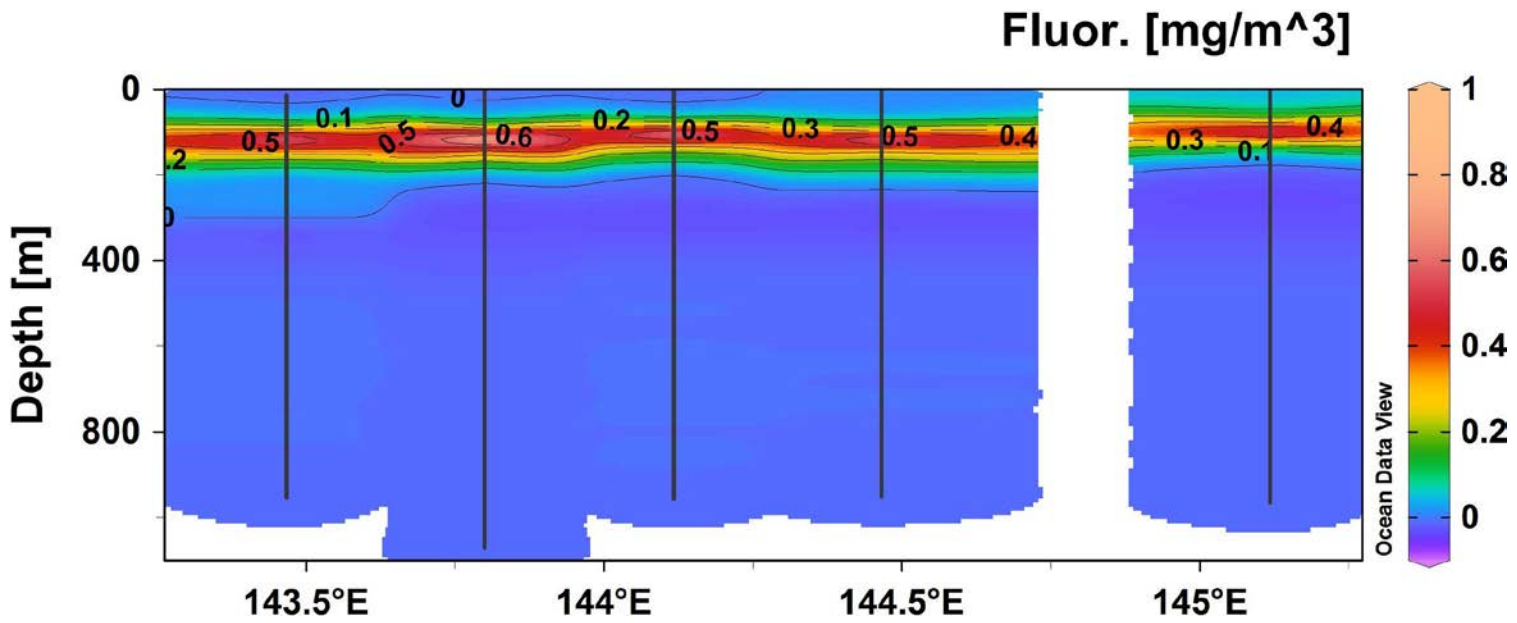

Figure 10$_{tm}$: Chlorophyll *a* along the E-W transect. Black lines indicate where sampling occurred.

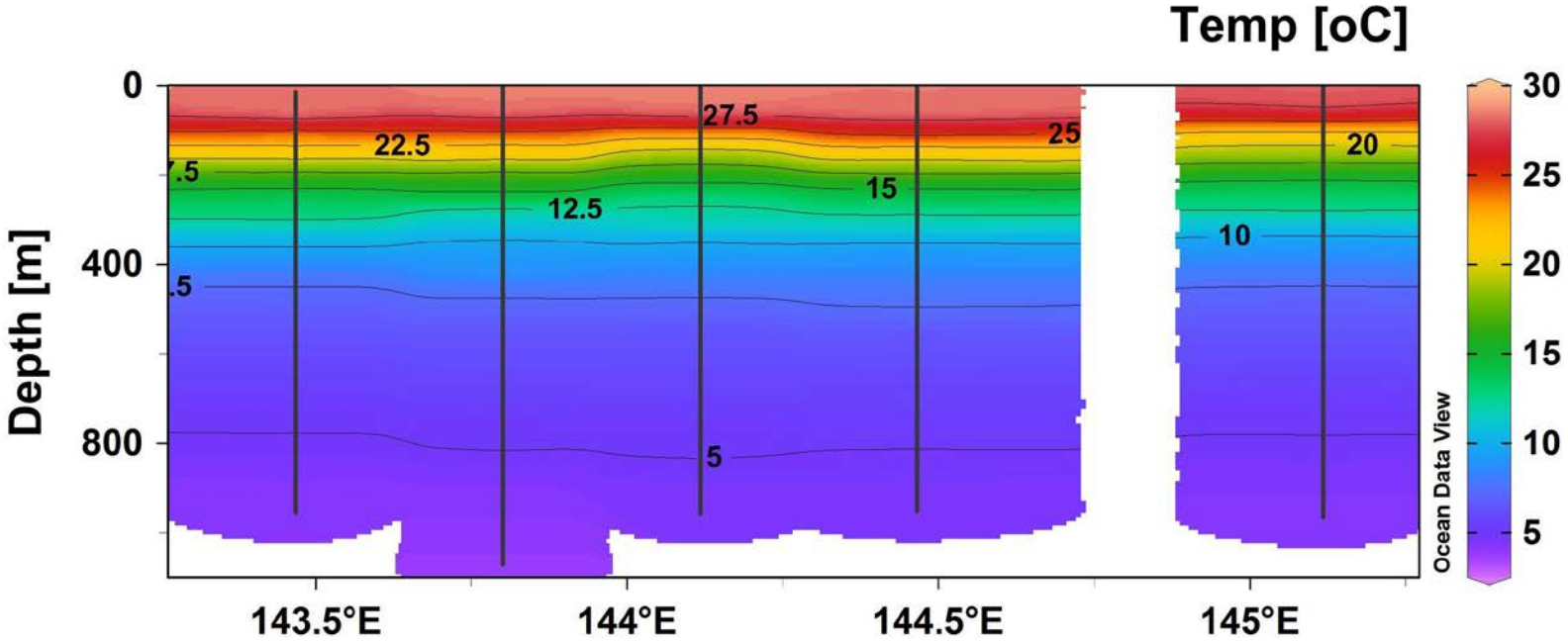

Figure 11$_{tm}$: Temperature along the E-W transect. Black lines indicate where sampling occurred.

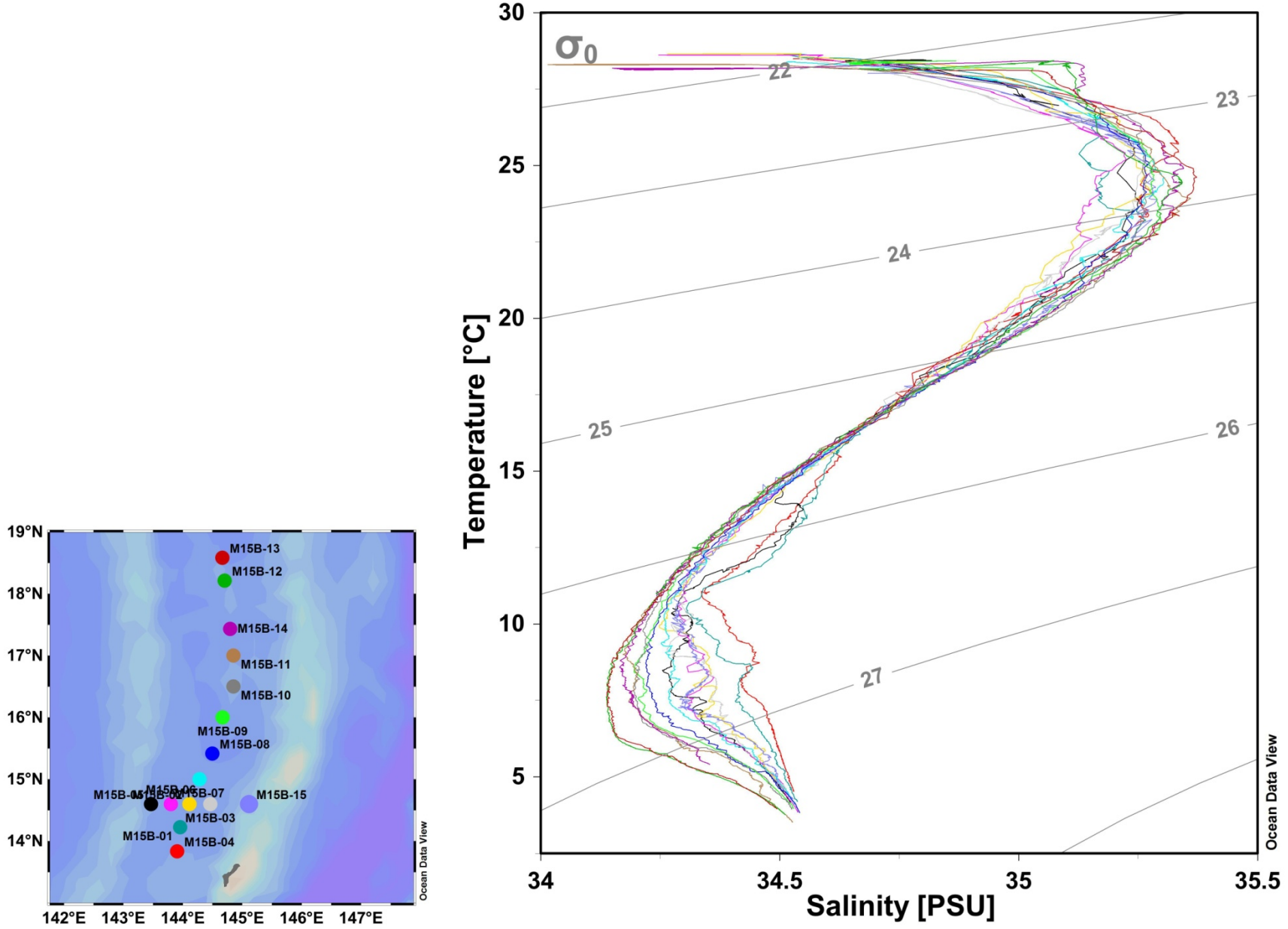

Figure 12$_{tm}$: Temperature-Salinity diagram for all stations sampled. The color of the station corresponds to the color of the T-S line, and the grey contours represent potential density (σ_θ).

Gas Chromatography

Dave Butterfield

The main goal of the gas chromatography work on this expedition was to measure dissolved methane and hydrogen concentrations in deep hydrocasts to help identify and characterize hydrothermal plume sources. The presence of enriched hydrogen gas concentrations in the water column indicates a nearby high-temperature vent fluid source. Extremely high hydrogen concentrations (e.g. > 50 nmol/L) are indicative of active eruption processes. Low-temperature vent fluids typically have very low hydrogen concentration, so enriched methane and low hydrogen in the water column may indicate a low-temperature source. Our intention was to use the GC results to try to characterize hydrothermal sources.

Methods and Setup

We installed Butterfield's SRI 8610 GC with flame ionization (FID, for methane) and pulsed discharge (PDD, for hydrogen) detectors. The instrument was set up in the starboard forward corner of the wet lab, with three gas tanks secured on the CTD bay deck. The hydrogen tank was kept inside a metal cabinet on deck with permanent ¼" stainless steel gas plumbing into the wet lab. High-purity air and helium were kept outside on the weather deck and 1/8" metal tubing was routed through a sealed opening into the wet lab.

Calibration standards at concentrations from 0.5 to 20 ppm were prepared from 100 ppm hydrogen or methane in nitrogen. Calibration was verified for every run day, and calibration slope was quite stable during the expedition. Additional lower level standards (0.05 ppm) were prepared and run to test detection limits. For small peaks (i.e. in most cases), we selected the baseline manually rather than use the auto-baseline feature of the software.

Samples for GC analysis were second in the overall draw order for Niskin samples, immediately following helium sampling. 140ml syringes with Luer slip stopcock valves were inserted directly into the Niskin sampling port valve, flushed with approximately 60 ml of sample, filled and flushed out to contain 100ml of sample with no air bubbles. The cast ID, Niskin rosette position, and unique syringe number were recorded on deck. 40 ml of high-purity helium was then added into the sample syringe (using a rubber septum attached to the sample syringe Luer fitting), excluding ambient air. Samples were shaken vigorously for 30 seconds to dissolved gas into the helium, allowed to equilibrate to room temperature, then shaken again. Gas was removed from the sample syringe into a dry syringe (to minimize water getting into the GC column through the ascarite/drierite injection tubes) and ~20ml slowly pushed into the injection port. Any suspect injections were repeated with the ~20ml gas remaining. Results were recorded on GC Data Sheets and transferred to an Excel spreadsheet for calculation of results.

Lab temperature and atmospheric pressure were recorded during each run, and used to calculate the molar volume of gas under lab conditions (24.45 liters/mole +/- 0.1). The concentration of the measured gas was calculated by dividing the peak area by the slope of the response curve,

and the original concentration of gas in the sample was calculated using the molar volume, the ratio of gas headspace to total sample volume, and the empirically determined efficiency of gas extraction into helium headspace (87%).

Results

We sampled the shallow trace metal casts as well as the deep hydrothermal casts. Dave Butterfield was the primary operator, but Tamara Baumberger also ran the GC when we had multiple CTD casts in a single day. Our techniques were identical, and there was no discernible difference in results between operators.

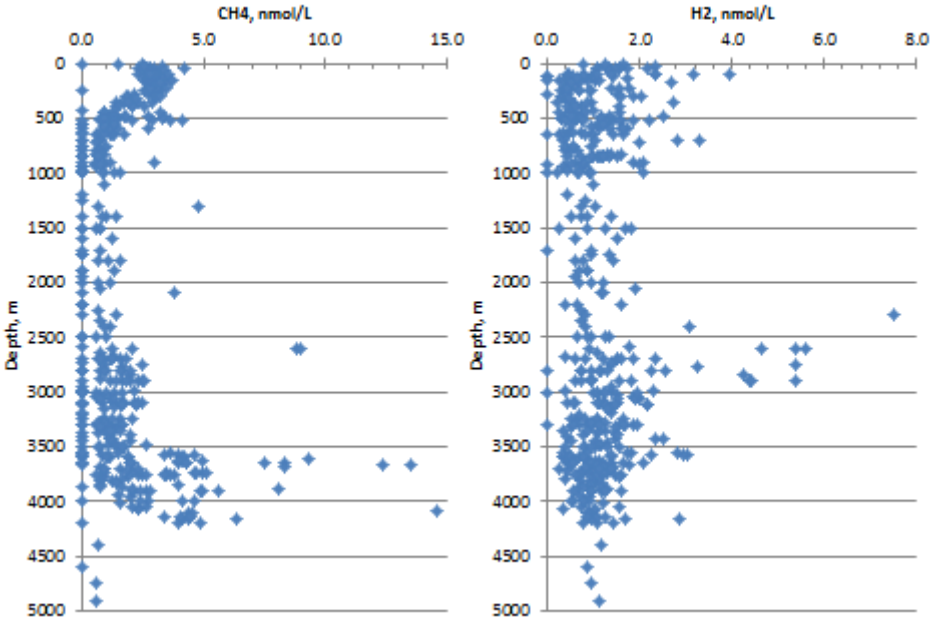

Figure 1_{gc}. Summary plot of methane and hydrogen versus depth for all samples. Surface water methane concentrations are near expected value for equilibrium with the atmosphere, and then decrease with depth. The same is generally true for hydrogen, but with much more variability in the upper 1000 meters. There is discernible (hydrothermal) methane enrichment from 2500 to 3500 meters, and substantial hydrothermal enrichment below 3500 m (generally < 500 m above seafloor). The largest hydrogen enrichment is much higher in the water column, suggesting it is associated with buoyant high-temperature sources rising through water with little density stratification. Methane close to the seafloor may be associated with very low-temperature, diffuse sources.

We analyzed nearly every Niskin sample collected (approximately 500), covering the entire depth range from the surface down to nearly 5000 meters. The summary plot (Figure 1) shows the general trends with depth, and Figure 2 shows how H2 and CH4 co-vary.

Note, many of the deep background samples are near or below the detection limit for methane, and to a lesser extent, for hydrogen. The detection limit for methane is determined by the noise level in the FID, and is approximately 1 nmol/liter for a 100/40 liquid/gas split. When it is working optimally, there is very little noise on the PDD where hydrogen elutes (near 0.9 minutes) resulting in a slightly lower detection limit near 0.6 nmol/liter for hydrogen. A typical

blank is shown in Figure 3. Opening the helium purge valve to fill syringes causes noise in the hydrogen detector, so we made it a practice not to fill syringes while running samples, and to wait for the detector to quiet down after using the helium supply.

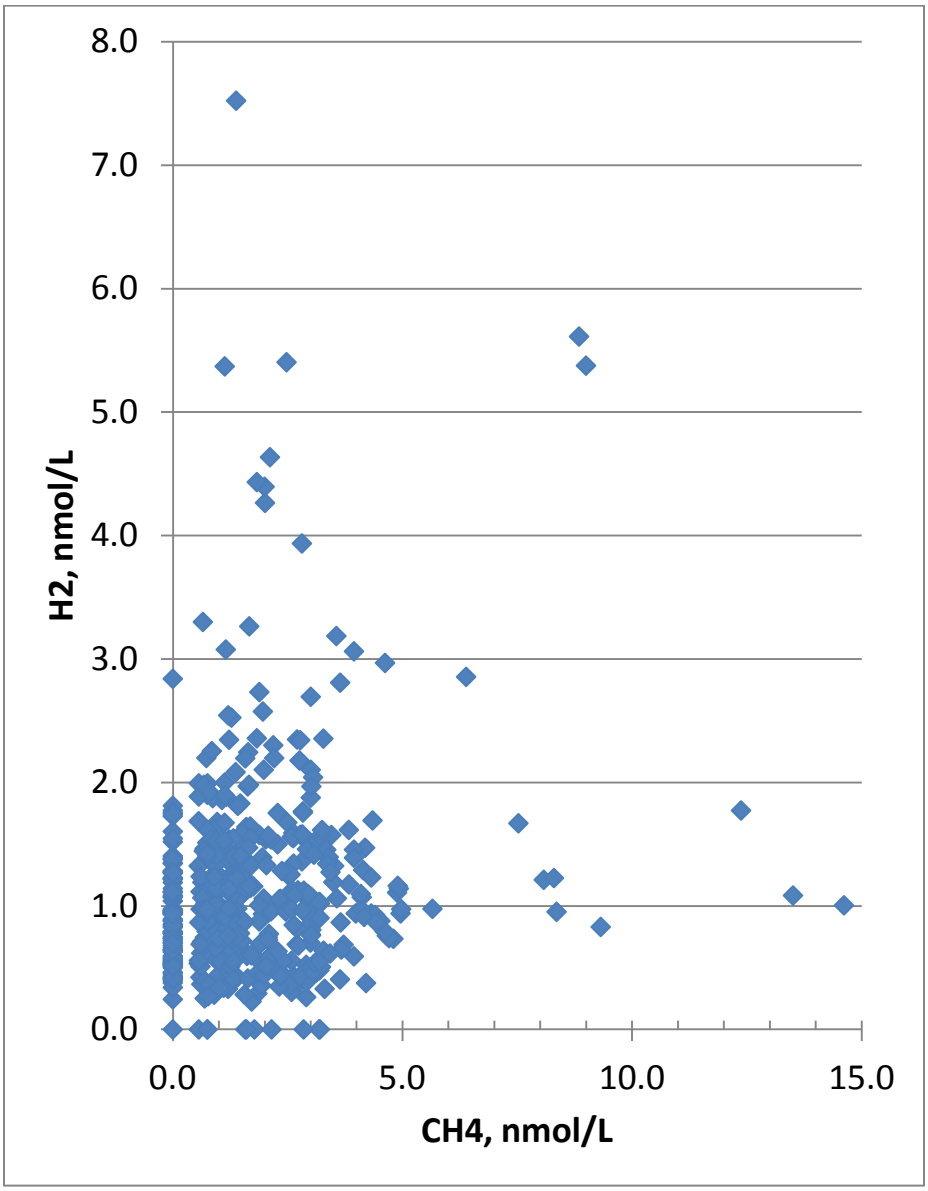

Figure 2_{gc}. Summary plot of hydrogen versus methane for all samples analyzed. Plumes are generally either high in hydrogen or high in methane, but not both.

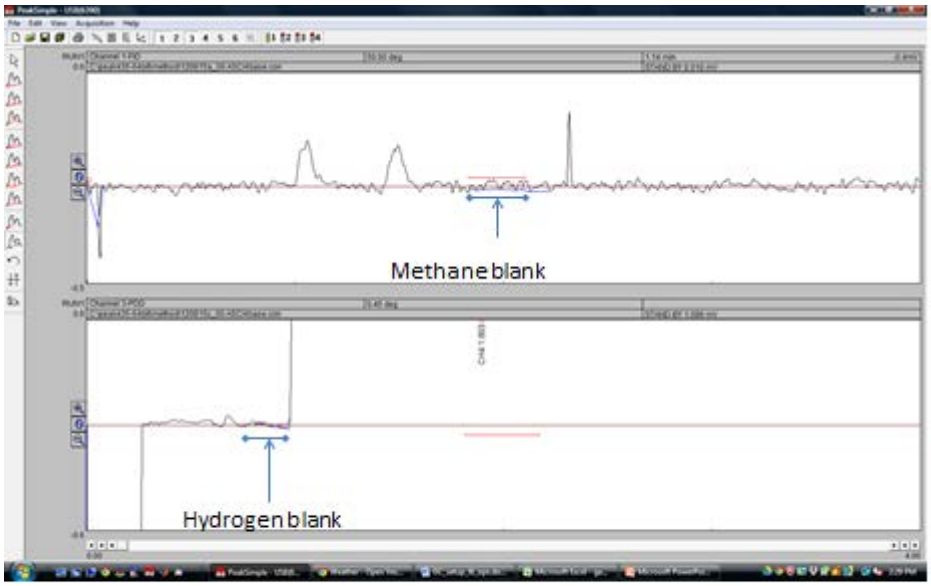

Figure 3_{gc}. Helium blank showing noise level for methane and hydrogen.

Near the end of the cruise, we conducted replicate tests, firing 6 Niskin samplers in rapid succession (as fast as triggering would allow, approximately once per second, over a vertical distance of 5-10 meters) and analyzing each of the samples for methane and hydrogen. One test was at 850 meters, and the other through the chlorophyll maximum near 100 m depth. The results are given in the table below. At 850 m, methane was below the detection limit, so RSD results are poor. Results for H_2 are representative of the precision for low-level H_2 (13% RSD, 1 sigma). Results for methane at 100 m are probably representative for levels slightly enriched above background (3 nM +/- 9%). There is an apparent fine-scale gradient in H_2 at the chlorophyll maximum, with concentration decreasing toward the surface, so the replicate results do not represent the precision of the analysis. The trend is intriguing and suggests photochemistry and/or active biological processes generating hydrogen. As this was found on the last day of the expedition, it could not be investigated further. Green algae are known to produce molecular hydrogen through photochemistry (Kruse and Hankamer, 2010, Current Opinion in Biotechnology). So far, I can find no reference of this chlorophyll-related hydrogen gradient phenomenon in the literature.

	Depth	Description	Average H2, nM	Std Dev H2, nM	RSD % H2	Average CH4, nM	Std Dev CH4, nM	RSD% CH4
n=6	850	deep low O2	1.23	0.16	13	0.24	0.37	155
n=6	100	Chlor Max	2.49	1.06	42	3.0	0.28	9.4

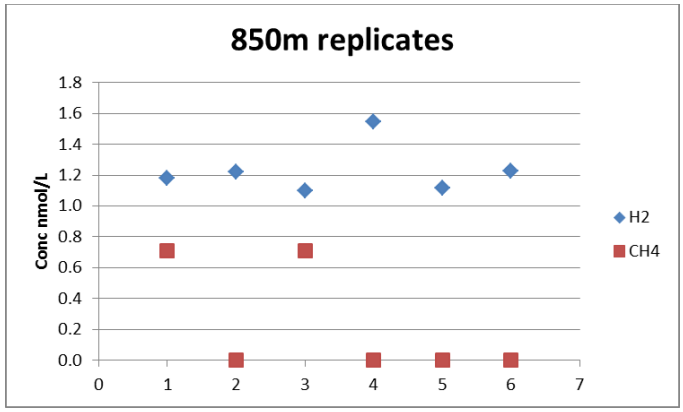

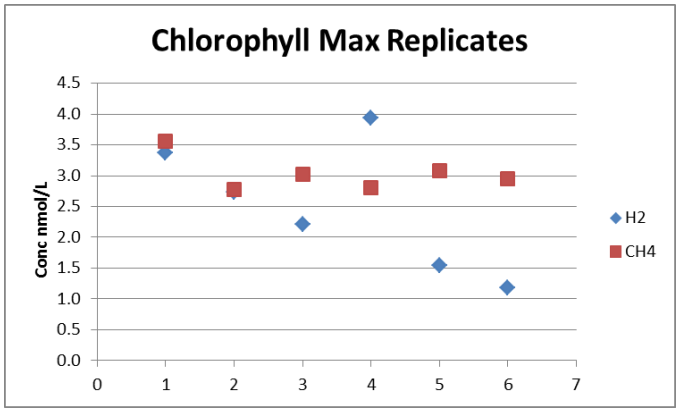

Figure 4_{gc}. Results of replicate sampling and analysis during upcasts. For the deep sample, CH4 is below the detection limit. For the chlorophyll max samples, there is an apparent trend of decreasing H2 (with one outlier) over a vertical distance of a few meters coming up through the feature.

For methane, we note that the surface waters are generally near the concentration expected for saturation with the atmosphere (approximately 3 nmol/L in surface water and 1.8 ppm in air). (We measured lab air and outside air frequently, and also verified air-saturation concentration of surface seawater experimentally). The lowest concentrations of methane are generally observed between 1000 and 2500 m depth. Samples below 2500 m show some influence from hydrothermal input.

Hydrogen concentration in air is approximately 0.4 ppm, and the air-saturated surface seawater concentration is approximately 1.3 nmol/liter. The hydrogen data show significant scatter because we are working close to the detection limit. Most of the surface ocean concentrations are close to the expected value for H_2, with some values in excess of air saturation. Non-plume samples below 1000 m depth are near or below the detection limit for H_2. The highest hydrogen concentration is close to 8 nmol/liter. The highest hydrogen concentrations do not occur in the same samples with the highest methane concentration, and we attribute this to fact that hydrogen is associated with high-temperature fluids (which may have relatively low methane), and methane may be enriched in low-temperature fluids. High concentrations of hydrogen are observed higher in the water column (more than 1000 m above the seafloor), consistent with a more buoyant, high-temperature source. Methane is more enriched near the seafloor, consistent with less buoyant, low-temperature sources. The extreme rise height of plumes as indicated by the hydrogen profiles is consistent with a negligent density gradient below 2500 m depth in the W. Pacific.

Helium Isotope Gas Sampling

Tamara Baumberger and John Lupton

Samples for water column helium isotopes were obtained from two different CTD rosette packages, the hydrothermal package and the trace metal package, respectively. Samples from the hydrothermal CTD were either collected during tow-yos or during vertical casts with focus on the deep water column to catch hydrothermal anomalies. To get an overview of the distribution of helium in the Mariana back-arc water column, 12 vertical water column profiles were done regularly geographically distributed. The most southern profile is located at 12°59' N and the most northern at 18°19' N with a spreading of roughly every 30'. The obtained samples cover the range from background seawater to strong hydrothermal anomalies right over active vents at the seafloor. In addition, vertical water column profiles for helium isotopes of the top 1000 m were collected during every trace metal cast. This will allow us to define if trace metals present in the shallow water column have a hydrothermal origin. All samples will be analyzed shore-based in the NOAA Helium Isotope Laboratory in Newport OR.

For helium isotope water column sampling at sea, a special hydraulic system is available for hermetically sealing seawater samples into copper tubing. Immediately upon recovery of the underwater CTD sampling package, air-free water samples were flushed through 24-inch long sections of refrigeration-grade Cu-tubing and sealed for later laboratory determinations of He isotope concentrations and ratios. At the Helium Isotope Laboratory in Newport OR, facilities available for the analysis of these samples include a high vacuum sample preparation system for processing copper tubing samples, and a 21-cm radius, dual-collector, sector-type mass spectrometer specially designed for helium isotope analyses. The mass spectrometer inlet is fitted with a low temperature cryotrap system that can separate He from Ne before the sample is analyzed. The mass spectrometer system can determine helium isotope ratios to a precision of 0.2 % in δ^3He, where δ^3He is the percentage deviation of ^{3}He/^{4}He from the atmospheric ratio.

During the Mariana back-arc cruise, 501 samples for helium isotope analysis were collected, 222 samples from tow-yos, 114 from vertical casts and 165 from trace metal casts.

Summary of samples obtained for helium isotope composition determination

Station	Tow	Vertical	Trace metal
T15B-01	19		
T15B-02	21		
M15B-01			11
T15B-03	20		
M15B-02			12
M15B-03			12
T15B-04	17		
M15B-04			10
M15B-05			9
T15B-05	19		
M15B-06			12
M15B-07			12
T15B-06	20		
M15B-08			11
V15B-01		17	
M15B-09			11
T15B-07	21		
M15B-10			10
T15B-08	6		
M15B-11			11
T15B-09	21		
V15B-02		20	
M15B-12			11
V15B-03		12	
M15B-13			10
T15B-10	17		
V15B-04		20	
M15B-14			11
M15B-15			12
V15B-05		14	
V15B-06		10	
T15B-11	20		
T15B-12	21		
V15B-07		21	
Total	222	114	165
Total overall 501			

AUV *Sentry* Dive Operations - Multibeam mapping and photo surveys

Bill Chadwick

The goals of the AUV *Sentry* dives were to supplement the CTD casts and tows to search for hydrothermal plumes along the Mariana back-arc, collect high-resolution multibeam bathymetry at the sites where new hydrothermal vent sites were found, and conduct photographic surveys of the seafloor in selected areas. AUV *Sentry* made 7 dives during the cruise. The first two dives (364 & 365) were "tow-yo dives" looking for plumes up in the water column 100's of meters above the seafloor. The last 5 dives (366-370) were focused on multibeam sonar mapping of sites where CTD ops had found hydrothermal plumes. Two of those dives (367 & 370) also included a photo survey of the seafloor. The following is a summary of the *Sentry* dives on this cruise:

AUV *Sentry* Dive Summary

• **363** - This was a test dive that was aborted before *Sentry* reached the bottom, due to problems with the acoustic communication and tracking. No useful science data were recorded, so this dive is ignored in the following.

• **364** - Tow-yo dive on 13.9°N back-arc segment (Map 3) - no plumes found. Initially had acoustic tracking but no comms. Acoustic troubleshooting found problems with interference from *Sentry*'s subbottom and with the ship's transducers. *Sentry* repeatedly overshot the top of tow-yo profiles. The PMEL ORP sensor was not logged by *Sentry* during this dive.

• **365** - Tow-yo dive on 14.5°N back-arc segment (Map 4) - small plume found. *Sentry* repeatedly overshot the top of tow-yo profiles. The PMEL ORP sensor was not logged by *Sentry* during this dive.

• **366** - Multibeam mapping dive on 14.5°N back-arc segment (Map 4) - in area where first plume was found on *Sentry* dive 365

• **367** - Multibeam mapping dive and photo survey on 15.1°N back-arc segment (Map 5) - after CTD tow-yo found venting. Centered *Sentry* dive on highest ORP anomalies. Discovered new lava flow in photos.

• **368** - Multibeam mapping dive on 18.2°N back-arc segment (Map 10) - centered on three previously known vent sites comprising the Alice Springs vent field.

• **369** - Multibeam mapping dive on 15.1°N back-arc segment (Map 5) - of the northern high-temp vent area found on CTD tow-yo (north of area mapped on *Sentry* dive 367).

• **370** - Multibeam mapping dive on 17.0°N back-arc segment (Map 8) - after CTD tow-yo found venting. Photo survey centered on highest ORP anomalies during CTD tow-yo and *Sentry*

multibeam survey (we shifted the photo survey 250 m N and E from its original position during the dive, based on the *Sentry* MAPR data, and that worked well).

AUV *Sentry* Operations Notes

Initially, there were problems integrating the *Sentry* and *Falkor* USBL acoustic communication systems. The problem was found to be related to incompatibility between firmware and software versions and was resolved after both were updated. The *Falkor* A-frame was used for launch and recovery of *Sentry* and that worked well.

The first two AUV *Sentry* dives that attempted to tow-yo in the water column were not as effective or efficient as we had hoped. When diving up from the bottom, the existing *Sentry* software put it in a panic mode that caused it to overshoot the desired upper depth limit, which could only be overridden manually by acoustic commands from the surface. The angle at which *Sentry* could drive up or down was also limited (~20-25°), and not as steep as we would have liked (~45-50°). *Sentry's* forward speed during tow-yos was also not as high as we had hoped. For these reasons, and because the *Falkor*'s CTD system proved to be capable of towing deeper than anticipated, after the first two *Sentry* dives, we decided to use the CTD for hydrothermal prospecting and limit the rest of the *Sentry* dives to multibeam mapping and photo surveys.

AUV *Sentry* Multibeam Surveys

The AUV *Sentry* multibeam sonar mapping dives were conducted such that the survey altitude was ~65-70 meters, the survey speed was ~1.8 knots, the line spacing of the survey tracklines was ~180 meters. This yielded a lateral resolution of about 1.5 meters. The dive durations varied from dive to dive (15-33 hours), so the area surveyed also varied. The multibeam surveys were rectangular boxes between 2.8-4.8 km in the long dimension and between 1.3-2.5 km in the short dimension. The areas surveyed ranged from 3.6 km^2 on dive 366 to 10.6 km^2 on dive 368. During the two photo surveys, the altitude above bottom was ~5 m and the trackline spacing was either 25 or 50 m. The photos survey areas were 450 x 900 m on dive 367 (~6 hours) and 600 x 800 m on dive 370 (~12 hours). During dive 370, acoustic data from the MAPR were transmitted to the surface and based on this information the photo block was re-targeted successfully.

The multibeam mapping sonar on the vehicle is a Reson 7125 400 kHz multibeam sonar. A MAPR instrument supplied by NOAA/PMEL was also integrated into the *Sentry* logging system (it also recorded internally) - those results are reported in a separate section of this report. USBL updates were given periodically throughout each mission when the AUV was within range of the ship and these were incorporated into the AUV navigation in post-processing. Vehicle configurations, sensor performance, vehicle statistics, and post-dive summaries are detailed in the WHOI operations report "*Sentry* Operations Report for the FK151121 Resing Cruise." The bathymetric maps that follow are preliminary and reflect the data processing that was done at sea by the WHOI/*Sentry* group. Additional data processing will be done to improve them further, but these maps show the extent of the surveys and the morphology of the seafloor at each site.

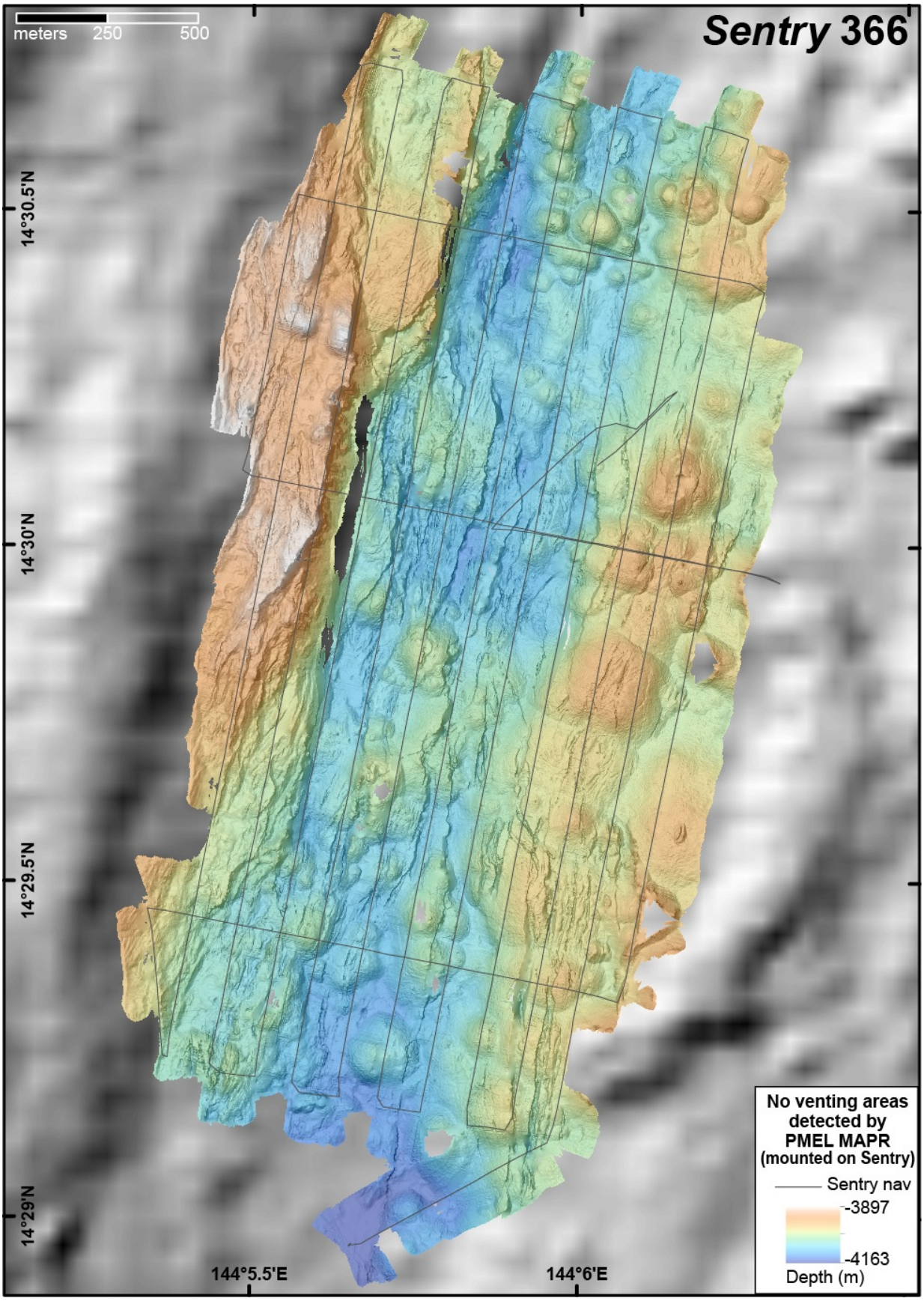
Sentry 366
meters 250 500
14°30.5'N
14°30'N
14°29.5'N
14°29'N
144°5.5'E
144°6'E
No venting areas detected by PMEL MAPR (mounted on Sentry)
Sentry nav
-3897
-4163
Depth (m)

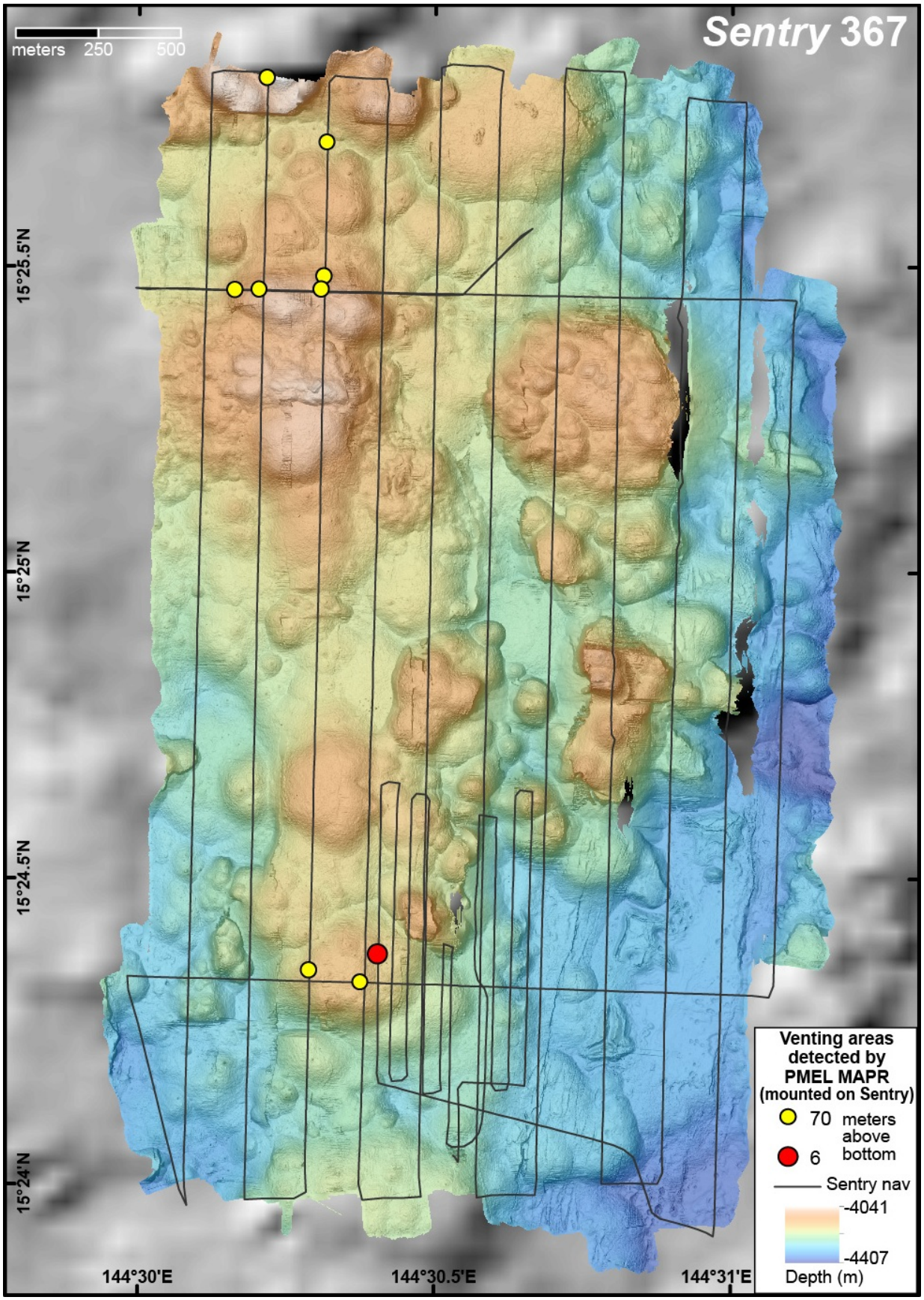
Sentry 367
meters 250 500
15°25.5'N
15°25'N
15°24.5'N
15°24'N
144°30'E
144°30.5'E
144°31'E
Venting areas detected by PMEL MAPR (mounted on Sentry)
70 meters above bottom
6
Sentry nav
-4041
-4407
Depth (m)

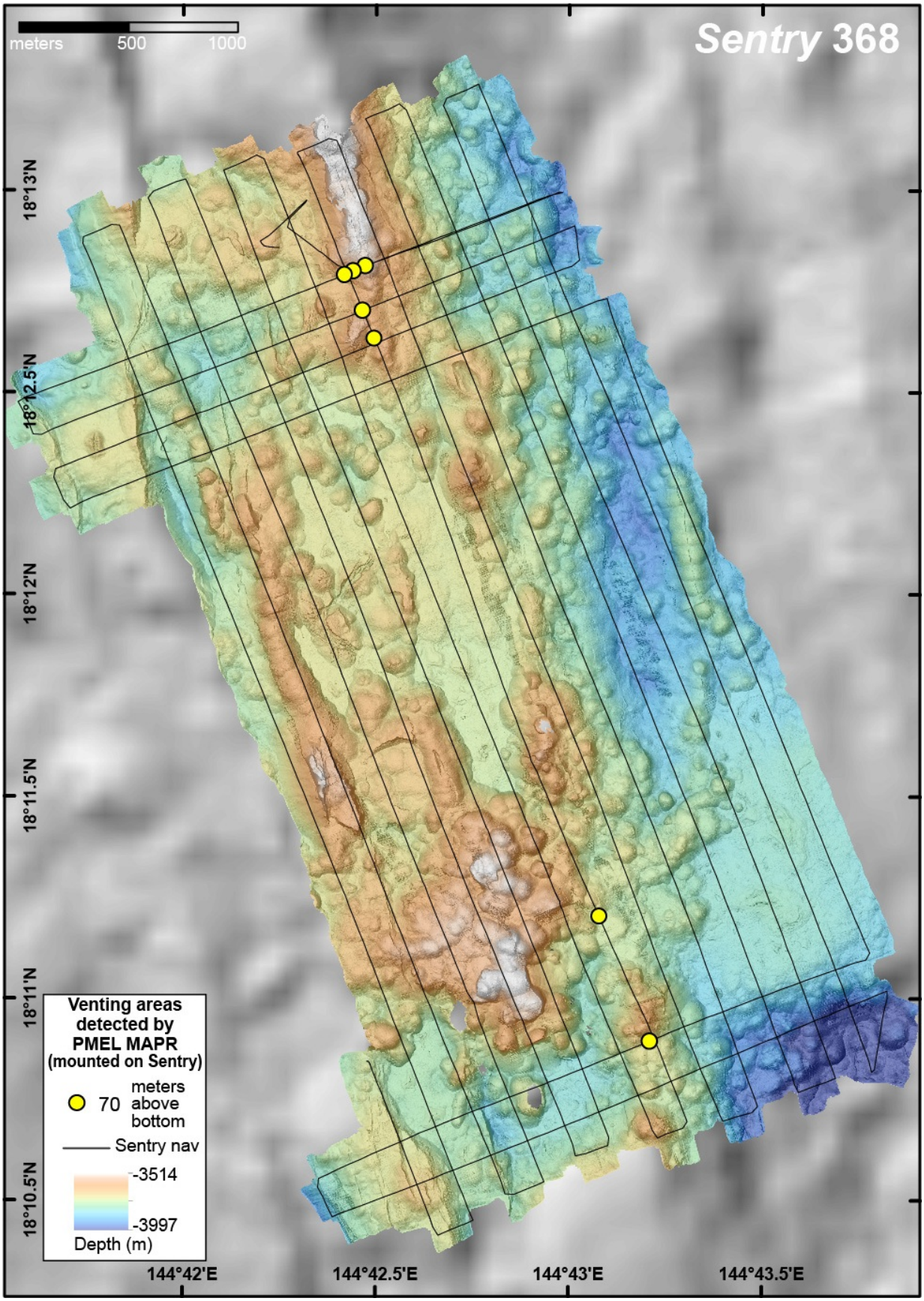
Sentry 368
meters
500
1000
18°13'N
18°12.5'N
18°12'N
18°11.5'N
18°11'N
18°10.5'N
144°42'E
144°42.5'E
144°43'E
144°43.5'E
Venting areas detected by PMEL MAPR (mounted on Sentry)
70 meters above bottom
Sentry nav
-3514
-3997
Depth (m)

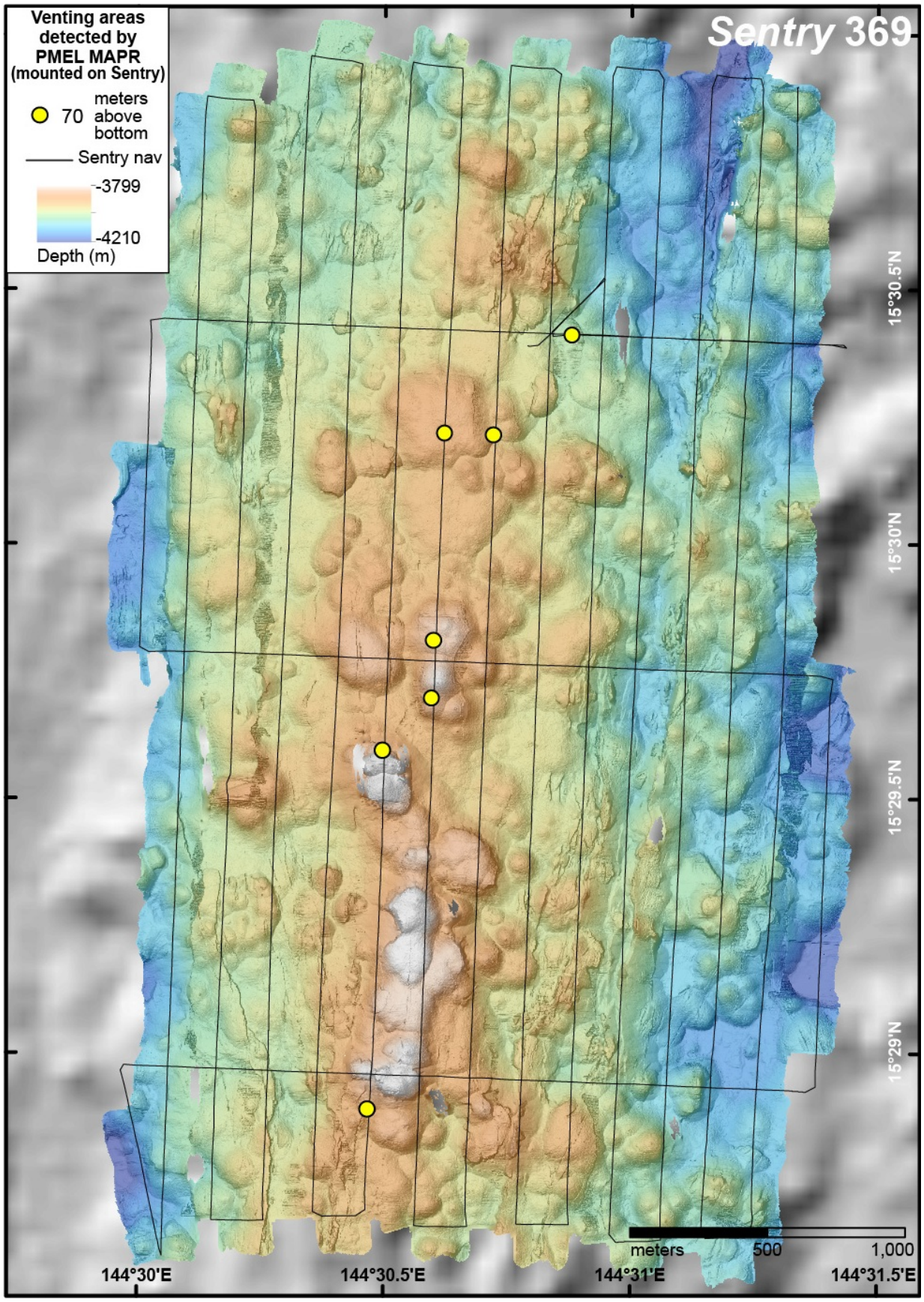
Venting areas detected by PMEL MAPR (mounted on Sentry)
70 meters above bottom
Sentry nav
-3799
-4210
Depth (m)
Sentry 369
15°30.5'N
15°30'N
15°29.5'N
15°29'N
meters
500
1,000
144°30'E
144°30.5'E
144°31'E
144°31.5'E

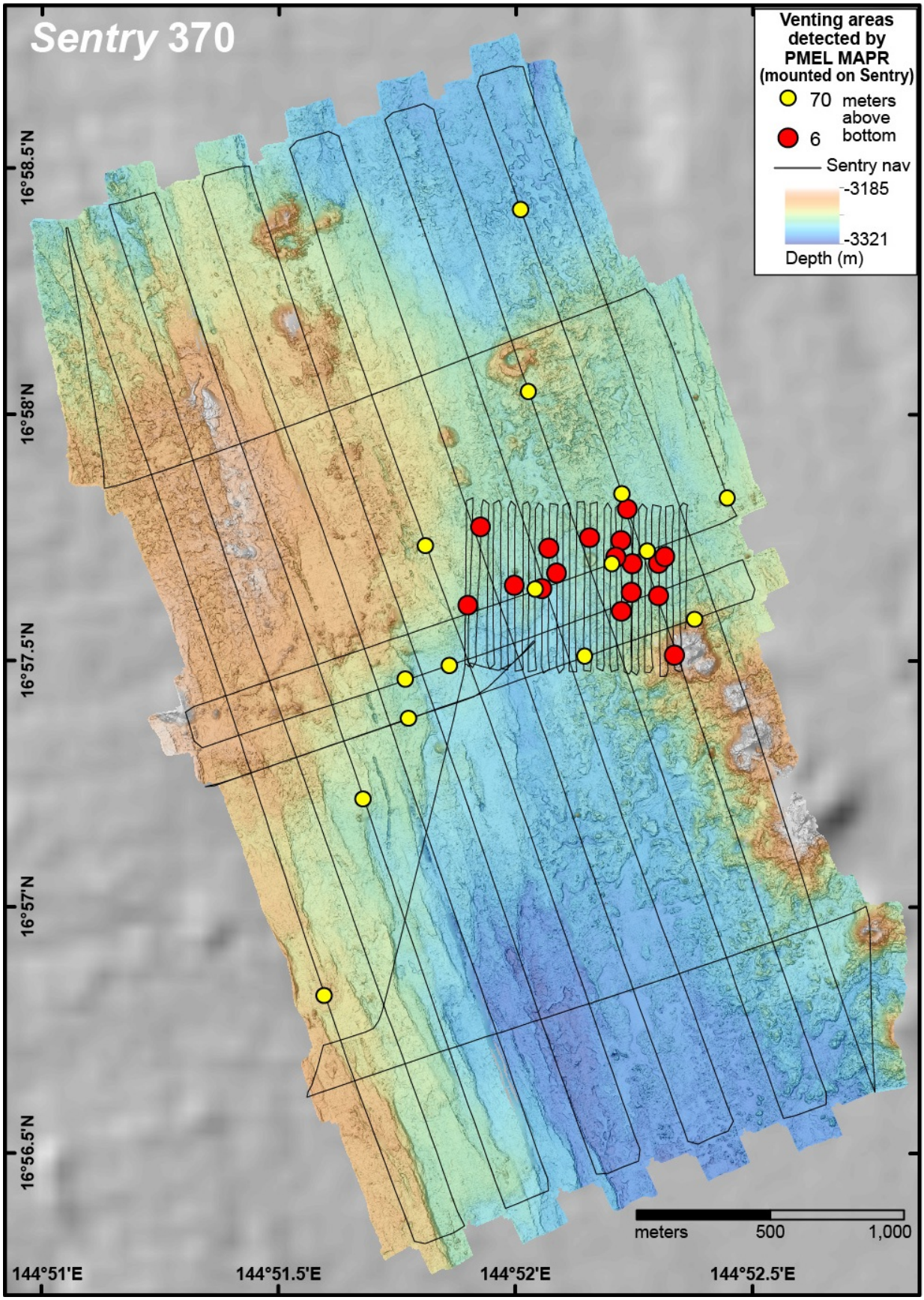
Sentry 370
Venting areas detected by PMEL MAPR (mounted on Sentry)
70 meters above bottom
6
Sentry nav
-3185
-3321
Depth (m)
16°58.5'N
16°58'N
16°57.5'N
16°57'N
16°56.5'N
144°51'E
144°51.5'E
144°52'E
144°52.5'E
meters
500
1,000

AUV *Sentry* Photo Surveys

The two photo surveys on AUV *Sentry* dives 367 and 370 provide valuable geologic data. The photos from dive 367 on back-arc segment 15.5°N (Map 5) can be used to map part of the boundary of the 2013-2015 lava flows.

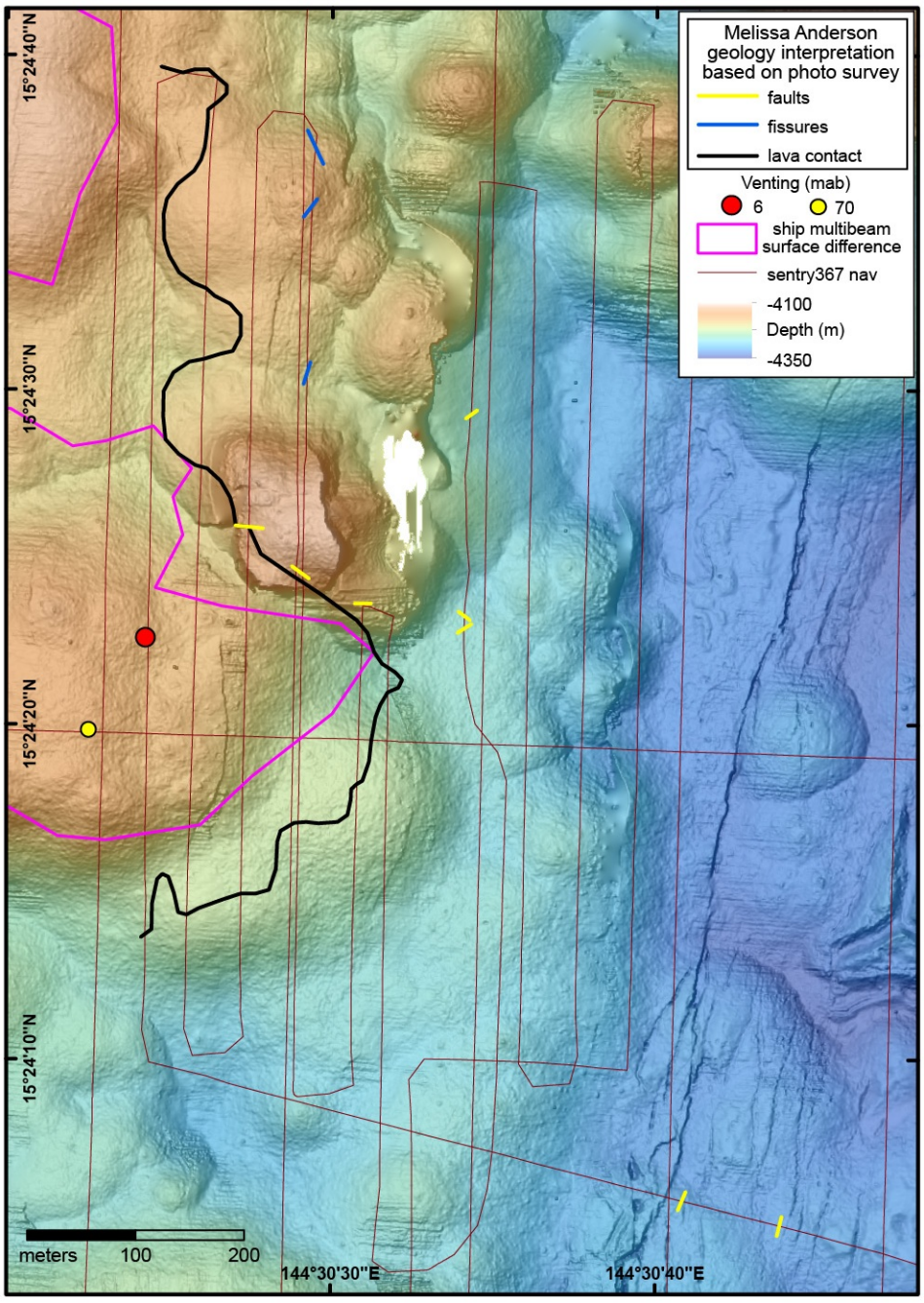

The photo survey during AUV *Sentry* dive 370 on back-arc segment 17.0°N (Map 8) photographed many sulfide chimney - most inactive, but several that were clearly active. The photos also show microbial mats and vent animals (squat lobsters, anemones, possibly snails) living at some of the vents.

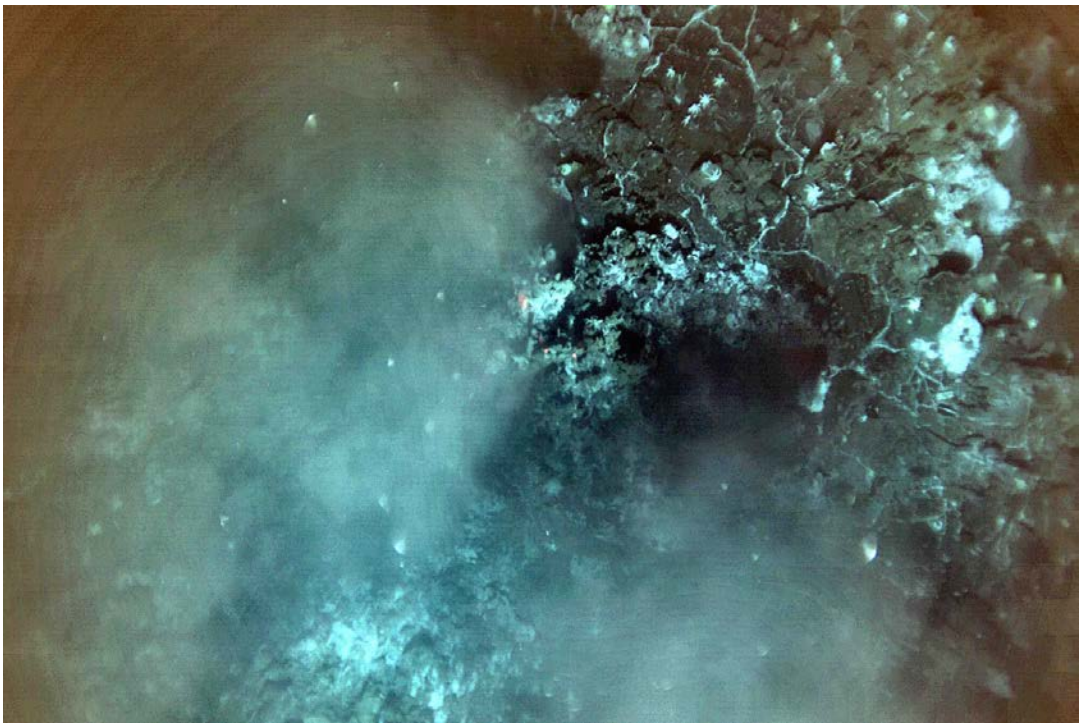

Sentry photo (2015-12-15-13:51:05) showing smoke from an active sulfide chimney and vent animals.

.

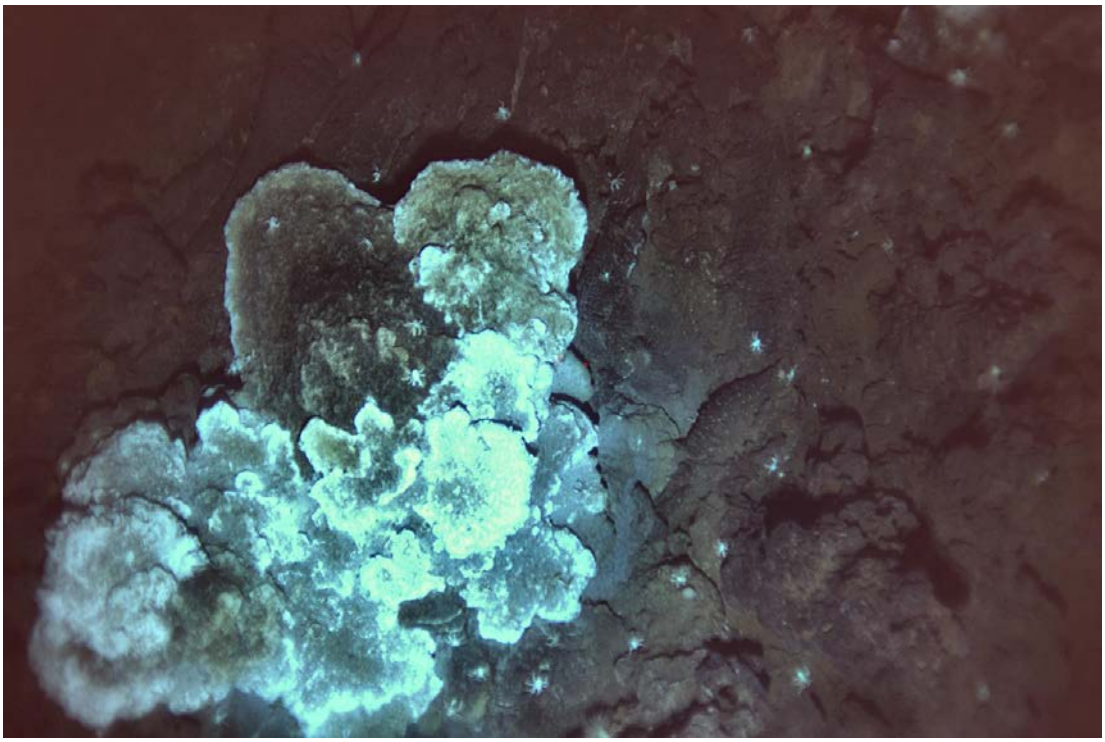

Sentry photo (2015-12-15-20:29:22) showing an active sulfide chimney covered with microbial mats and animals with shimmering water visible in lower left.

AUV *Sentry* MAPR Data Summary

Sharon Walker

One PMEL MAPR (Miniature Autonomous Plume Recorder) was mounted onto AUV *Sentry* for all eight (8) dives. While *Sentry* has optical backscatter and ORP sensors integrated into its sensor suite, the MAPR provided redundancy in case of sensor failure and cleaner data because the MAPR sensors were powered independently and isolated from the *Sentry* power system which causes the integrated sensors to be much noisier. The data described here are from the MAPR sensors. We utilized a new capability for MAPR use on *Sentry* this cruise - the MAPR data were integrated into the *Sentry* data pipeline by capturing the serial output string from the MAPR and combining it with *Sentry* navigation data. We discovered during the cruise that a time offset between MAPR time and *Sentry* time developed through the course of a dive, resulting in ~1.5 minute mismatch by the end of a 24 hr dive. Corrections have not been applied. Target positions identified below (Table 1_{MAPR}) are based on temperature, dNTU, ΔE_{max}, and/or dE/dt anomalies in the MAPR data downloaded from the instrument. Assuming an average Sentry speed of 1.2 m/s (2.3 knots) during mapping missions at ~70 meter above bottom (mab), these positions may have an uncertainty of up to ~50-100 m.

***Sentry*-363:** This dive was intended to be a tow-yo mission to compare *Sentry* tow-yo results with CTD tow-yo results in the area of the known "Snail" vent on the Mariana back-arc segment centered at 12.8°N (Map 1). The dive was aborted due to *Sentry* navigation system failures. MAPR data are useful as a background profile to 1665 m (specific location will have to be obtained from the ship navigation records).

***Sentry*-364:** Tow-yo mission to explore the Mariana back-arc along-axis from 13°52.8'N to 14°06.1'N (13.88-14.1°N; Map 3) for hydrothermal activity. No significant dNTU or ORP anomalies were found during this dive.

***Sentry*-365:** Tow-yo mission to explore the Mariana back-arc along axis from 14.44-14.58°N (Map 5). A weak particle anomaly ($dNTU_{max}$ = 0.012) with associated ORP signals (ΔE_{max} = -1.7 and -2.3 mv) occurred between 14°29.64'N and 14°30.18'N (14.4440-14.5030°N) at 3750-3800 m water depth. CTD tow T15B-05 repeated the *Sentry* trackline through the plume area to obtain water samples. Figure 2_{CTD} shows results from both *Sentry*-365 and CTD tow T15B-05 in the area of this plume for comparison (see also summary of results for T15B-05).

***Sentry*-366:** This dive was a high-resolution mapping mission in the area of the plume found during *Sentry*-365 and CTD tow T15B-05. *Sentry* altitude was ~70 mab; no significant dNTU or ORP anomalies were found. Additional analysis will determine if any temperature anomalies were present.

***Sentry*-367:** The first 16.5 hours of this dive were dedicated to high-resolution mapping of the seafloor (altitude ~70 m) in the area of the particle-poor/ORP-intense plume discovered during

CTD tow T15B-06 (between 15°18'N and 15°28'N (15.3000-15.4667°N)). The final 6 hours of the dive were spent doing a photo survey at an altitude of ~6 m (which revealed a new lava flow in this area). The dNTU profile for *Sentry*-367 descent showed a particle layer (dNTU = 0.013) at 3360 m that was separate from a less intense deeper layer (dNTU = 0.004) at 3700-4000 m. The shallower particle anomaly was not seen during CTD tow T15B-06 because the vertical excursions were all below this depth through this plume area. It is worth noting that neither particle layer was seen during vertical cast V15B-06 ten days later, however this cast did reveal an ORP anomaly (ΔE_{max} = -14 mv) from 3750 m to the bottom (i.e., the bottom 400 m of the water column). The mapping portion of the dive showed a broad area of ORP anomalies overlying the new lava flows (as defined by repeat ship-based multibeam mapping – see mapping section). Seafloor target locations (Table 1_{MAPR}) were selected based on greatest ΔE_{max} values and/or dE/dT exceeding -1.5 mv/5-seconds. MAPR data are included as separate objects (temperature, dNTU, ΔE_{max}, and dE/dt < -1.5 mv/5 sec) for each portion (mapping and photo survey) of the dive in Fledermaus scene file "Map5-NewLavaFlow-*Sentry*367-369-T15B06.scene".

***Sentry*-368:** This dive was a high-resolution mapping mission (~70 mab) in the area of previously known vent sites (Ilium, Alice Springs, Burke and Central Trough; from Hessler 1989). There were six obvious temperature spikes (ΔT = 0.03-0.09°C) during this dive at altitudes of 70-90 mab. The temperature spikes were short-lived (~30-seconds to 1.5 min) and were all concurrent with ORP anomalies (ΔE_{max} = -1.5 to -20 mv). The only prominent dNTU anomaly encountered during *Sentry*-368 (dNTU = 0.011) was located over the "Burke" vent site, which was also directly beneath the particle/ORP plume seen during T15B-09 (see Figure 4_{CTD} and Fledermaus scene file "AliceSpringsSegment-CTDandMAPRdata.scene"). Target locations for seafloor sources are based on these anomalies (Table 1_{MAPR}) and line up very closely with the published locations for the previously-known vent sites. These vents were reported to have temperatures as high as 287°C, but were described as "clear" in earlier papers, so our results suggest these vents, with the exception of the Burke vent, continue to emit particle-poor fluids.

***Sentry*-369:** This dive was a mapping mission (~70 mab) in the area of the higher-intensity particle plumes see during T15B-06 (north of the new lava flow; Map 5). Anomalies were characterized by dNTU anomalies correlated with ORP signals (dNTU = 0.017; ΔE_{max} = -49 mv). Potential seafloor targets were identified by dNTU, ΔE_{max}, dE/dt (Table 1_{MAPR}). Only one of these positions also has an obvious temperature anomaly. The data from this dive are also included in the "Map5-NewLavaFlow-*Sentry*367-369-T15B06.scene" Fledermaus scene file.

***Sentry*-370:** The final *Sentry* dive of the cruise was a combination mapping/photo survey dive in the area of the plume found during CTD tow T15B-12 (Map 8). This site has a broad swath of hydrothermal anomalies (dNTU = 0.028; ΔE_{max} = -104 mv; and ΔT = 0.13°C) at 70 mab that are oriented SW-NE relative to the CTD tow trackline. This is quite different from the anomalies seen at Alice Springs and above the new lava flows which appear to have more focused

anomalies (except for the ORP anomalies which are broadly distributed over the new lava flow). The photo survey (~6 mab) covered a small portion of the total area where anomalies were seen during the mapping survey, but several significant anomalies were detected (maximum values for dNTU = 0.036; ΔE_{max} = -80 mv; and ΔT = 0.32°C). Seafloor targets were selected from both the mapping and photo survey portions of the dive (Table 1_{MAPR}; see Fledermaus scene file "Map8-*Sentry*370-T15B12.scene").

NOTE: Contact Sharon Walker for Fledermaus scene files discussed in this summary. sharon.l.walker@noaa.gov Fledermaus scenes can be viewed with free software (iView4D) downloadable at: http://www.qps.nl/display/fledermaus/iview

Positions listed in following Table1_{MAPR} are plotted on the *Sentry* maps in previous section "AUV *Sentry* Multibeam Surveys".

Table 1_{MAPR} Target positions based on temperature, particle (dNTU), and ORP (ΔE or dE/dt) anomalies from MAPR data during *Sentry* dives (unless otherwise noted)

Location/Operation	Longitude °E	Latitude °N	Anomaly type
15.5 N - New Lava Flow (Map 5)			
***Sentry*-367 (70 mab)**	144.506258	15.405505	dE/dt > 1.5 mv/5sec
	144.504804	15.405836	dE/dt > 1.5 mv/5sec
	144.505193	15.424734	dE/dt > 1.5 mv/5sec
	144.505276	15.428390	dE/dt > 1.5 mv/5sec
	144.503373	15.424378	dE/dt > 1.5 mv/5sec
	144.502695	15.424366	dE/dt > 1.5 mv/5sec
	144.505119	15.424377	largest ΔE
	144.503592	15.430146	largest ΔE
***Sentry*-367 (6 mab)**	144.506743	15.406271	ΔT, ΔE, slight dNTU
***Sentry*-369 (70 mab)**	144.507803	15.481481	ΔT, ΔE, dNTU
	144.508293	15.493226	ΔE and dNTU
	144.510005	15.496834	ΔE and dNTU
	144.509944	15.494938	ΔE and dNTU
	144.510372	15.503623	ΔE and dNTU
	144.512023	15.503563	ΔE and dNTU
	144.514673	15.506838	ΔE only
T15B-06	144.513002	15.528015	location below dNTU plume seen in tow
17 N (Map 8)			
***Sentry*-370 (70 mab)**	144.864338	16.958176	ΔT, dNTU, ΔE
	144.867358	16.960760	ΔT, dNTU, ΔE
	144.870069	16.961617	ΔT, dNTU, ΔE
	144.870403	16.963991	ΔT, ΔE
	144.863504	16.962221	ΔT, dNTU, ΔE
	144.871304	16.962048	ΔT, dNTU, ΔE
	144.859947	16.946986	ΔT, dNTU
	144.861303	16.953641	ΔT, dNTU, ΔE
	144.862910	16.956373	ΔT, dNTU, ΔE
	144.862786	16.957707	ΔT, dNTU, ΔE
	144.869107	16.958493	ΔT, dNTU, ΔE
	144.867123	16.967440	ΔT, dNTU, ΔE
	144.866837	16.973609	ΔT, dNTU
	144.872972	16.959729	ΔT, dNTU, ΔE

Location/Operation	Longitude °E	Latitude °N	Anomaly type
	144.874120	16.963839	ΔT, dNTU, ΔE
***Sentry*-370 (6 mab)**	144.865000	16.960200	ΔT, ΔE, dNTU
	144.865448	16.962855	ΔT, ΔE
	144.866632	16.960889	ΔT, ΔE, dNTU
	144.867600	16.960770	ΔT, ΔE, dNTU
	144.867840	16.962142	ΔT, ΔE
	144.871700	16.961630	ΔT, ΔE, dNTU
	144.870600	16.963460	ΔT, ΔE, dNTU
	144.868120	16.961296	ΔT, ΔE, dNTU
	144.870377	16.962394	ΔT
	144.870781	16.961621	ΔT, ΔE
	144.870196	16.961845	ΔT, ΔE, dNTU
	144.871696	16.960530	ΔT, ΔE, dNTU
	144.870397	16.960002	ΔT, ΔE, dNTU
	144.871931	16.961866	ΔT, ΔE
	144.870743	16.960649	ΔT, ΔE
	144.869278	16.962501	ΔT, ΔE, dNTU
	144.872264	16.958532	dNTU generally elevated in southeast corner of photo survey box. Slight temp increases and ORP anomalies
18 N - Alice Springs Area (Map 10)			
***Sentry*-368 (70 mab)**	144.707869	18.213564	ΔT, ΔE
	144.707341	18.213336	ΔT, ΔE
	144.706975	18.213190	ΔT, ΔE
	144.707748	18.211714	ΔT, ΔE
	144.720180	18.181568	ΔT, ΔE, dNTU
	144.708262	18.210553	ΔT, ΔE
	144.717994	18.186712	ΔT, ΔE

Geologic Observations and *Falkor* EM302 Multibeam Bathymetric Mapping

Bill Chadwick, Susan Merle, & Melissa Anderson

The 2013-2015 lava flows discovered on the 15.5°N back-arc segment

One of the most surprising discoveries during the cruise was finding glassy unsedimented lava flows on the 15.5°N segment (Map 5), indicating that there had been a recent eruption on this segment. The area was identified by a bottom hugging hydrothermal plume with no optical signals and high ORP signals during CTD tow T15B-06. We thought that this indicated a large area of diffuse, low-temperature venting that could readily be mapped and photographed by *Sentry*. We targeted AUV *Sentry* dive 367 in the area of those CTD signals, and the dive collected multibeam bathymetry and then did a photo survey of the seafloor centered on the location of the highest ORP signal from the CTD tow. Our reasoning was that we might have a good chance of seeing vent animals in an area with low-temperature venting. Instead, when we got the photos back we found an amazingly pristine lava flow with dark glassy pillow and lobate lavas with little or no sediment on them!

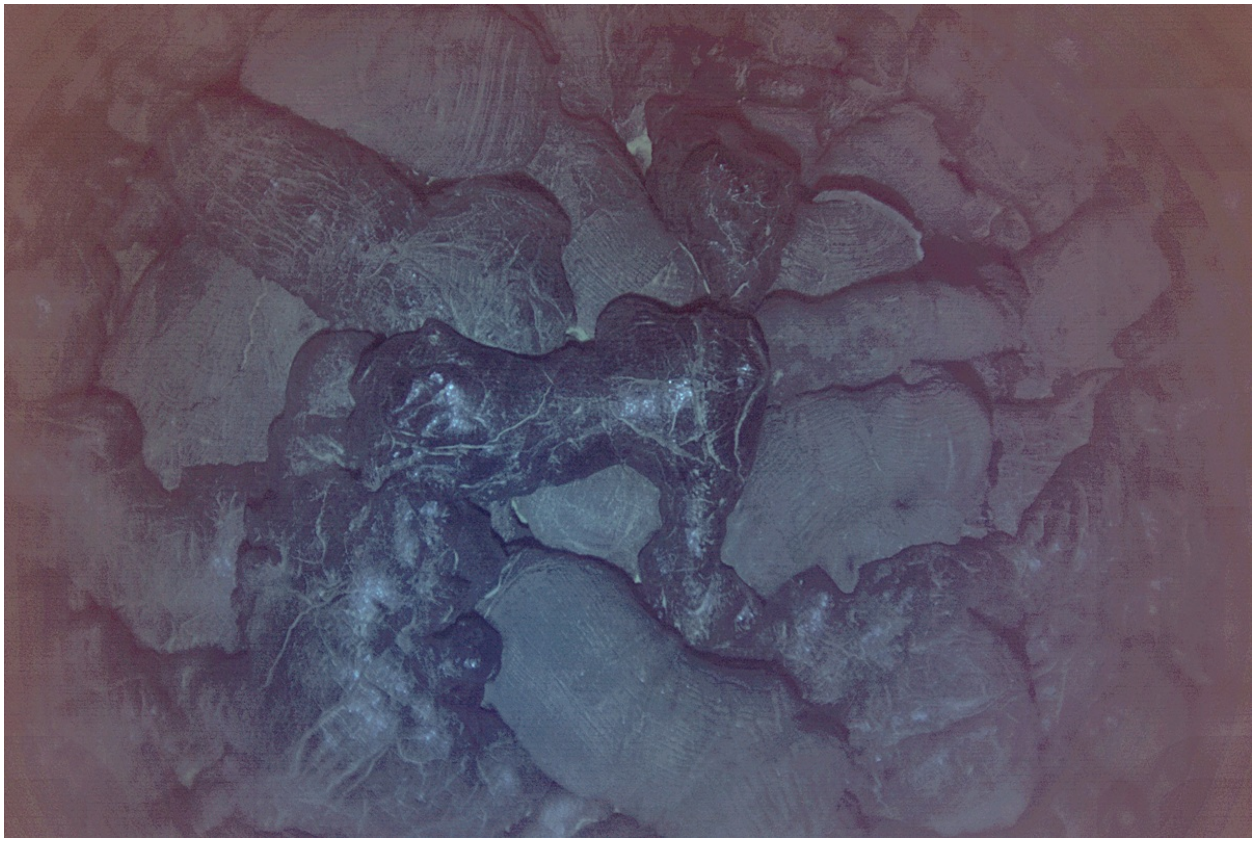

We also photographed at least one area with cloudy water venting out of the lava flow (2015-12-03, 07:05:53), evidence that it was still warm. We could map the young lavas to some extent from the photo survey, but the area of the lava flow(s) was clearly much larger than the relatively small photo survey (roughly 900 m x 450 m). The multibeam bathymetry from *Sentry* dive 367

shows the new lava flows are clearly constructed of steep-sided hummocky pillow mounds and are surrounded by older flows with the same morphology.

The next step was to compare the *Falkor* EM302 bathymetry we had just collected over this segment (on December 1) to the most recent previous survey that we knew of. Fortuitously, we had asked Doug Weins and Patrick Shore to collect some multibeam data over the back-arc axis in 2013 during an ocean-bottom seismometer cruise. That earlier survey (Cruise MV1302a on R/V *Melville* with an EM122 system) collected data over the site on Feb 14, 2013, which effectively brackets the timing of the eruption within a window of less than 3 years. However, the very appearance of the lava flows, the lack of sediment, and the hydrothermal venting all suggest the time since the eruption was much less than that - perhaps on the order of months. On the other hand, the lack of hydrogen in the CTD water samples over the site means that the eruption had to be older than a few weeks or a month (and that it was certainly not still on-going).

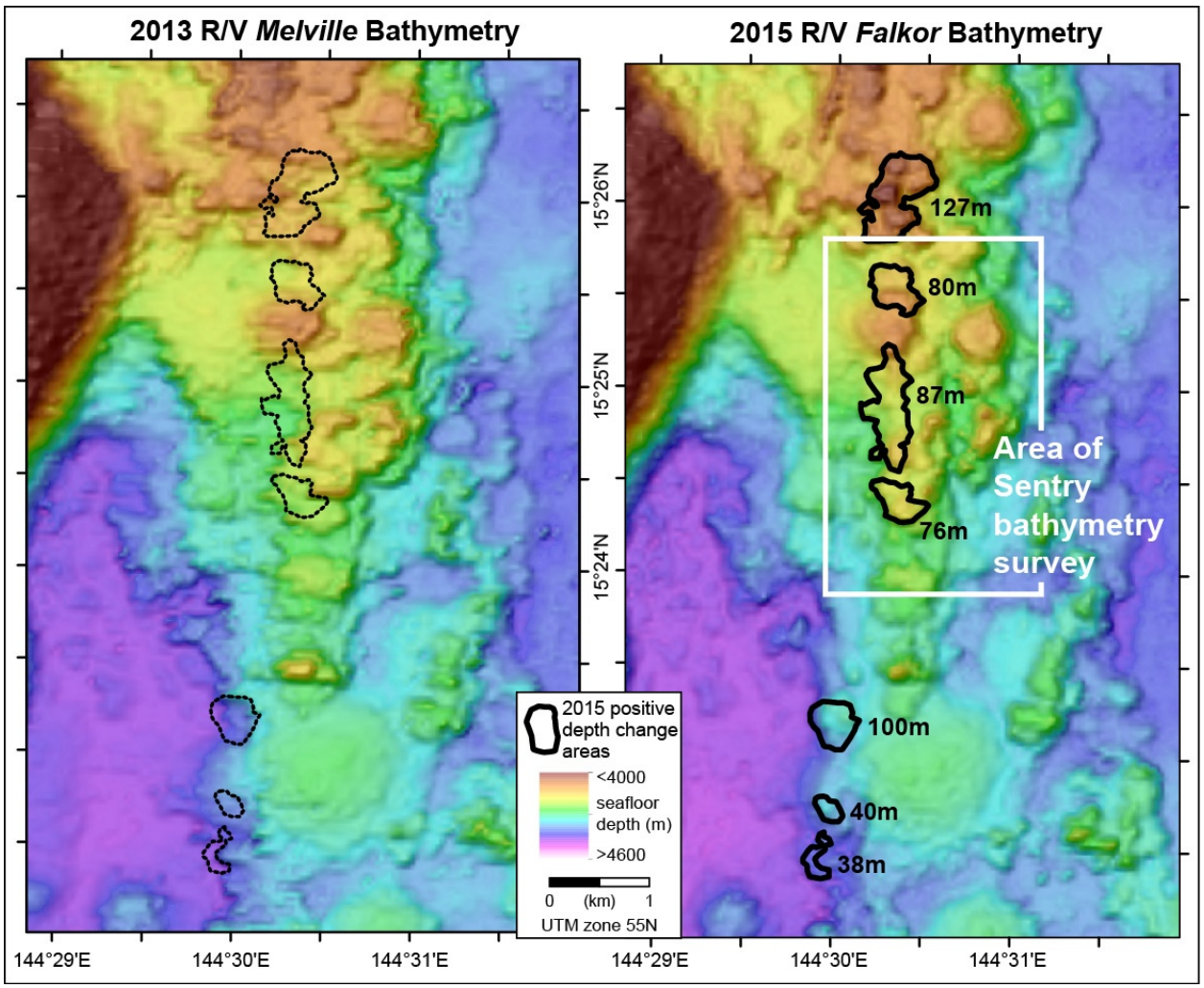

Surface difference showing positive depth changes derived from ship hull-mounted multibeam data

The comparison of the two multibeam sonar surveys from 2013 and 2015 shows that there are 7 distinct areas of significant depth changes. While there may be 7 separate lava flows a few of them are likely connected by much thinner lava flows that are not detected by our analysis. The depth changes range from 38 m on the southern-most mound to 127 m on the northern-most mound. The lava flows extend over a distance of 7.3 km, or from 15° 22.3' to 15° 26.3'N. The cross-axis width of the lava flows is 300-600 m. The depth at the eruption site ranges from 4050 m in the north to 4450 m in the south.

General observations from the AUV *Sentry* Bathymetry

The high-resolution bathymetric maps created from AUV *Sentry's* multibeam sonar data show that the seafloor in most of the surveyed areas (dives 366, 367, 368, 369) is characterized by pillow-lava mounds and ridges. The first survey (dive 366) on segment 14.5°N (Map 4) is distinctly older seafloor than the other areas, based on the number of faults running through the area. At the other end of the spectrum, the survey of the 2013-2015 lava flows (dive 367) is obviously the newest seafloor mapped. In stark contrast, the last *Sentry* dive (370) at segment 17.0°N (Map 8) revealed a completely different morphology than the other sites, characterized by very smooth seafloor formed by extensive sheet flow lavas, confirmed by the photo survey. This is also reflected in the unusually smooth ship-based bathymetry at this segment high. It is not clear why this segment has such a different morphology. It will be interesting to compare its lava chemistry and vent fluid chemistry to the other segments we will visit in 2016.

Multibeam Sonar Mapping

We used R/V *Falkor*'s EM302 multibeam sonar to collect new bathymetric data during most ship transits, especially along the axis of the Mariana back-arc, where little or no modern bathymetric data existed (see summary figure at the beginning of this report). The new data are far superior to what existed previously, and we were very impressed with the high-quality of the *Falkor* bathymetry data and the great support for mapping from the ship's marine technicians. The total area mapped was 24,054 km^2. In general, our experience was the swath width we got was about twice the water depth along the deep back-arc axis (for example, 7000-8000 m swath width at depths of 3500-4000 m), and the system worked well down to about 5000 m, after which the swath width progressively narrowed. The ship's crew were particularly adept at "edge mapping", which entailed interactively adjusting the ship's position and heading, based on the real-time EM302 display to achieve an optimal overlap with previously collected swath data. This made adding to existing data very easy and efficient. The multibeam data were used for broad scale geologic mapping in the section that follows.

Structures and Predicted Geology of the Mariana Back-Arc

Melissa O. Anderson (*University of Ottawa / GEOMAR)*
Schmidt Student Opportunities Participant

1. Introduction

Geological mapping is employed as a powerful tool to elucidate the evolution of the Mariana back-arc and determine the relationships between the geodynamic setting and volcanism. Importantly, these maps are useful in determining the tectonic *versus* magmatic controls on hydrothermal venting, and may help to distinguish terrains with high resource potential from those that are associated with small, uneconomic hydrothermal systems. On land, geological mapping is a vital component of resource assessment, but these maps are rare on the ocean floor. By taking the first steps towards building a robust geological map guided by seafloor morphologies, we can assess the accuracy of these predictions when compared to future ground-truthing provided by ROV dives during the second leg of the Hydrothermal Hunt in the Mariana back-arc.

2. Methods

Ship-based multibeam bathymetric data from the Mariana back-arc were collected during the FK151121 Hydrothermal Hunt cruise in 2015. The R/V *Falkor* was equipped with a Kongsberg EM 302 multibeam echosounder with an operating frequency of 30 kHz. The collected bathymetric data were gridded with a cell size of 40 m using MBSystem and ArcGIS software, and then reprocessed using a "Terrain Texture Shading" (TTS) technique developed by Brown (2010). This technique combines basic hill shading with curvature analysis to add texture to shaded relief to reveal subtle surface and structural features that can be directly correlated with volcanic geomorphology (e.g., Anderson et al., 2016; Augustin et al., Submitted). The process uses the Terrain Texture Shader software of L. Brown, available as freeware from Natural Graphics (http://www.naturalgfx.com/tts.htm). The TTS software analyzes digital elevation or bathymetric data and creates a visual hierarchy of texture and elevation that solves many of the problems associated with traditional hill shading, including improving edge detection and maintaining contrast ratios at every zoom level (Fig. 1_{geo2}). After processing, the rendered GeoTIFF images were merged in ArcGIS with weighted shaded relief (translucency of 50%) to create shaded base maps for each back-arc segment. Predicted geological maps of the newly surveyed back-arc were constructed from interpreted seafloor texture, slope, and rugosity derived from the bathymetric surfaces. Observations from other similar studies (e.g., Yeo et al., 2012; Anderson et al., 2016) allow us to assign geological contacts following well-established approaches for classifying volcanic geomorphology (cf. Walker et al., 1993; Thouret, 1999; Sigurdsson, 2000). Relative ages of the mapped units were established from overlapping and cross-cutting relationships, and backscatter evidence of young volcanic flow features. This approach allows us to predict the geology that will be encountered on the seafloor; however, direct seafloor observations that

will be obtained during Leg 2 of this cruise will provide the ground-truthing necessary to refine the geological maps

.

3. Map units

The southern Mariana back-arc area was arbitrarily divided into 10 sections (Maps) during cruise planning. The sections generally follow the most recent spreading axis, and comprise individual segments with lengths up to ~100 km long, and widths ranging from ~5.5 to 13.8 km wide. Predicted geological maps were constructed only for segments that were surveyed during this cruise. The mapped units follow the legend shown in Fig. 2_{geo2}.

3.1 Old arc crust

The basins are generally bound by steeply-faulted escarpments that expose the older Mariana arc basement. In some areas, the basin walls are hummocky with a highly rugose (rough) surface dotted by numerous small volcanic edifices with minor faulting. This hummocky old arc crust grades into heavily faulted crust with steep slopes and very few small volcanic edifices. The old arc crust is interpreted to be sedimented in areas that have flat slopes, less relief, and a generally smooth morphology. The contacts between the old arc crust units are gradational.

3.2 Basin floor

The main features of the basin floors are hummocky volcanic terrain, smooth volcanic terrain, faulted basins, and sedimented basins. The hummocky volcanic terrain occurs along the axis of the spreading centers and dominates basin floors for most of the segments. This unit ranges from heavily faulted to unfaulted, reflecting the different ages of the extrusive products. The surface morphology has a high rugosity, with “hummocks” up to 200 m high, interpreted to represent thick onlapping lava flows (pillows and lobes) with steep flow fronts (cf. Yeo et al., 2012). One flow was visited during an AUV dive, with still photographs revealing both young and old pillow flows. The hummocky volcanic terrain grades into smoother volcanic terrain, generally more prevalent towards the basin walls. This terrain may be sedimented volcanic flows, or flat-lying sheet flows. Photographs from an AUV dive to this flow morphology near 17°N revealed sheeted flow. Sediment-filled topographic lows occur throughout the back-arc, and are divided into faulted and sedimented basin units based on the abundance of faults. These units have a very low slope and smooth surfaces (low rugosity).

Two larger conical volcanoes occur off-axis near 13°0’N and 16°20’N. These volcanic edifices are identified in the multibeam data by their circular morphology, steep sides, and high relief relative to the surrounding units. In addition, a large rifted-volcano near 17°N is interpreted based on the flat, circular morphology and comparisons to similar rifted volcanoes in other spreading centers (e.g., Menez Gwen volcano, EPR).

3.3 Structural features

Numerous lineaments occur throughout the Mariana back-arc. Major faults are identified as linear to curvilinear traces with scarps >100 m in height, and minor faults have scarps <100 m in height. The faults are all steeply-dipping normal faults, with dip directions indicated on the geological maps. The inferred faults are generally east-dipping on the west side of the back-arc segments, and west-dipping on the east side. In some areas, particularly near transfer zones between back-arc segments, the fault strikes have a wide range of orientations, while some segments have more uniform orientations, reflecting the changing regional stress fields. A total of 1664 major fault segments between 93 m and 8478 m in length were measured, and a total of 5148 minor fault segments between 57 m and 11540 m in length were measured.

4. Structures and predicted geology

4.1 Back-arc Segment centered at 13.3°N

The structures and predicted geology of the back-arc segment centered at 13.3°N are shown in Fig. 3_{geo2}. The character of the seafloor is dominated by heavily faulted smooth volcanic morphologies with minor hummocky ridges. Faulted basin floor occurs on the western side of the back-arc. A total of 195 major faults and 618 minor faults were measured. In the south between 12°53'N and 13°4'N, the faults (major and minor) are oriented over a narrow range with a mean of 39.3° ± 0.9° (95% confidence interval, n = 325). In this area, the faults tend to dip towards the center of the back-arc. There is an abrupt change in the orientation of the faults at 13°4'N (towards 13°26'N), rotating counter-clockwise with a mean of 23.8° ± 0.6° (95% confidence interval, n = 488). Unusually, the faults in this area dip towards the west on the western side of the back-arc, and to the east on the east side. This may indicate that the surveyed area is slightly off-axis to the back-arc spreading axis. The axes of volcanic ridges tends to follow the fault orientations in the center of the back-arc, except near the large volcanic cone in the south where the ridges are oriented in a more E-W direction, possibly reflecting a radial stress field associated with this volcano. The volcanic ridge axes have a mean of 34.8° ± 21.7° (95% confidence interval, n = 7), with a large uncertainty in data reflecting these variable orientations and a small sample size.

4.2 Back-arc Segment centered at 13.9°N

The structures and predicted geology of the back-arc segment centered at 13.9°N are shown in Fig. 4_{geo2}. The seafloor is dominated by hummocky volcanic terrain with minor smooth volcanic terrain on the basin floor, bounded primarily by faulted old arc crust in the west and hummocky old arc crust in the east. A total of 166 major faults and 496 minor faults were measured. The faults show a uniform orientation over the entire length of this segment between 13°40'N and 14°18'N, with a mean of 15.6° ± 0.6° (95% confidence interval, n = 662). The orientation of these faults is further rotated counter-clockwise relative to the

previous segment to the south. The volcanic ridge axes have a mean orientation of 13.0° ± 4.4° (95% confidence interval, n = 14), which shows a more northerly orientation relative to the faults. Most ridges trend between 0–20°, and while 17% of the structures trend between 20–30°, only 7% of the volcanic ridge segments follow this orientation.

4.3 Back-arc Segment centered at 14.5°N

The structures and predicted geology of the 14.5°N segment are shown in Fig. 5_{geo2}. The seafloor shows a wide range in morphologies and fault orientations. The basin floor is dominated by heavily faulted hummocky volcanic terrain and sedimented basins, bound by faulted and hummocky old arc crust. A total of 555 major faults and 377 minor faults were measured. The faults show a wide range of orientations throughout this segment between 14°10'N and 14°53'N, with a mean of 16.7° ± 0.9° (95% confidence interval, n = 932), reflecting a complicated regional stress field. The zigzag orientation of the faults is common in other *en echelon* basins. The abundance of faulting within the hummocky volcanic terrain suggests that there are episodes of tectonic extension punctuated by magmatism, and that most of the volcanic flows in this segment are relatively older than those in unfaulted hummocky areas. The volcanic ridge axes follow the dominant structural trend, and have a mean orientation of 16.7° ± 8.2° (95% confidence interval, n = 10). One volcanic ridge axis follows a distinctly more E-W trend, indicating that while only a small number of faults follow this orientation, regional E-W structures may have an important control on volcanism.

4.4 Back-arc segments centered at 15.1°N and 15.5°N

The structures and predicted geology of the back-arc segments centered at 15.1°N and 15.5°N are shown in Fig. 6_{geo2}. The seafloor is dominated by sedimented basins bound by sedimented to faulted old arc crust in the south, and hummocky to smooth volcanic flows bound by hummocky to faulted old arc crust to the north. A total of 177 major faults and 284 minor faults were measured. Between 14°59'N and 15°12'N, there is a wide range of fault orientations marking the top of the transfer zone with the back-arc segment to the south. The mean fault orientation is 14.6° ± 3.7° (95% confidence interval, n = 217). This is a slightly more northerly direction than the previous segment to the south. Between 15°12'N and 15°33'N, the seafloor is dominated by relatively recent volcanism, manifested by unfaulted hummocky volcanic terrain on the basin floor bound by hummocky old arc crust. Here, there is a smaller range of fault orientations, with a mean of 7.5° ± 2.5° (95% confidence interval, n = 151). Over this length of back-arc there are relatively less fault segments than previous back-arc areas. Finally, there is a clock-wise rotation in fault orientations between 15°33'N and 15°39'N, with a mean of 21.5° ± 2.7° (95% confidence interval, n = 93), representing the beginning of the transfer zone between this segment and the one to the north. Despite the wide range of fault orientations, the volcanic ridge axes follow a narrow trend with a mean orientation of 15.9° ± 6.9° (95% confidence interval, n = 11).

4.5 Back-arc segment centered at 16.1°N

The structures and predicted geology of the back-arc segment centered at 16.1°N is shown in Fig. 7_{geo2}. The seafloor is dominated by sedimented basins bound by sedimented to faulted old arc crust in the south, and hummocky to smooth volcanic flows bound by hummocky to faulted old arc crust to the north. A total of 131 major faults and 541 minor faults were measured. The wide range of fault orientations between 15°41'N and 15°48'N marks the southern transfer zone, with a mean fault orientation is 16.4° ± 3.0° (95% confidence interval, n = 130). In contrast, the area from 15°48'N to 16°13'N has a narrow range of fault orientations, with a mean of 2.7° ± 1.3° (95% confidence interval, n = 429). Between 16°13'N and 16°28'N, the northern transfer zone shows a slightly wider distribution of fault orientations, rotated clock-wise from the faults to the south, with a mean of 9.3° ± 2.7° (95% confidence interval, n = 113). The volcanic ridge axes have a mean orientation of 18.6° ± 3.6° (95% confidence interval, n = 39); however, two distinct populations occur between 0–20° (41% of the data) in the central part of the back-arc, and between 30–50° (31% of the data) in the northern part of the back-arc associated with a radial pattern at the base of a large volcanic cone.

4.6 Back-arc segment centered at 16.5°N

The structures and predicted geology of the back-arc segment centered at 16.5°N is shown in Fig. 8_{geo2}. The seafloor is dominated by a large volcanic cone flanked by hummocky flows near 16°20'N. This cone appears to be growing on top of old arc crust rather than from the basin floor, although the flows extend onto the basin floor. To the north of this narrow basins occur almost entirely covered with hummocky and smooth volcanic terrains. The old arc crust is heterogeneous, with hummocky, faulted, and sedimented units. A total of 125 major faults and 1036 minor faults were measured. Over the entire segment between 16°19'N and 16°54'N, there is a narrow range of fault orientations, with a mean of 1.0° ± 0.9° (95% confidence interval, n = 1161). The volcanic ridge axes have a mean orientation of 174.3° ± 2.4° (95% confidence interval, n = 43), suggesting that volcanism is controlled by a narrower range of structures than represented by the orientations of the faults.

4.7 Back-arc segment centered at 17.0°N

The structures and predicted geology of the back-arc segment centered at 17.0°N is shown in Fig. 9_{geo2}. Near 17°N, a large rifted volcano is interpreted based on the morphology of the seafloor. The center of this cone is dominated by smooth volcanic terrain, determined to be sheeted lava flows during an AUV photo survey, with small hummocky volcanic ridges. This smooth volcanic terrain extends to the south and north of the rifted volcano, where it grades into hummocky volcanic terrain. These volcanic terrains occupy the entire width of the basin south of 17°13'N, and are bound primarily by hummocky old arc crust. To the north of this, deep sedimented basins are bound by very steeply dipping old arc crust that grades from

hummocky to faulted to sedimented. A total of 108 major faults and 715 minor faults were measured.

Between 16°54'N and 17°3'N, there is a wide range of fault orientations, although this back-arc segment is only slightly offset from the one to the south. The mean fault orientation is 170.4° ± 1.8° (95% confidence interval, n = 175), showing a further counter-clockwise rotation of the fault orientations with increasing latitude. From 17°3'N to 17°20'N, the fault trends are further rotated and occupy a very narrow range, with a mean of 174.3° ± 0.9° (95% confidence interval, n = 423). In the north between 17°20'N and 17°27'N, the northern transfer zone again reveals a wider range of fault orientations that are further rotated, with a mean of 179.4° ± 2.0° (95% confidence interval, n = 225). The volcanic ridge axes have a mean orientation of 163.2° ± 3.4° (95% confidence interval, n = 26), which demonstrate a structural control that has a more E-W trend than the primary structures in the central back-arc area.

4.8 Back-arc segment centered at 17.8°N

The structures and predicted geology of the 17.8°N segment is shown in Fig. 10_{geo2}. The southern part of this back-arc segment between 17°28'N and 17°40'N represents a transfer zone between the segment to the south. The back-arc between 17°40'N and 18°0'N is dominated by hummocky flows bound by hummocky old arc crust. North of 18°0'N, the back-arc spreading axis is offset to the west but the transfer zone in between is poorly defined.

A total of 82 major faults and 530 minor faults were measured. In the southern transfer zone between 17°28'N and 17°40'N, the mean fault trend is 10.4° ± 1.8° (95% confidence interval, n = 226). The back-arc area between 17°40'N and 18°0'N has a mean fault trend of mean fault trend is 172.8° ± 1.9° (95% confidence interval, n = 386). Similar to the previous back-arc, the volcanic ridge axes occupy a very narrow range, showing a strong structural control on volcanism from structures associated with a mean orientation 167.1° ± 2.0° (95% confidence interval, n = 31).

4.9 Back-arc segment centered at 18.2°N

The structures and predicted geology of the northernmost back-arc segment centered at 18.2°N is shown in Fig. 11_{geo2}. The basin floor between 18°0'N and 18°20'N is almost entirely occupied by hummocky volcanic terrain, bound by faulted to hummocky old arc crust. Between 18°20'N and 18°35'N, the seafloor terrains are more heterogeneous, including smooth volcanic terrain onlapping on top of sedimented basins, bound primarily by hummocky old arc crust.

A total of 125 major faults and 551 minor faults were measured. There is a slight offset between this back-arc segment and the one to the south, although there is no well-defined transfer zone between them. The back-arc spreading area between 18°0'N and 18°22'N has a mean fault orientation of 168.4° ± 1.1° (95% confidence interval, n = 478). There is an abrupt change in fault orientations at 18°22'N, with a clockwise relative rotation in fault orientations. The data suggest a wide range in fault orientations north of 18°22'N, with a mean of 0.3° ± 4.0° (95% confidence interval, n = 198). The volcanic ridge axes have a mean orientation of 171.3° ± 2.7° (95% confidence interval, n = 21), closely following the orientations of the faulting.

5. Controls on hydrothermal venting

Slow-spreading back-arcs are ideal environments for generating large deposits of seafloor massive sulfides, as deeply-penetrating faults up to 10 km below the seafloor allow seawater to penetrate the ocean crust, providing conduits to focus hydrothermal fluid flow over long periods of time (Hannington et al., 2005; Andersen et al., 2015; German et al., 2016). Importantly, the depth of the Mariana back-arc provides a high ambient pressure that prevents boiling of the hydrothermal fluids during their ascent to the seafloor. The temperature at which the hydrothermal fluids discharge at the seafloor is limited by boiling, which is reflected in the mineralogy of the hydrothermal precipitates (Monecke et al., 2014). Black smoker chimneys in the Mariana back-arc are expected to have a high-temperature mineral assemblage, dominated by chalcopyrite, pyrite, and anhydrite.

In the study area, hydrothermal venting occurs in the back-arc on segments centered at: 14.5°N, 15.5°N, 16.5°N, 17.0°N, and 18.2°N In addition, previously-discovered venting occurs in the southern back-arc, an area that is not covered by this study. In the mapped areas, the hydrothermal vent sites inevitably occur in the center of the back-arc spreading axis associated with volcanic terrains. Several vent sites occur on volcanic terrains that are unfaulted (15.5°N, 16.5°N, and 17.0°N), suggesting that hydrothermal venting is associated with relatively recent eruptions. Vent sites also occur on volcanic terrains that are moderately to extensively faulted (14.5°N and 18.2°N). In these areas, the presence of active venting may indicate renewed volcanism following a period of quiescence and tectonic extension. These faulted terrains are predicted to have larger accumulations of massive sulfides relative to their unfaulted counterparts due to the presumably increased efficiency of hydrothermal fluid flow and focusing along faults. All of the vent sites in this study are classified as magmatically-hosted, although there is potential for undiscovered tectonically-hosted deposits to occur in other areas of the back-arc basin, similar to what is found in slow-spreading mid-ocean ridge environments (German et al., 2016).

6. Next steps

The predicted geological maps presented here are the first step towards understanding the evolution of the Mariana back-arc and controls on hydrothermal venting. Important next

steps include: (1) establishing individual lava flows based on sediment cover interpreted from backscatter data, (2) comparing the predicted map to observations from ROV dives conducted during Leg 2 of the Hydrothermal Hunt, as well as any previous cruises, in order to provide ground-truthing, (3) refine the maps as necessary, (4) extend the map to other areas that have bathymetric data, (5) compare the mapped structures with the large-scale regional structures that permeate the entire back-arc, and (6) compare the results to geodynamic models of the formation of the Mariana back-arc. This work is part of an ongoing effort between the University of Ottawa, GEOMAR Helmholtz Centre for Ocean Research Kiel, and our many partners, to provide geological context interpreted from bathymetric data in a wide range of tectonic environments.

References

Andersen, C., Rüpke, L., Hasenclever, J., Greveymeyer, I., Petersen, S., 2015. Fault geometry and permeability contrast control vent temperatures and the Logatchev 1 hydrothermal field, Mid-Atlantic Ridge. Geology 43, 51–54.

Anderson, M.O., Hannington, M.D., Haase, K., Schwarz-Schampera, U., Augustin, N., McConachy, T.F., Allen, K., 2016. Tectonic focusing of voluminous basaltic eruptions in magma-deficient backarc rifts. Earth and Planetary Science Letters 440, 43–55.

Augustin, N., van der Zwan, F.M., Devey, C.W., Ligi, M., Kwasnitschka, T., Feldens, Bantan, R.A., and Basaham, A.S. Geomorphology of the Central Red Sea Rift: Determining spreading processes. Geomorphology (submitted).

Brown, L., 2010. A new technique for depicting terrain relief [abstract]. NACIS Annual Meeting, 2010 Oct 13–17, St. Petersburg, Florida.

German, C.R., Petersen, S., Hannington, M.D., 2016. Hydrothermal exploration of mid-ocean ridges: Where might the largest sulfide deposits be forming?. Chemical Geology 420, 114–126.

Hannington, M.D., de Ronde, C.E.J., Petersen, S., 2005. Sea-floor tectonics and submarine hydrothermal systems. Economic Geology 100th Anniversary volume, 111–141.

Monecke, T., Petersen, S., Hannington, M.D., 2014. Constraints on water depth of massive sulfide formation: Evidence from modern seafloor hydrothermal systems in arc-related settings. Economic Geology 108, 2079–2101.

Sigurdsson, H., 2000. Volcanic episodes and rates of volcanism. In: Sigurdsson, H., Houghton, B., McNutt, S.R., Rymer, H., Stix, J. (Eds.), Encyclopedia of Volcanoes. Academic Press, San Diego, pp. 271–279.

Thouret, J.-C, 1999. Volcanic geomorphology, an overview: Earth Sci. Rev., v. 47, p. 95–131.

Walker, G.P.L., 1993. Basaltic-volcano systems. Geological Society of London, Special Publication 76, 3–38.

Yeo, I., Searle, R.C., Achenbach, K.L., Le Bas, T.P., Murton, B.J., 2012. Eruptive hummocks: Building blocks of the upper ocean crust. Geology 40 (1), 91–94.

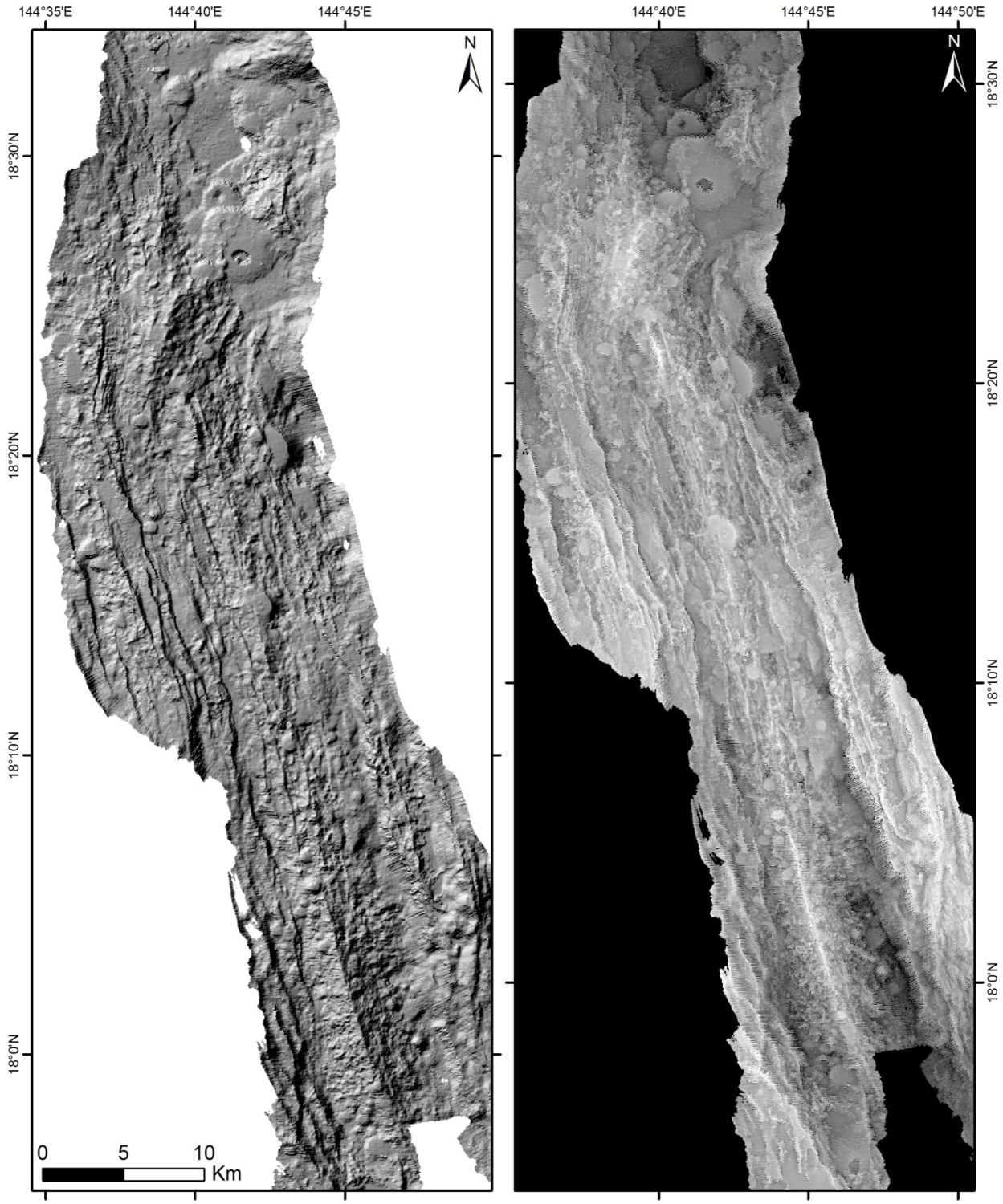

Figure 1 $_{geo2}$ – Layers that were combined to create the basemaps for this study include traditional hillshaded bathymetry (left) that uses a directional light source, and terrain-texture shaded bathymetry (right) that has a uses a diffuse light source.

Figure 2_{geo2} – Legend of the structures and mapped units for all subsequent geological maps.

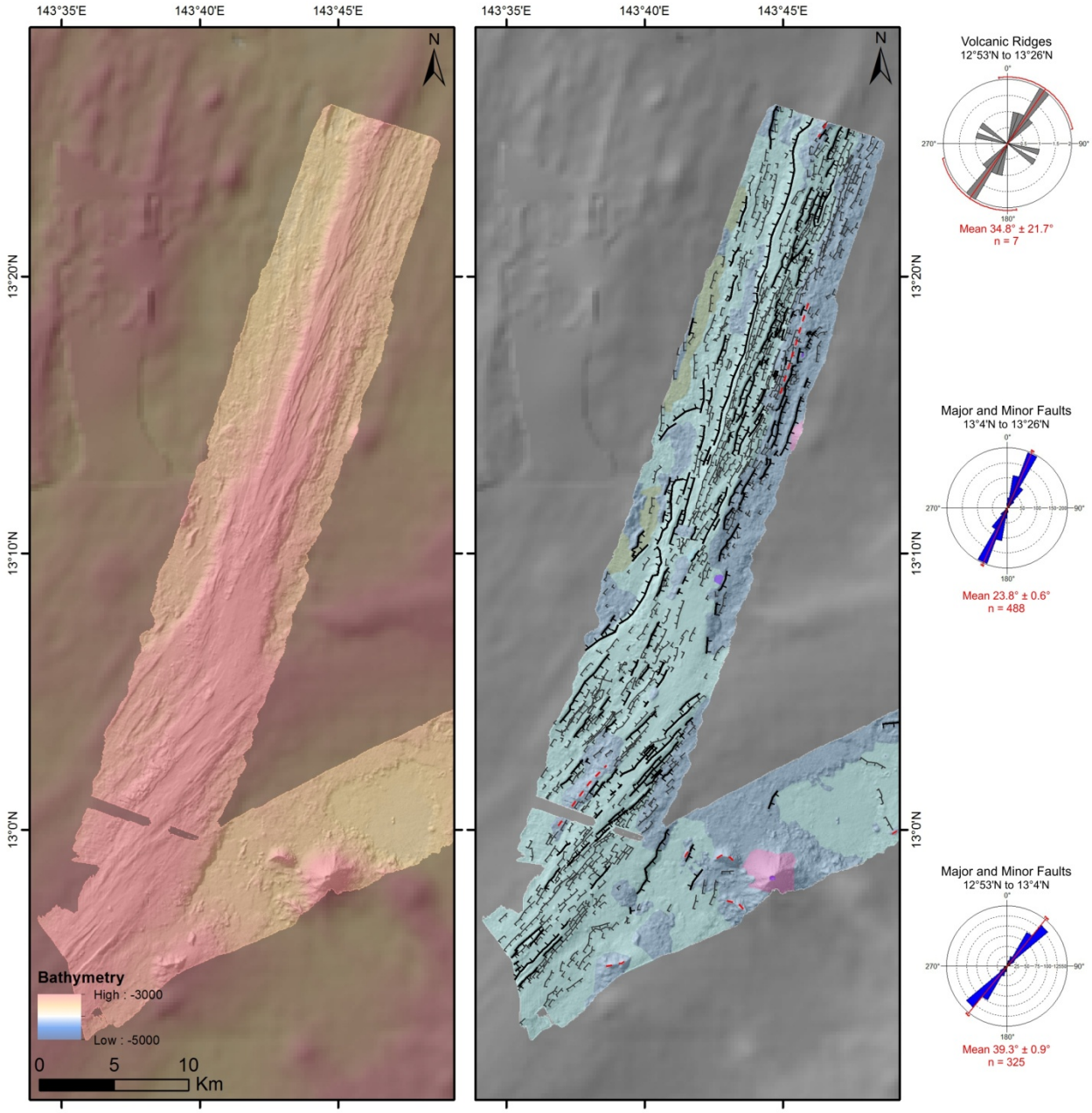

Figure 3$_{geo2}$ – Bathymetry (left) and predicted geological map (right) of the segment centered at 13.3°N (Segment 2), with a rose diagram of the volcanic ridge axes of the entire segment, as well as rose diagrams for the major and minor faults from 12°53’N to 13°4’N, and 13°4’N to 13°26’N.

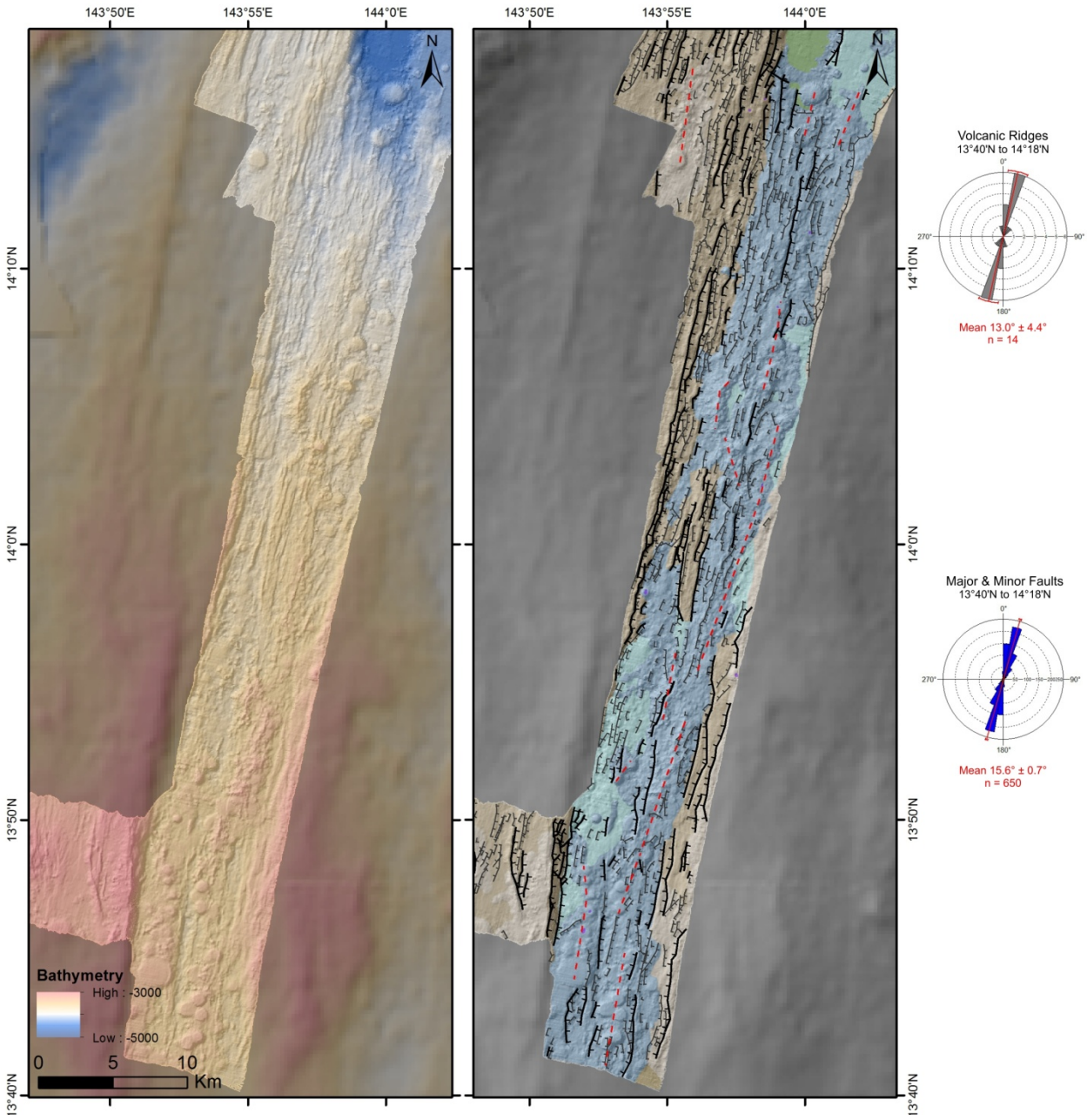

Figure 4$_{geo2}$ – Bathymetry (left) and predicted geological map (right) of the segment centered at 13.9°N (Segment 3), with rose diagrams of the volcanic ridge axes and major and minor faults of the entire segment, from 13°40'N to 14°18'N.

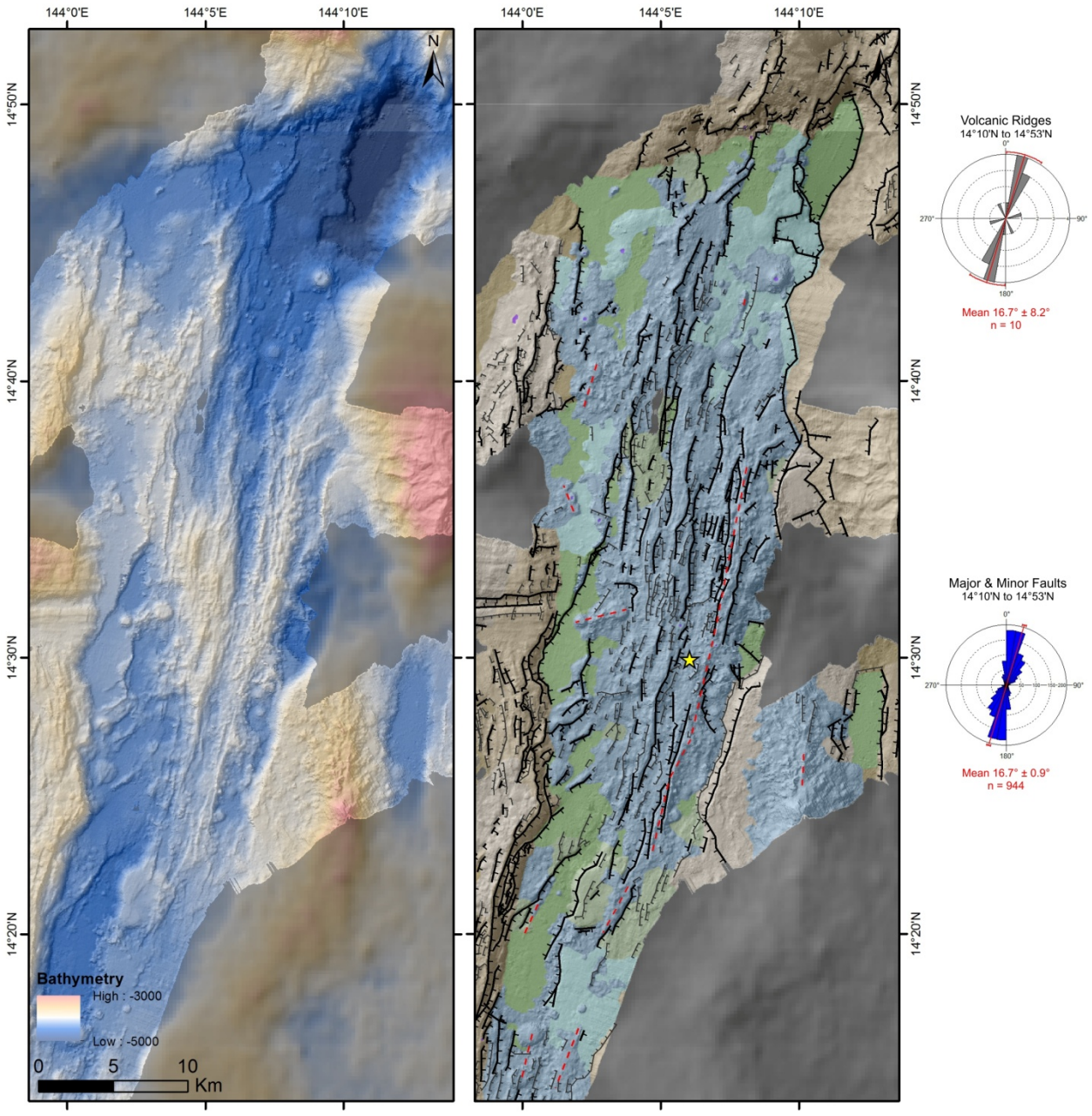

Figure 5$_{geo2}$ – Bathymetry (left) and predicted geological map (right) of the segment centered at 14.5°N (Segment 4), with rose diagrams of the volcanic ridge axes and major and minor faults of the entire segment, from 14°18'N to 14°53'N. Approximate location of hydrothermal venting indicated by yellow star.

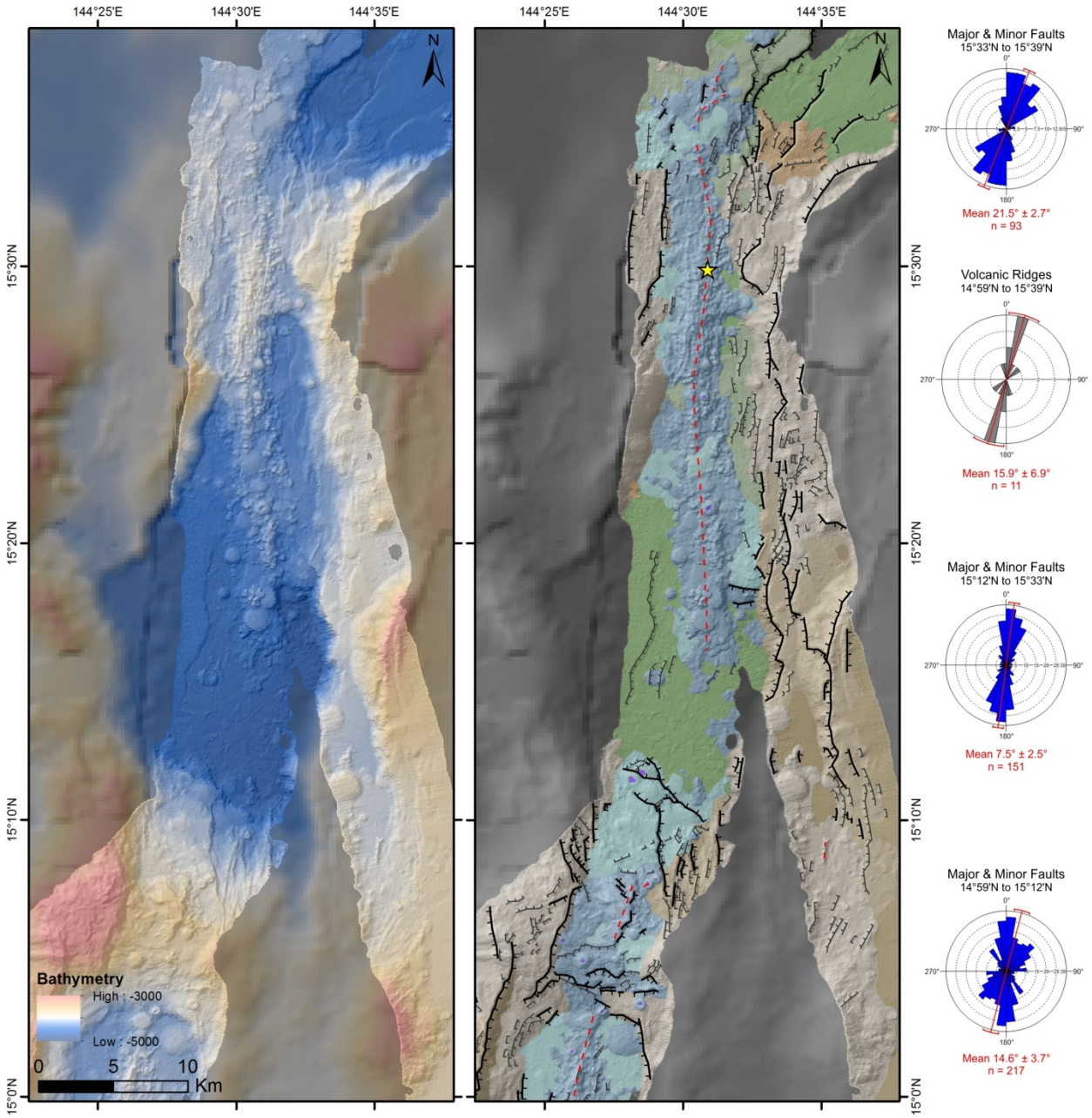

Figure 6$_{geo2}$ – Bathymetry (left) and predicted geological map (right) of the segments centered at 15.1°N and 15.5°N (Segment 5), with a rose diagram of the volcanic ridge axes of the entire segment, as well as rose diagrams for the major and minor faults from 14°59'N to 15°12'N, 15°12'N to 15°33'N, and 15°33'N to 15°39'N. Approximate location of hydrothermal venting indicated by yellow star.

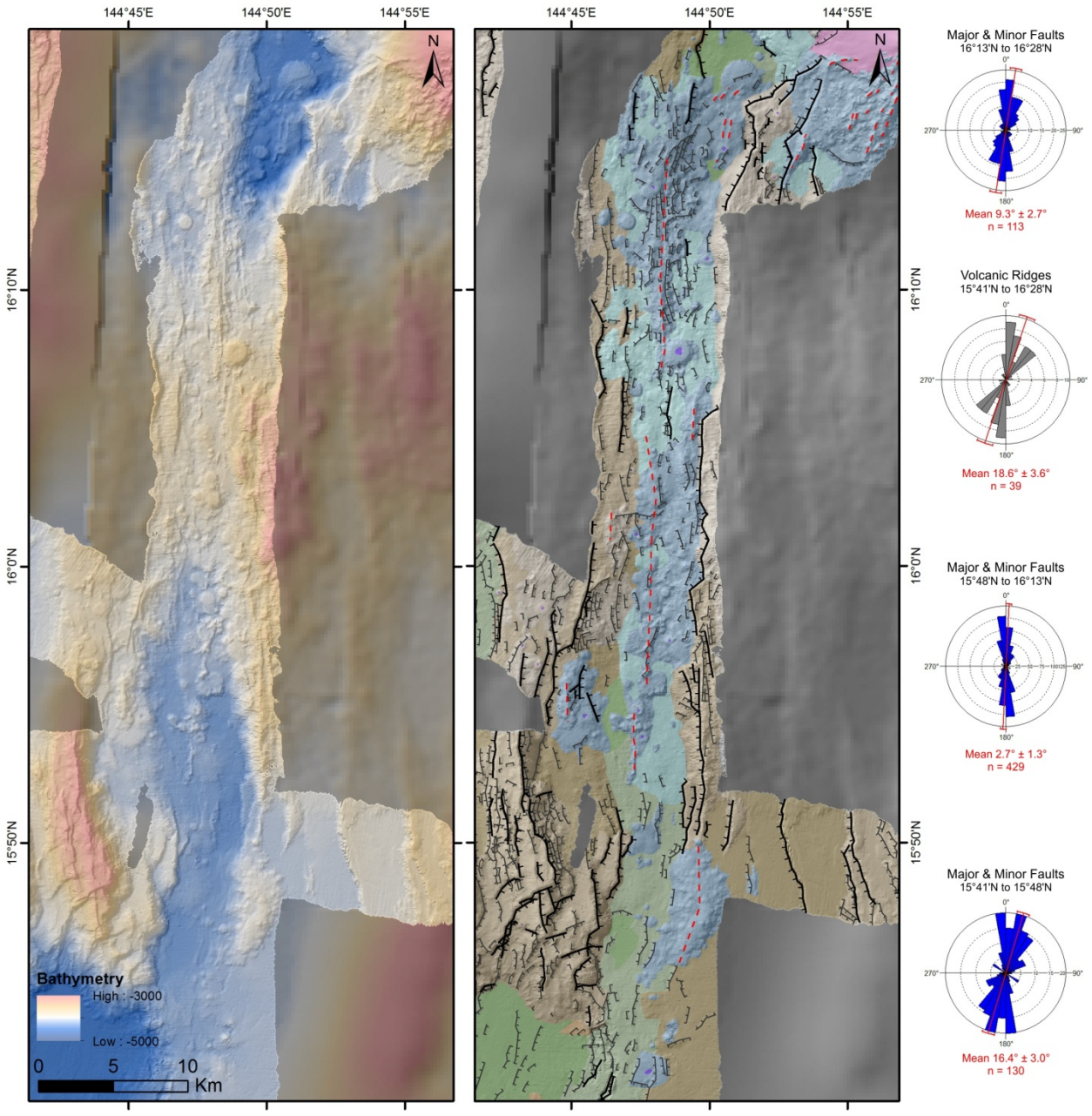

Figure 7$_{geo2}$ – Bathymetry (left) and predicted geological map (right) of the segment centered at 16.1°N (Segment 6), with a rose diagram of the volcanic ridge axes of the entire segment, as well as rose diagrams for the major and minor faults from 15°41'N to 15°48'N, 15°48'N to 16°13'N, and 16°13'N to 16°28'N.

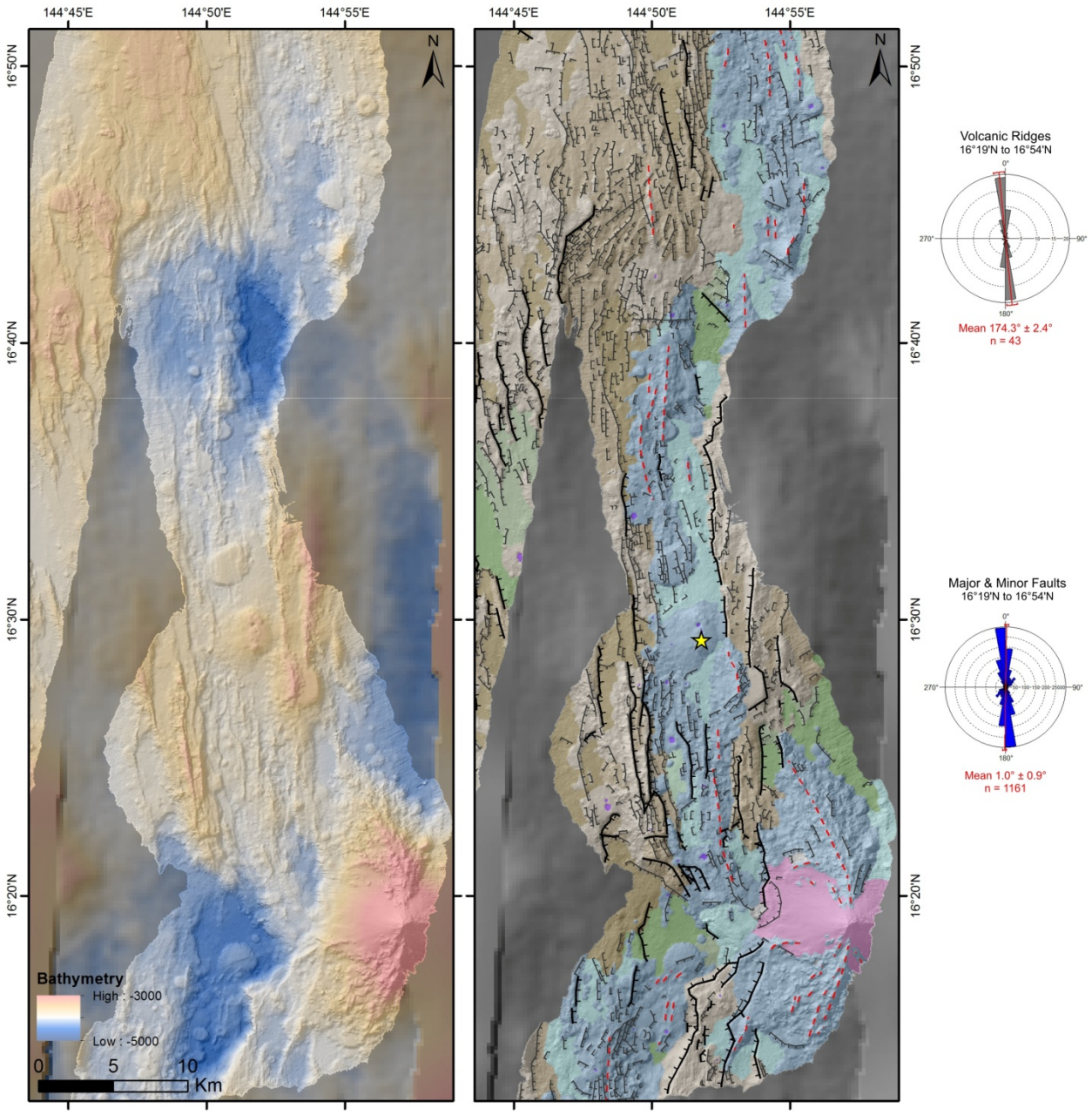

Figure 8$_{geo2}$ – Bathymetry (left) and predicted geological map (right) of the segment centered at 16.5°N (Segment 7), with rose diagrams of the volcanic ridge axes and major and minor faults of the entire segment, from 16°19'N to 16°54'N. Approximate location of hydrothermal venting indicated by yellow star.

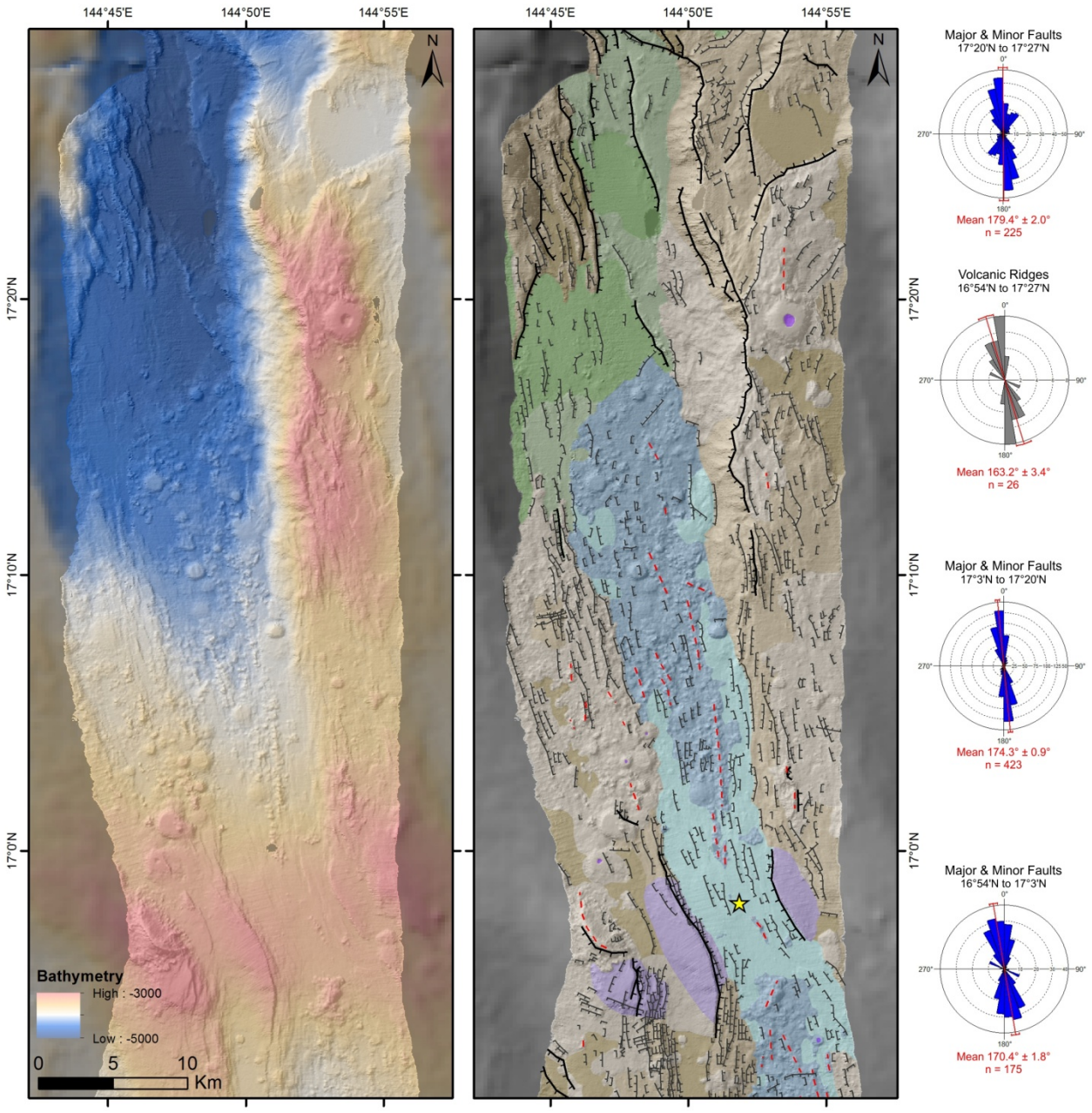

Figure 9$_{geo2}$ – Bathymetry (left) and predicted geological map (right) of the segment centered at 17.0°N (Segments 7 and 8), with rose diagrams of the volcanic ridge axes and major and minor faults of the entire segment, from 16°54'N to 17°27'N. Approximate location of hydrothermal venting indicated by yellow star.

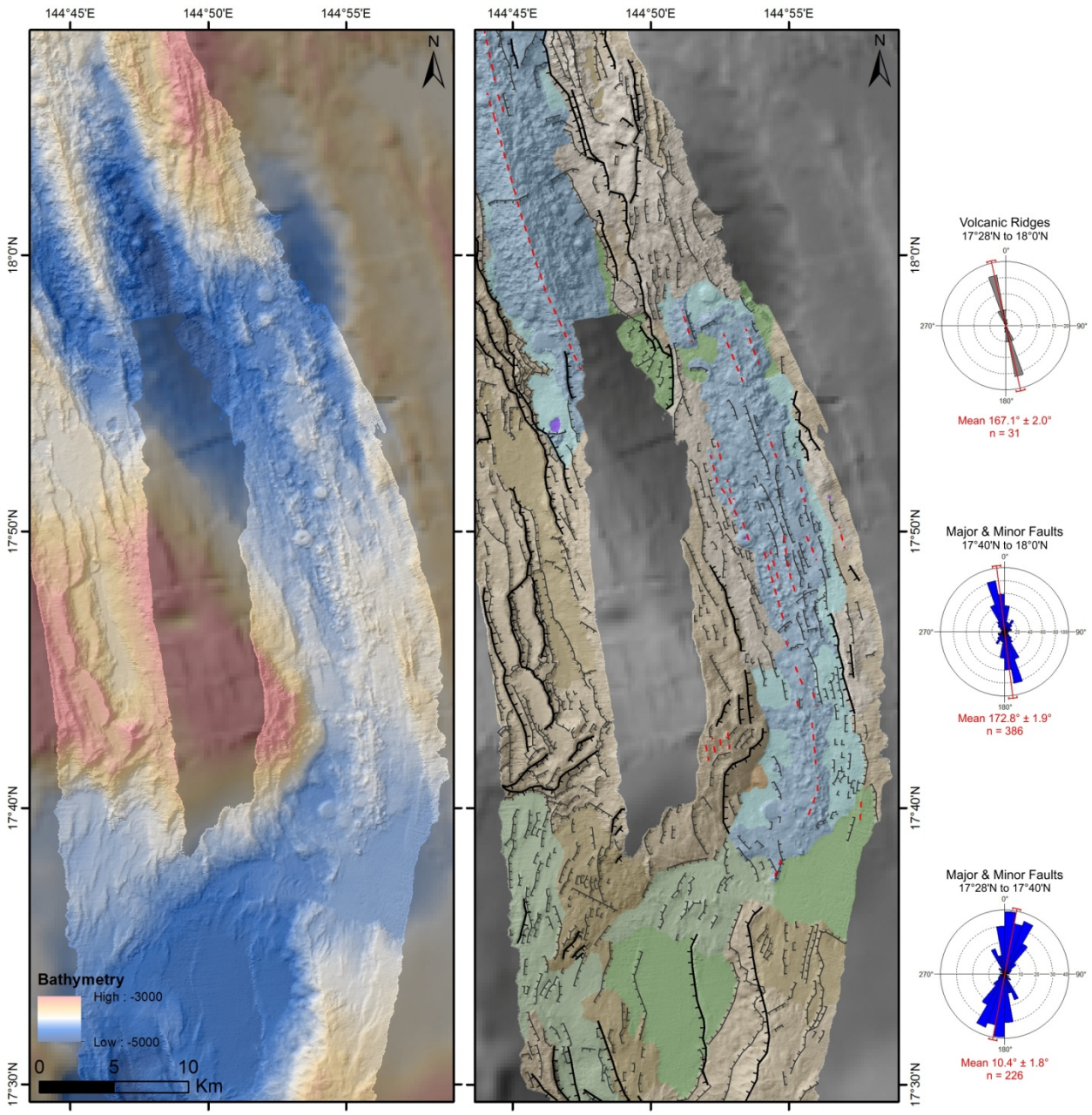

Figure 10 $_{geo2}$ – Bathymetry (left) and predicted geological map (right) of the segment centered at 17.8°N (Segment 9), with rose diagrams of the volcanic ridge axes and major and minor faults of the entire segment, from 17°28’N to 18°0’N.

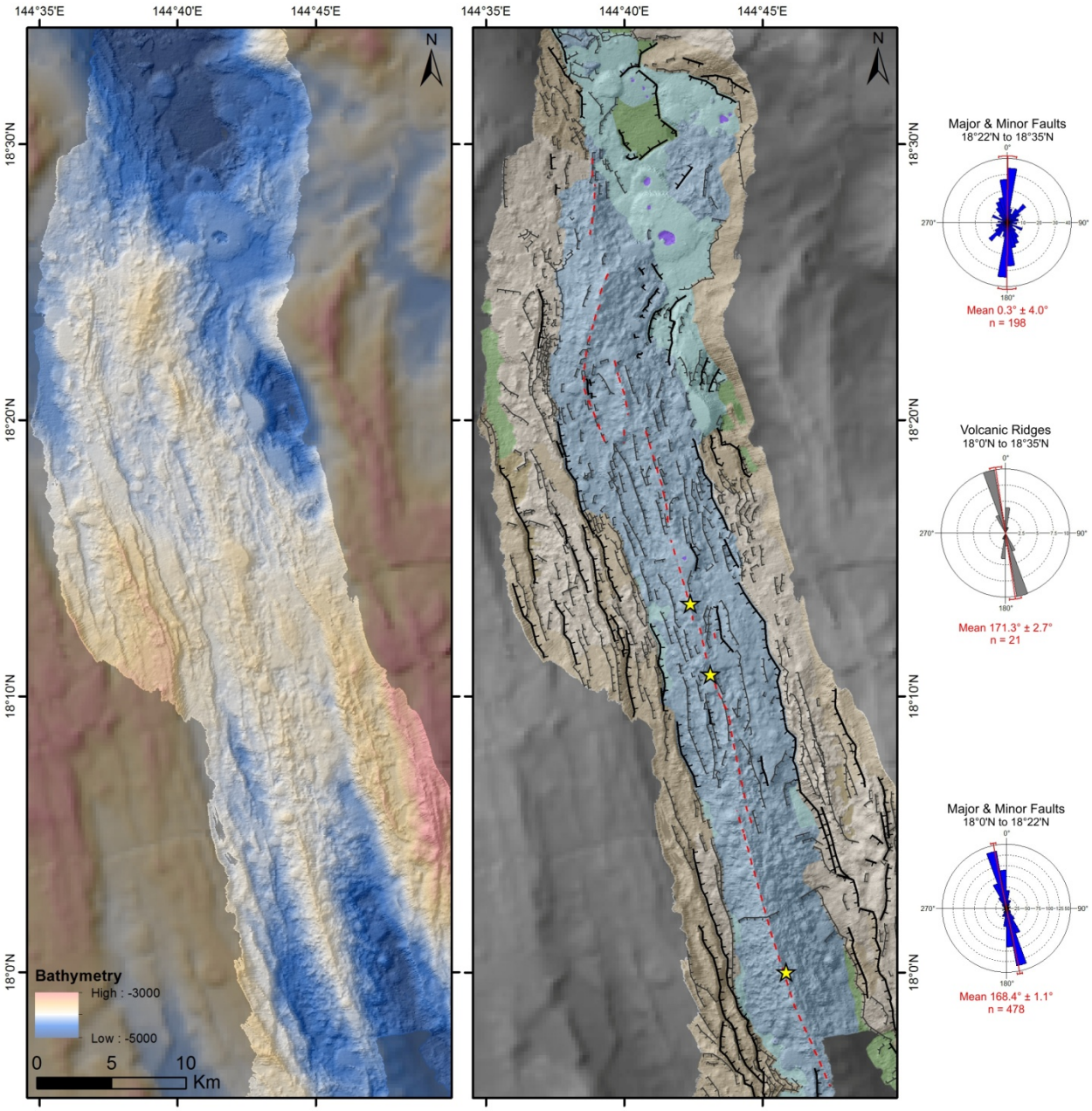

Figure 11$_{geo2}$ – Bathymetry (left) and predicted geological map (right) of the segment centered at 18.2°N (Segment 10), with rose diagrams of the volcanic ridge axes and major and minor faults of the entire segment, from 18°0'N to 18°35'N. Approximate locations of hydrothermal venting indicated by yellow stars.

Public Outreach

Bill Chadwick

Public outreach for this expedition was primarily through the Schmidt Ocean Institute web site at this URL: http://schmidtocean.org/cruise/hydrothermal-hunt-at-mariana/
(note the SOI web site went through a major re-design after our expedition and the original URL was different). We posted blog entries to the cruise web site nearly daily and Thom Hoffman (our videographer, see below) created excellent video updates at least weekly. Early on, we decided to start a betting pool to guess which Mariana back-arc segment would host the largest hydrothermal signal, and besides being fun for us, this turned out to be a surprisingly effective way to engage the ship's crew and the public in the goals of our expedition. We also made 12 ship-to-shore video calls to grade school, middle school, high school, and a community college in Guam, Oregon, and Washington (some part of the Oregon Coast STEM Hub). In addition, we made a call to Ocean Science Bowl (high school) teams in Oregon and Washington, and to a public audience at the Hatfield Marine Science Center in Newport, Oregon. Carlie Wiener and Logan Mock-Bunting (SOI shore-side outreach specialists) were extremely helpful in coordinating the cruise web site outreach and the ship-to-shore calls.

Multimedia

Thom Hoffman

Filmmaker and general outreach humanoid Thom Hoffman came on board the Hydrothermal Hunt, and got to annoy everyone with questions, a messy workspace and interview requests. The scientists and crew were extremely skilled and enthusiastic in writing blog posts and collaborating. Everyone put in a great, creative, effort to tell the story of a hugely successful trip. Live outreach to schools and public events went down a storm, including a wobbly iPad tour of the ship providing an authentic deep ocean experience. (Reports of seasickness in the audience were widely exaggerated). From Bill starring in a series of gifs, Susanna's origami skills explaining the magic of Towyos, and Melissa's gambling pool which we extended to the world. We tried a load of things and engaged people in a broad range of ways.

Some things I learned:

- The Gambling pool/breakdown/competition is a good hook, particularly in cruises where there is less 'to see' or that involve more abstract concepts.
- Short films on the key areas/concepts are probably a more efficient approach than pure chronology. 'Week one'/'week two' loses relevance quickly.
- The 'photo project' with the crew got loads of engagement, wish I'd done one with the science team too… Next time.
- Getting everyone's perspective on the key concepts needed to explain their work, before we leave. So we have all the right tools/animations in place to do so.

It was my first cruise and there was so much to learn at the same time as having so much to do! Thanks for all your help, you taught me so much, and shared generously. If you have any thoughts feedback for me let me know. I'll be back in November for round two…

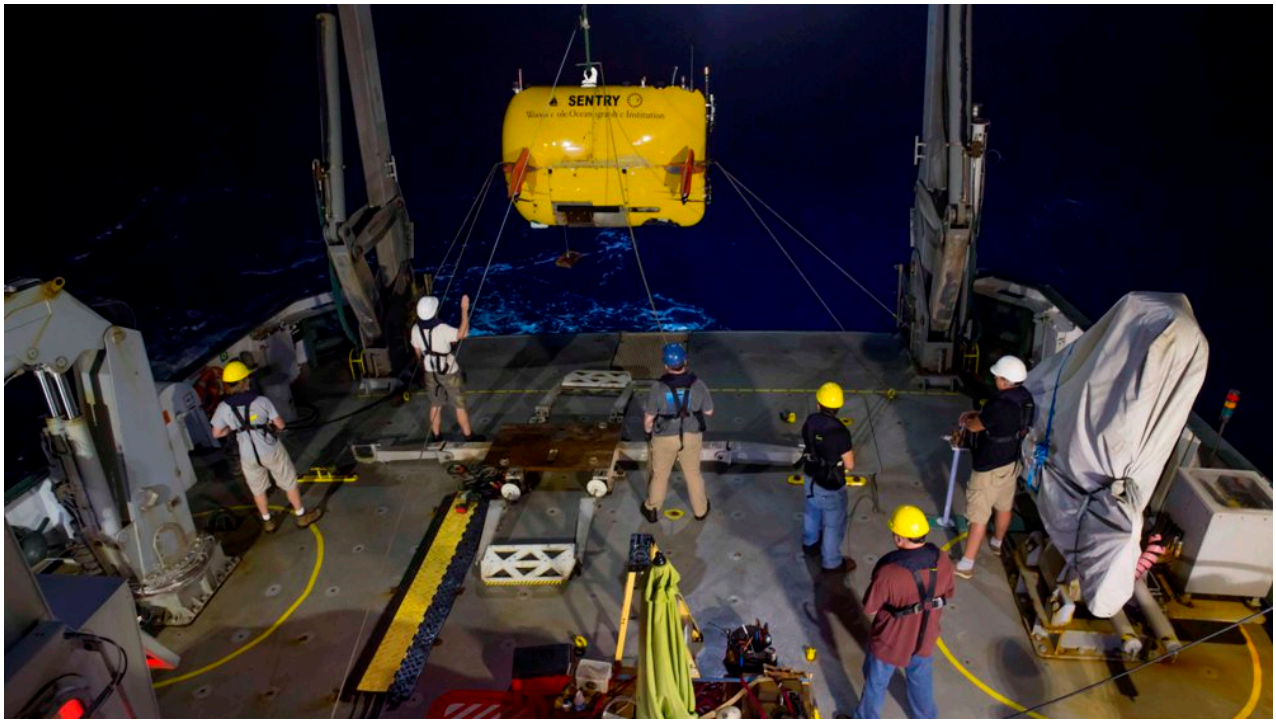
SENTRY